UFRJ

CENTRO DE CIÊNCIAS DA SAÚDE

CURSO DE PÓS-GRADUAÇÃO EM BIOTECNOLOGIA VEGETAL E BIOPROCESSOS

Efeitos induzidos por NaCl e KCl nas relações iônicas, fotossíntese e crescimento de espécies C_4

Ana Carolina Mendes Bezerra

2021

UNIVERSIDADE FEDERAL DO RIO DE JANEIRO

CENTRO DE CIÊNCIAS DA SAÚDE

CURSO DE PÓS-GRADUAÇÃO EM BIOTECNOLOGIA VEGETAL E BIOPROCESSOS

Efeitos induzidos por NaCl e KCl nas relações iônicas, fotossíntese e crescimento de espécies C_4

ANA CAROLINA MENDES BEZERRA

Sob a Orientação dos Professores

Fernanda Reinert, UFRJ

Leonardo Oliveira Medici, UFRRJ

Bianca Ortiz da Silva, UFRJ

Tese apresentada como requisito parcial para obtenção do grau de **Doutor (a) em Biotecnologia Vegetal** no curso de pós-graduação em Biotecnologia Vegetal e Bioprocessos da Universidade Federal do Rio de Janeiro - UFRJ.

Rio de Janeiro, RJ

Setembro de 2021

CIP - Catalogação na Publicação

Bezerra, Ana Carolina Mendes
BB574e Efeitos induzidos por NaCl e KCl nas relações iônicas, fotossíntese e crescimento de espécies C4 / Ana Carolina Mendes Bezerra. -- Rio de Janeiro, 2021.
136 f.

Orientadora: Fernanda Reinert.
Coorientadora: Bianca Ortiz-Silva.
Tese (doutorado) - Universidade Federal do Rio de Janeiro, Decania do Centro de Ciências da Saude, Programa de Pós-Graduação em Biotecnologia Vegetal, 2021.

1. Fisiologia Vegetal . 2. Estresse abiótico. 3. Salinidade do solo. 4. Fotossíntese. I. Reinert, Fernanda, orient. II. Ortiz-Silva, Bianca, coorient. III. Título.

Elaborado pelo Sistema de Geração Automática da UFRJ com os dados fornecidos pelo(a) autor(a), sob a responsabilidade de Miguel Romeu Amorim Neto - CRB-7/6283.

Universidade Federal do Rio de Janeiro
Centro de Ciências da Saúde

Coordenação de Pós-Graduação em Biotecnologia Vegetal e Bioprocessos

ATA DO EXAME DE DEFESA DE TESE DE DOUTORADO DE ANA CAROLINA MENDES BEZERRA, COMO PARTE DOS REQUISITOS NECESSÁRIOS À OBTENÇÃO DO GRAU DE DOUTOR EM CIÊNCIAS (BIOTECNOLOGIA VEGETAL E BIOPROCESSOS).

Aos vinte e sete dias do mês de setembro do ano de dois mil e vinte e um, às 14 horas e 15 minutos, reuniu-se via videoconferência, a Banca Examinadora abaixo discriminada, para avaliação da Tese de Doutorado da aluna **Ana Carolina Mendes Bezerra**, intitulada: "Efeitos induzidos por NaCl e KCl nas relações iônicas, fotossíntese e crescimento de espécies C_4" desenvolvida sob a orientação da **Profª. Fernanda Reinert Thomé Macrae.** A apresentação feita pela candidata foi acompanhada da arguição pelos componentes da Banca. Em seguida, esta se reuniu para sua avaliação e a tese foi (A) (inserir letra apropriada).

A) Aprovado;
B) Aprovado com pequenas modificações* a serem combinadas com o Presidente da Banca dentro de um mês;
C) Não aprovado ainda, é necessária a apresentação das modificações/correções* em uma nova versão do documento para o Presidente da Banca e uma carta do Presidente com prazo de máximo 3 meses para ser aprovada; se não reprovada
D) Não aprovado ainda, é necessária uma nova apresentação*, oral e escrita, para a mesma ou nova banca examinadora dentro de um prazo combinado com a comissão do Programa.
E) Reprovado, razões da reprovação* escritas no espaço destinado.

*As modificações/correções/razões para reprovação precisam ser discriminadas e o Presidente da Banca e o(a) aluno(a) precisam estar cientes.

E, para constar, foi lavrada a presente ata que vai devidamente assinada pelo coordenador, pelos membros da Comissão Examinadora e pela orientadora do aluno. A aluna deve ficar com uma cópia da ata e a outra deve ser entregue para a secretaria do PBV pelo Presidente da Banca.

Rio de Janeiro, 27 de setembro de 2021.

Centro de Ciências da Saúde – Bloco K
Sala K2-032 – 2º andar – Cidade Universitária
CEP: 21941-590 – Rio de Janeiro – RJ – Brasil
Tel: 3938-6676 - E-mail: pbv@ccsdecania.ufrj.br

Universidade Federal do Rio de Janeiro
Centro de Ciências da Saúde

Coordenação de Pós-Graduação em Biotecnologia Vegetal e Bioprocessos

ATA DO EXAME DE DEFESA DE TESE DE DOUTORADO DE ANA CAROLINA MENDES BEZERRA, COMO PARTE DOS REQUISITOS NECESSÁRIOS À OBTENÇÃO DO GRAU DE DOUTOR EM CIÊNCIAS (BIOTECNOLOGIA VEGETAL E BIOPROCESSOS).

Drª. Fernanda de Ávila Abreu – Coordenadora

Drª. Fernanda Reinert Thomé Macrae – UFRJ

Drª. Marcia Alves Ferreira - UFRJ

Dr. Marcos Leal Costa - IFF

Drª. Cristina Moll Hüther - UFF

Dr. Ricardo Antunes Azevedo - USP

Drª. Fernanda Reinert Thomé Macrae (Orientadora)

Ana Carolina Mendes Bezerra (Doutoranda)

LISTA DE MODIFICAÇÕES, CORREÇÕES OU RAZÕES PARA REPROVAÇÕES:

Ciente,

Presidente da Banca

Ciente,

Aluno(a)

Centro de Ciências da Saúde – Bloco K
Sala K2-032 – 2º andar – Cidade Universitária
CEP: 21941-590 – Rio de Janeiro – RJ – Brasil
Tel: 3938-6676 - E-mail: pbv@ccsdecania.ufrj.br

AGRADECIMENTOS

Esta tese de doutorado reúne contribuições de diversas pessoas. Como tal, agradeço a disponibilidade, acompanhamento atento e colaboração de todos. Nomeadamente:

Aos meus orientadores prof.[as] Fernanda Reinert, Bianca Ortiz e professor Leonardo Medici, pelos inestimáveis ensinamentos e apoio em todas as etapas de desenvolvimento desta tese. Aos meus orientadores no exterior, professores Timothy Colmer e Lukasz Kotula, pelo acolhimento, apoio e ensinamentos inestimáveis.

Ao professor Ricardo Vieira por tão generosamente permitir que nosso grupo de pesquisa se tornasse parte integrante de seu laboratório. Obrigada por todo o incentivo, apoio e contribuição.

Ao professor Márcio Alves Ferreira, pela estreita colaboração com nosso grupo de pesquisa e por disponibilizar a infraestrutura de seu laboratório para realização de experimentos e análises, tornando essa pesquisa possível. Obrigada também pela revisão deste documento.

Aos professores Camila Pinho e Júnior Borella-UFRRJ e à professora Iracema Takase-UFRJ, pelo auxílio e disponibilização de infraestrutura para realização de análises. À equipe do Numpex-Bio-UFRJ, pela utilização de equipamentos e apoio técnico.

Aos amigos e integrantes do Laboratório de Fisiologia Vegetal, David, Diego, Cattem, Filipe, Isabela, Alice, Gabriel e Camila, pelo apoio e estímulo intelectual e emocional. À minha querida amiga Nícia, por seu acolhimento, por me proporcionar ótimos momentos e oportunidades de aprendizado. Á professora Cristina Möll Huther, pela ajuda e orientação.

Aos membros da banca, por aceitarem avaliar esse trabalho e contribuir para sua melhoria com seus conhecimentos e experiência.

Ao Programa de Pós-Graduação em Biotecnologia Vegetal, em especial ao Prof. Andrew Macrae e à Thayline Tasaka.

Ao CNPQ e à CAPES, pelo suporte financeiro.

À Universidade Federal do Rio de Janeiro e à University of Western Australia.

Aos meus pais, irmãos e todos os familiares por todo apoio e esforço despendido.

Aos amigos por todo apoio e companheirismo, especialmente Halina, Gabriela, Paula, Bruno, Mariane e Mayara.

A todos que torceram e contribuíram, direta ou indiretamente, para o sucesso deste trabalho.

O meu profundo agradecimento!

LISTA DE FIGURAS

CAPÍTULO I – INTRODUÇÃO, JUSTIFICATIVA E OBJETIVOS

CAPÍTULO 3 – ARTIGO I

LISTA DE TABELAS

CAPÍTULO 3 – ARTIGO I

CAPÍTULO 4 – ARTIGO II

SUMÁRIO

CAPÍTULO I – INTRODUÇÃO, JUSTIFICATIVA E OBJETIVOS

1. INTRODUÇÃO

1.1. Estresse Salino

O processo de salinização de solos constitui um dos principais problemas de degradação das áreas aráveis (Dias *et al*., 2016; Pedrotti *et al*., 2015) e detém alto potencial para afetar o desempenho de culturas agrícolas de maneira severa, mediante o impacto direto causado no crescimento e desenvolvimento vegetal (Deilein *et al.*, 2014; Zhao *et al*., 2020). A ocorrência de salinização é típica de regiões áridas e semiáridas, nas quais a taxa de evaporação excede a de precipitação (Dias *et al*., 2016; Pedrotti *et al*., 2015). No entanto, pode advir também de características locais, como formação geológica predominante, condições climáticas, altura do lençol freático e/ou drenagem deficiente dos solos, incluindo as ações antrópicas (Dias *et al*., 2016).

O termo salinidade se refere à presença de sais solúveis em quantidade que interfere no desenvolvimento vegetal e é caracterizado pela condutividade elétrica do solo superior a 4 dS m^{-1} (Cordeiro, 1983; EMPRAPA Solos, 2006; Pedrotti *et al.*, 2015). A ocorrência de salinidade é frequentemente associada ao conceito de sodicidade, e solos salino-sódicos apresentam excesso de sódio trocável (>15%) e condutividade elétrica do solo superior a 4 dS m^{-1} na solução do solo (EMPRAPA Solos, 2006). No mundo, estima-se que mais de um bilhão de hectares são afetados por excesso de sais e há previsão que esse número aumente com o passar dos anos (Ivushkin *et al.*, 2019). A salinização e/ou sodização de solos por uso antrópico, também denominada secundária, é ocasionada pela exploração agrícola inadequada, sobretudo relacionada ao uso incorreto de técnicas de irrigação e adubação (Munns *et al.*, 2004; Sreenivasuli *et al*., 2000).

No Brasil, a área afetada por salinidade e/ou sodicidade é de, aproximadamente, 16 milhões de hectares, representando cerca de 30% da área total cultivada (Pedrotti *et al.*, 2015). As regiões onde encontram-se solos salinos e sódicos no Brasil são concentradas no Rio Grande do Sul, Pantanal Mato-grossense e, predominantemente, na região semiárida do Nordeste (Ribeiro *et al.*, 2009). Além disso, mais de 35% das áreas irrigadas no nordeste brasileiro vêm apresentando declínio na produtividade resultante de aumento de salinidade do

solo, geralmente atribuído ao manejo deficiente e uso incorreto de técnicas de irrigação associado a utilização de água de baixa qualidade (Cavalcante, 2016).

A utilização de cloreto de sódio (NaCl) é bastante difundida para fins de compreensão dos efeitos de estresse no crescimento e nas respostas fisiológicas das plantas (Ashraf *et al.*, 2001; Kaddour *et al.*, 2009; Kim *et al.*, 2000; Siringam *et al.*, 2013). O efeito da exposição à presença de sais, em geral, torna-se mais deletério quanto maior for sua concentração no solo e a susceptibilidade de cada espécie (Tester & Davenport, 2003). Na maioria das plantas glicófitas, a taxa de crescimento começa a reduzir quando a concentração do sal atinge um limiar em torno de 40 mM de NaCl (Kataria & Verma, 2018) e ao serem submetidas a concentrações maiores que 200 mM, têm o crescimento severamente inibido ou sofrem morte prematura (Munns & Tester, 2008; Kataria & Verma, 2018). Espécies halófitas, no entanto, sobrevivem e se reproduzem em ambientes onde a concentração de sal é igual ou maior a 200 mM NaCl (Flowers & Colmer, 2008).

As respostas das plantas em ambiente salino ocorrem de duas maneiras. Através da redução do potencial hídrico, decorrente da incorporação de sais no ambiente radicular, afetando a homeostase hídrica, e por meio do acúmulo dos íons sódio (Na^+) e cloro (Cl^-), afetando a homeostase iônica (Zhao *et al.*, 2020), gerando efeitos de toxidez e desequilíbrio nutricional. A sobrevivência das plantas em ambiente salinizado depende da utilização de mecanismo de homeostases hídrica (ajuste osmótico) e iônica (exclusão e compartimentalização de íons) (Figura 1), que possuem papéis fundamentais na manutenção do crescimento e do metabolismo da planta (Deilein *et al.*, 2014; Kataria & Verma, 2018; Zhao *et al.*, 2020).

Figura 1. Resumo simplificado dos componentes do estresse salino (osmótico e iônico) aos quais as plantas são expostas quando submetidas a condições de alta salinidade e/ou sodicidade, e as respostas correspondentes necessárias para sua sobrevivência (Adaptado: Kataria & Verma, 2018).

A absorção de água pelas plantas acontece a favor do gradiente de potencial hídrico entre solo, planta e atmosfera, que é contínuo e dinâmico, uma vez que o status de energia da água na planta se encontra em constante desequilíbrio com o solo e a atmosfera (Passioura, 1982). O movimento da água ocorre do potencial menos negativo para o mais negativo, logo, o transporte de água acontece do solo para a atmosfera, passando pela planta (Cowan, 1965; Jackson *et al.*, 2000; Novák, 2012). Quando o potencial hídrico do solo é reduzido, devido ao acúmulo de sais na região radicular, a absorção de água pela planta passa a ser comprometida e a magnitude desse comprometimento será tão maior quanto maior for a concentração de sal (Cha-Um *et al.*, 2010; Deinlein *et al.*, 2014; Munns, 2002). Logo, a exposição das culturas a solos salinizados interfere nas relações hídricas entre o contínuo solo-planta, afetando adversamente o seu crescimento e a produtividade, gerando prejuízos em cultivos já estabelecidos ou inviabilizando a exploração agrícola (Munns *et al.*, 2006; Zhao *et al.*, 2020).

Algumas plantas são capazes de se ajustar osmoticamente, ao aumentar a concentração

de osmólitos, permitindo redução do potencial hídrico e manutenção do processo de absorção de água (Deinlein *et al.*, 2014). Tal redução pode ser alcançada tanto através de absorção de íons já presentes na solução do solo (Na^+, Cl^-, etc.), quanto por meio da síntese de osmólitos compatíveis com o metabolismo no citosol, através de um processo energicamente mais dispendioso (Tester & Davenport, 2003). Os solutos compatíveis provêm de natureza distinta como, por exemplo, aminoácidos (prolina), compostos amino-quaternários (glicinabetaína, β-alanina betaína), polióis (pinitol e manitol) e açúcares solúveis ou poliméricos, entre outros, e apresentam distribuição e funções específicas variáveis de acordo com a espécie (Hasegawa *et al.*, 2000; Bray *et al.*, 2000; Willadino *et al.*, 1996). Por ocasião da absorção de íons para fins de redução do potencial osmótico, a compartimentalização desses íons no vacúolo torna-se essencial para a manutenção do metabolismo celular no citosol (Bose *et al.*, 2017). A capacidade de sintetizar e acumular compostos orgânicos no citosol está diretamente relacionada à aclimatação das plantas sob estresse, fazendo frente ao baixo potencial osmótico do vacúolo nessas condições (Cha-Um & Kirdmanee, 2009; Saneoka *et al.*, 1995). Nesse caso específico, a importância é atribuída não somente à redução de potencial osmótico celular, mas também à função protetora destes compostos sobre macromoléculas, como proteínas e lipídeos, bem como do sequestro de espécies reativas de oxigênio (EROs) (Flowers & Colmer, 2015; Munns & Tester, 2008; Tester & Davenport, 2003).

A produção de EROs ocorre em condições naturais no metabolismo da planta, geralmente associada aos processos metabólicos de fotossíntese, fotorrespiração e respiração aeróbia (Chaves *et al.*, 2009). Apesar de citotóxicas e altamente reativas, quando em concentrações compatíveis com a homeostase redox celular, as EROs são componentes de diversas vias de sinalização, podendo, inclusive, aumentar a tolerância a estresses abióticos (Mitler, 2017; Sharma *et al.*, 2012). As principais EROs formadas sob condição de estresse são o oxigênio singleto ($^1O_2$), como resultado de excitação direta do oxigênio molecular; o radical superóxido ($O^{2\cdot-}$), o peróxido de hidrogênio (H_2O_2) e radical hidroxila (OH^-), por meio de sucessivas adições de elétrons (Acosta-Motos *et al.*, 2017). O H_2O_2 é moderadamente reativo, porém, ao interagir com íons metálicos ou quelatos de metais, leva a formação de radicais hidroxila (OH^-). Os radicais OH^-, assim como o $^1O_2$, possuem grande potencial oxidativo, atacando, sem discriminação, diversas moléculas biológicas, como lipídios, proteínas e ácidos nucléicos, ocasionando peroxidação, desnaturação e mutações,

respectivamente, por meio de reações de oxidação (Hasanuzzaman *et al.*, 2012; Sharma *et al.*, 2012).

Devido ao alto potencial oxidativo das EROs, moléculas de ácidos graxos insaturados, componentes estruturais dos fosfolipídios constituintes das membranas celulares, perdem um átomo de hidrogênio (Buege & Aust, 1978). O subsequente rearranjo das ligações duplas, após o ataque por oxigênio molecular, produz radicais peroxilipídicos e endoperóxidos (Figura 2) (Gutteridge & Halliwell, 1990), afetando a fluidez e seletividade de membranas, podendo ocasionar a inativação de receptores e canais iônicos e, inclusive, formação adicional de EROs (Gill & Tuteja, 2010) e perda massiva de K^+ (Shabala, 2000). Dessa forma, para detecção da ocorrência de estresse oxidativo, medidas de extravasamento de eletrólitos através da membrana (Demidchick *et al.*, 2014) e/ou quantificação da formação de produtos formados a partir da decomposição de subprodutos da peroxidação lipídica, como o malondialdeído (MDA), são amplamente utilizadas (Noctor *et al.*, 2015; Prisco *et al.*, 2016).

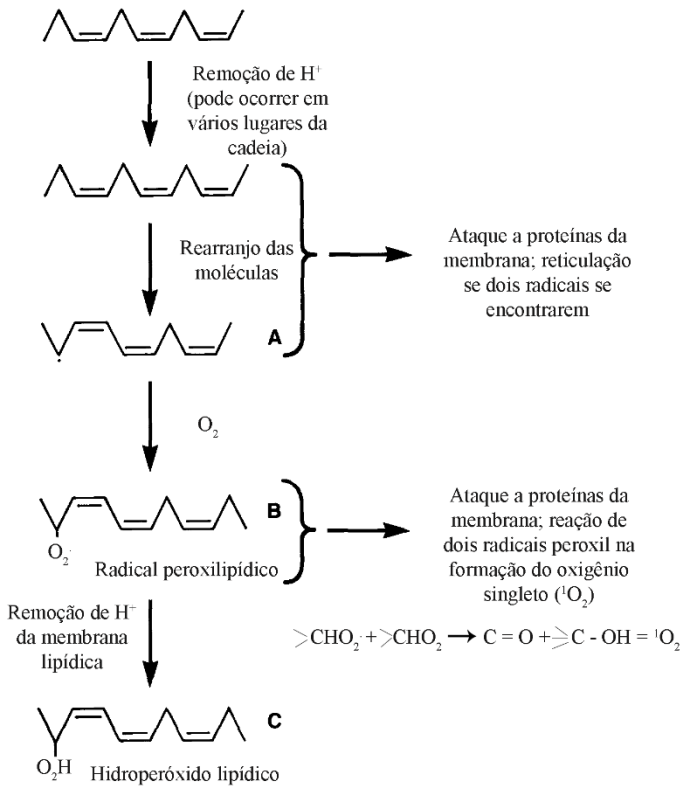

Figura 2. Mecanismo de peroxidação lipídica. Remoção de hidrogênio de um ácido graxo com três duplas ligações. (Adaptado: Gutteridge & Halliwell, 1990).

Nas células vegetais, a produção excessiva de EROs, em condições de estresse salino, está especialmente associada aos cloroplastos no processo fotossintético; aos peroxissomos, durante processo de fotorrespiração; às NADPH-oxidases da membrana plasmática e às mitocôndrias, durante a respiração celular (Gill & Tuteja, 2010; Navrot *et al.*, 2006). Decorrente do processo fotossintético, a produção de EROs é desencadeada pelo desequilíbrio entre a excitação de clorofilas do complexo antena e centros de reação por meio de fótons e a dissipação dessa energia pela fixação do carbono (Chaves *et al.*, 2009; Hasanuzzaman *et al.*, 2012).

A formação de EROs associada à cadeia de transporte de elétrons (CTE) durante o processo fotossintético é consequência de danos induzidos pela luz no fotossistema II (FSII), quando a energia armazenada na clorofila não é dissipada e, posteriormente, transferida para o O_2, ocasionando sua excitação e gerando oxigênio singleto (Figura 2) (Bhattacharjee, 2010). Esse processo ocorre, em menor escala, em condições naturais e não adversas sendo caracterizado pela inativação e reconstrução da proteína D1 do centro de reação do FSII devido à sua alta susceptibilidade a danos induzidos pela luz, e, nessas condições, a planta possui um sistema eficiente de reparação de danos (Foyer *et al.*, 2012). A produção do radical aniônico superóxido associado ao processo fotossintético durante a CTE ocorre no lado aceptor do fotossistema I (FSI). Esse processo consiste na transferência de elétrons no final da CTE para o O_2 (Figura 3) (Foyer *et al.*, 2012).

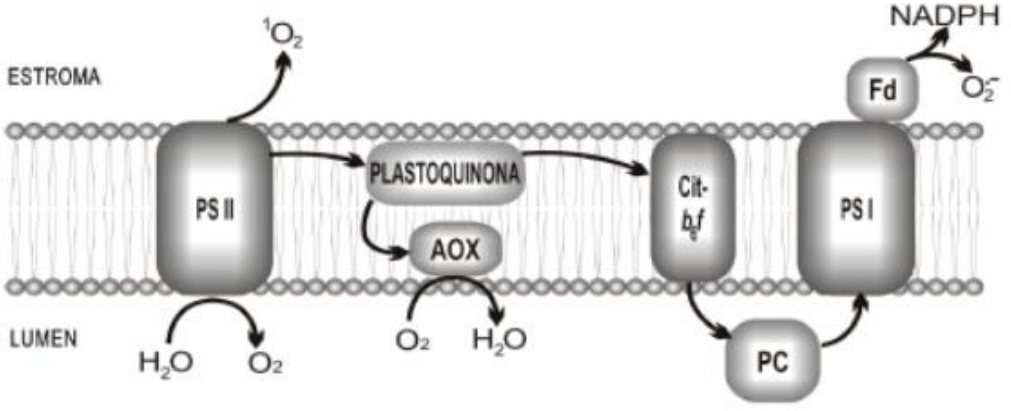

Figura 3. Formação de EROs durante a cadeia fotossintética de transporte de elétrons (Barbosa *et al.*, 2014).

A geração de EROs também pode ser ocasionada por meio de limitações estomáticas. A limitação estomática, uma das respostas iniciais da planta em situações de restrição hídrica, pode ocasionar drástica redução no conteúdo de dióxido de carbono (CO_2) na célula que, por sua vez, gera desequilíbrio na fase fotoquímica da fotossíntese (Tester & Davenport; 2003) e consequente redução na difusão de CO_2 nas células do mesofilo (Baker, 1993; Chaves *et al.*, 2009; Chaves & Oliveira, 2004). A fixação de carbono pode, ainda, ser afetada através da inibição das enzimas do ciclo de Calvin, como a ribulose-1,5-bisfosfato carboxilase oxigenase (RuBisCO) e a fosfoenolpiruvato carboxilase (PEPcase) (Chaves *et al.*, 2009; Kataria & Verma, 2018), devido a presença de altas concentrações celulares de peróxido de hidrogênio (Guan & Scandalious, 2000; Gadjev *et al.*, 2008).

A atividade de enzimas consiste em um dos principais sistemas antioxidantes da planta (Gill & Tuteja, 2010) (Figura 4). Entre elas, a superóxido dismutase (SOD) atua na primeira linha de defesa contra os danos ocasionados pelas EROs, sendo responsável pela rápida dismutação de dois radicais O^{2-} por meio da sua redução em O_2 e H_2O_2. A catalase (CAT), outra enzima chave do processo, converte H_2O_2 resultante do processo de fotorrespiração e da β-oxidação de ácidos graxos, em água e oxigênio. Adicionalmente, a enzima glutationa redutase (GR) é responsável pela catálise da redução da glutationa oxidada (GSSG), necessária para formação de ascorbato (AA) e a enzima ascorbato peroxidase (APX), que por sua vez, converte o H_2O_2 em H_2O utilizando AA como substrato. Outras peroxidases são igualmente importantes para a eliminação de EROs (Acosta-Motos *et al.*, 2017; Chen & Asada, 1989; Kataria & Verma, 2018; Sharma *et al.*, 2012).

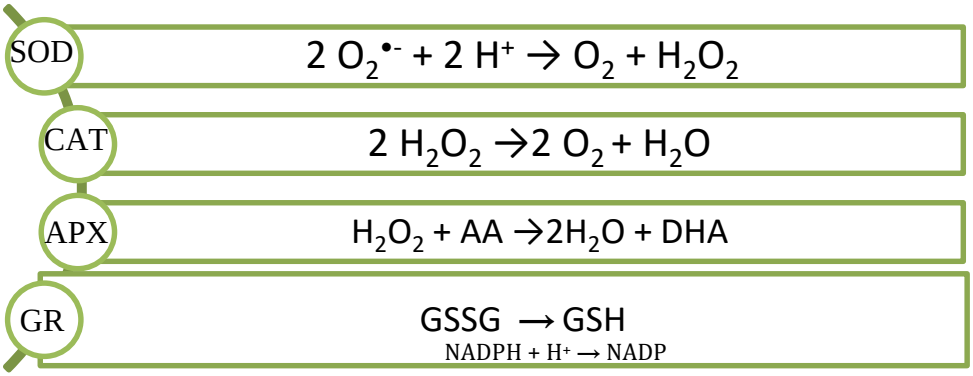

Figura 4. Reações catalisadas pelas principais enzimas antioxidantes

As plantas possuem ampla rede de defesa antioxidante para proteção contra EROs (Gill & Tuteja, 2010; Munns & Tester, 2008). No entanto, a consequência direta às plantas em situações de exposição ao estresse salino constitui o acúmulo, muitas vezes excessivo, de EROs culminando em estresse oxidativo (Silveira *et al.*, 2016). Quanto menor for a capacidade de neutralização dessas EROs através da produção de antioxidantes, enzimáticos ou não enzimáticos, maior o potencial de dano (Tester & Davenport, 2003).

Assim, quando expostas ao excesso de sais, as plantas são submetidas a diversos efeitos morfofisiológicos que culminam na redução no acúmulo de biomassa, com consequências diretas sob a produtividade das culturas agrícolas. Morfologicamente, a principal alteração nas plantas em resposta a um ambiente salinizado diz respeito a diminuição no comprimento e do acúmulo de biomassa de raízes e redução da área foliar, podendo ou não ser mais severa para raízes dependendo da concentração salina a qual a planta esteja submetida (Kataria *et al*., 2017; Kataria & Verma, 2018). Essa redução pode ser atribuída à presença de íons em níveis tóxicos e/ou desequilíbrio nutricional na planta (Deinlen *et al.*, 2014; Munns & Tester, 2008) ou como estratégia de aclimatação ao ambiente salinizado, por meio da utilização dos recursos hídricos e energéticos para sobrevivência em detrimento do crescimento (Chaves *et al.*, 2009).

O segundo componente do estresse salino diz respeito ao desequilíbrio iônico, relativo à absorção e ao acúmulo dos íons Na^+ e Cl^- até níveis tóxicos (Munns & Tester, 2008; Prisco *et al.*, 2016). Majoritariamente, o Na^+ é o principal componente na contribuição para toxidez em situação de exposição da planta a ambientes salinos, como é o caso com gramíneas (Tester & Davenport, 2003). O Cl^-, embora seja um nutriente essencial para o crescimento das plantas, é requerido em pequenas quantidades (micronutriente) e seu excesso pode ocasionar efeitos deletérios, como interferir na absorção de nitratos e no transporte de ácidos orgânicos. No entanto, a maioria das culturas anuais e perenes, entre elas cereais, milho (*Zea mays L.*) e cana-de-açúcar (*Saccharum officinarum* L.), são moderadamente tolerantes aos cloretos (Dias *et al*., 2016). A absorção contínua dos íons Na^+ e Cl^- ocasiona efeito negativo no crescimento, especialmente quando atingido o ponto onde a absorção excede a capacidade da planta de expulsar ou compartimentalizar esses íons, que podem, então, se acumular no citoplasma (Deinlein *et al.*, 2014; Munns, 2002).

A manutenção da homeostase iônica adequada no interior da célula pode ser alcançada por meio da extrusão através do sistema antiporte de H^+/Na^+ do citoplasma para o apoplasto, e/ou compartimentalização dos íons Na^+ nos vacúolos, mediado por proteínas presentes no tonoplasto, H^+ATPases e H^+-PPases (Figura 5) (Jiang *et al.*, 2010; Silveira *et al.*, 2016; Tester & Davenport, 2003; Xue *et al.*, 2004). O equilíbrio iônico pode também mantido por meio da capacidade de manter maior seletividade na absorção dos íons de K^+ em condição de presença abundante de sais na solução do solo (Kaddour *et al.*, 2009; Shabala & Pottosin, 2014), assim como a habilidade de secretar o excesso de íons tóxicos para o exterior da planta por meio de estruturas especializadas localizadas na lâmina foliar, presente em algumas espécies (Flowers & Colmer, 2008).

O mecanismo específico de seletividade e transporte de K^+ sobre Na^+ é complexo e não completamente claro, mas sabe-se que está ligado a 1) a regulação de canais catiônicos seletivos e não seletivos de alta e baixa afinidade que favorecem a absorção de K^+ pela raiz, como HTK e transportadores AKT; 2) a atividade de H^+-ATPases na membrana plasmática e no tonoplasto, inibindo a despolarização das membranas e fornecendo a força próton-motriz necessária para o transporte secundário de nutrientes, como o efluxo e regulação da absorção de Na^+; 3) sistemas de transporte que controlam o carregamento de K^+ do xilema e o transporte de K^+ de longa distância; 4) atividade de proteínas trocadoras, NHXs, catalisando o sequestro vacuolar de Na^+ em vacúolos e mediando o influxo de K^+ para o citoplasma (Assaha *et al.*, 2017; Kaddour *et al*., 2009; V'ery & Sentenac, 2003). Além disso, a formação de EROs e o aumento e retenção de Ca^{+2} no citosol em estágios iniciais do estresse estão diretamente envolvidos nas vias de sinalização e regulação do estresse, exercendo, portanto, papel essencial para a tolerância ao estresse e homeostase iônica, via regulação de canais de influxo e de minerais e partição de íons (Demidchik *et al.*, 2018; Flowers & Colmer, 2008; Garcia-Mata, 2010; V'ery & Sentenac, 2003).

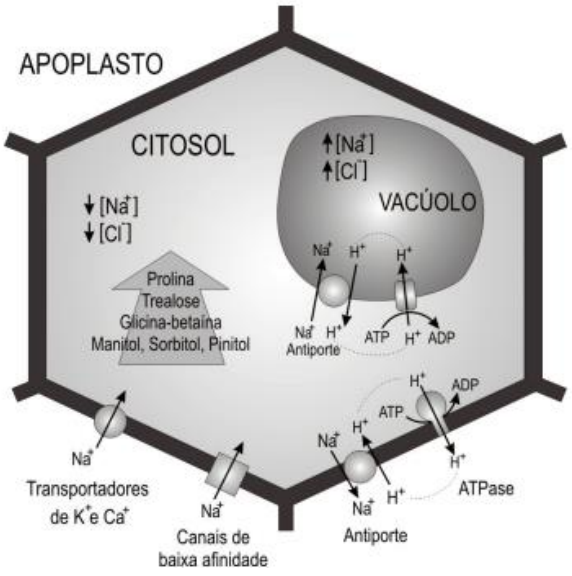

Figura 5. Canais iônicos e transportadores que determinam os mecanismos de absorção, compartimentalização e extrusão de Na^+ e ajuste osmótico, com acúmulo de solutos compatíveis no citoplasma. (Willadino & Camara, 2010; adaptado de Willadino & Camara, 2005).

A manutenção da homeostase iônica adequada pode ainda ser alcançada através da redistribuição dos íons tóxicos no interior da planta (Asshaha *et al.*, 2017; Munns & Tester, 2008). A redistribuição dos íons que causam toxidez no interior da planta pode ser alcançada por meio da alocação destes íons para determinados órgãos e tecidos da planta, como, por exemplo, para folhas mais velhas, uma vez que folhas mais jovens são metabolicamente mais ativas e possuem escassez de vacúolos para compartimentalização dos íons; e, em nível celular, por meio da alocação destes íons em células da epiderme, que são igualmente menos ativas metabolicamente, além de possuírem grande quantidade de vacúolos para armazenamento destes íons (Deinlein *et al.*, 2014; Tester & Davenport, 2003). Uma espécie particular de planta pode possuir um ou mais desses mecanismos de tolerância ou escape coordenadamente.

Espécies halófitas possuem adaptações que garantem tolerância a uma ampla gama de concentrações salinas (Flowers & Comer, 2015). Embora a fisiologia básica de mecanismos de tolerância de espécies halófitas e glicófitas seja semelhante – ajuste osmótico, síntese de solutos compatíveis no citosol e compartimentalização de íons inorgânicos no vacúolo, balanço e regulação iônica, sistema antioxidante – a eficiência na regulação de mecanismos

de tolerância de espécies halófitas para lidar com o estresse salino é superior (Munns & Tester, 2008; Flowers & Colmer, 2008; Shabala, 2013). Os mecanismos adaptativos e grau de tolerância apresentem alta variação dependendo da espécie e concentração salina, porém, de maneira geral, estão relacionados ao controle de absorção, alta e rápida capacidade de retenção e compartimentalização de íons inorgânicos e síntese de solutos orgânicos compatíveis no citosol, favorecendo a manutenção da absorção de água e pressão de turgor (Flowers & Colmer, 2008; Shabala, 2013). A presença de estruturas excretoras de sais, encontradas em cerca de 50% das espécies halófitas, também representa característica chave na capacidade dessas plantas de reduzir continuamente o excesso de Na^+ e garantir a proteção de sítios metabólicos sensíveis (Flowes & Colmer, 2008).

1.2. O potássio e a mitigação do estresse

A absorção de nutrientes em solos salinos é prejudicada, especialmente a de íons de K^+ e Ca^{2+} (Cakmak, 2005; Demidchik *et al.*, 2014; Verslues *et al.*, 2006). Devido a propriedades físico-químicas semelhantes, os íons K^+ e Na^+ competem por locais de absorção nas raízes e membrana plasmática (Cakmak, 2005; Hasanuzzaman *et al.*, 2018; Shabala & Pottosin, 2014, Siringam *et al.*, 2013). Assim, altas concentrações de íons Na^+ costumam reduzir a captação de K^+. A entrada dos íons Na^+ pode ocorrer através de canais não específicos, e/ou, através de canais específicos de alta afinidade por K^+. Os sistemas de absorção de alta afinidade (HAT) possuem alta especificidade para K^+ e são associados à sua captação em concentrações muito baixas (faixa de µm). Enquanto sistemas de absorção de K^+ de baixa afinidade (LAT) estão ligados à absorção de K^+ em concentrações maiores (faixa de mM). No entanto, a seletividade não é absoluta e canais específicos podem absorver e transportar outros íons, como o Na^+, mesmo que sob diferentes eficiências (Assaha *et al.*, 2017; Maathuis et al., 1997). O transporte de Na^+, no entanto, está principalmente ligado a canais catiônicos não seletivos (NSCC), que não discriminam entre os íons K^+ e Na^+ (Wakeel, 2013).

O status nutricional, especialmente em condições de estresse ambiental, desempenha papel fundamental sobre a capacidade de sobrevivência das plantas (Cakmak, 2005; Hasanuzzaman *et al.*, 2018; Shabala & Pottosin, 2014). Entre os nutrientes essenciais situa-se o potássio (K^+), que é requerido em grandes quantidades (macronutriente) e desempenha funções fundamentais no crescimento e metabolismo das plantas durante todo o seu ciclo de

vida, inclusive na tolerância a estresses abióticos (Cakmak, 2005; Hasanuzzaman *et al.*, 2018). Manutenção da pressão de turgor, controle de abertura e fechamento estomático, síntese de proteínas, ativação de sistemas enzimáticos e carregamento e transporte no xilema são alguns dos múltiplos papéis aos quais o potássio é relacionado (Abbasi *et al.*, 2014; Assaha *et al.*, 2017; Cakmak, 2005; Shabala & Pottosin, 2014).

Em condições fisiológicas normais, a concentração de K^+ no citosol é de ~ 100 a 200 mM e a de Na^+ ~10 a 30 mM (Tester & Davenport, 2003). No entanto, quando ocorre o aumento da concentração externa de íons Na^+, sua concentração citosólica pode chegar a 100mM, oferecendo sérios riscos a processos celulares básicos. Processos como a síntese de proteínas, que dependem da manutenção de alto conteúdo celular de K^+, e a ativação de mais de 50 enzimas, que podem ser inibidas sob altas concentrações de Na^+, são seriamente prejudicados (Bhandal & Malik, 1988; Blumwald *et al.*, 2000). Dessa forma, costuma-se relacionar a capacidade das plantas de manter os níveis de K^+ em condições de estresse salino como um importante caracterizador de espécies tolerantes, visto que a manutenção da aquisição de íons K^+ em condições de estresse salino parece balancear os efeitos tóxicos da acumulação de Na^+ (Assaha *et al.*, 2017; Cakmak, 2005; Hasanuzzaman *et al.*, 2018; Shabala & Pottosin, 2014).

Existem diversos relatos na literatura de que o aumento do suprimento de K^+ pode atuar como mitigador do estresse salino, no entanto, essa resposta é dependente da espécie, e dentro de uma mesma espécie, da variedade e do estádio de desenvolvimento da planta (Abbasi *et al.*, 2014; Ashraf *et al.*, 2001; Kaddour *et al.*, 2009; Sangakkara *et al.*, 2000). Em estudo com milho (*Zea mays* L.), a aplicação exógena de 9 mM de KCl em meio com concentração salina de 70 mM de NaCl melhorou a capacidade fotossintética, favoreceu o acúmulo de K^+ nas folhas e aumentou a atividade de enzimas antioxidantes (Abbasi *et al.*, 2014). Em arroz (*Oriza sativa* L.), a aplicação exógena foliar de aproximadamente 12 mM de KNO_3 em plantas que se encontravam sob concentração salina de 200 mM diminuiu a geração de EROs, conduziu à melhora do equilíbrio iônico, estabilização de pigmentos, redução da emissão de fluorescência de clorofila e maior taxa fotossintética, levando a uma maior taxa de crescimento (Cha-Um & Kirdmanee, 2009).

A aplicação exógena de nutrientes como ferramenta para mitigação de efeitos

relacionados ao estresse salino foi também observada em estudos com: milho (Studer *et al.*, 2017), arroz (Cha-Um & Kirdmanee, 2009; Siringam *et al.*, 2013) e *Arabidopsis* (Kaddour *et al.*, 2009). Entretanto, um estudo com milheto (*Pennisetum glaucum* (L.) R. Br.) não resultou em efeitos significativos no crescimento das plantas quando o estresse salino foi aplicado em conjunto com adubações potássicas acima do ótimo recomendado (Ashraf *et al.*, 2001). No entanto, os tratamentos com suplemento na adubação potássica, que já se encontravam sob estresse, apresentaram incremento relevante no ajustamento osmótico.

1.3. A fotossíntese nas plantas C_4

Processo que converte energia luminosa em energia química, a fotossíntese consiste no principal responsável pela entrada de energia na biosfera (Taiz & Zeiger, 2009). A fotossíntese é dividida em duas fases. A primeira consiste na etapa fotoquímica, onde a luz absorvida por meio do complexo antena promove uma série de reações envolvendo o transporte de elétrons entre complexos de proteínas causando reações de oxirredução e resultando na oxidação da H_2O, formação de $NADP^+$ reduzido e oxigênio molecular. A energia liberada durante a etapa fotoquímica resulta na formação de gradiente eletroquímico, gerando ATP (Chaves *et al.*, 2009; Heldt, 2005). Na fase bioquímica (Ciclo de Calvin-Benson), ATP e poder redutor gerados na fase fotoquímica são utilizados para formação de trioses-fosfato e assimilação de CO_2 atmosférico (Sage, 2004). O processo fotossintético de assimilação de carbono é subdividido em 3 subgrupos principais: C_3, C_4 e CAM (Taiz & Zeiger, 2009).

As plantas que apresentam metabolismo fotossintético C_4 correspondem a aproximadamente 1% de todas as espécies conhecidas (Taiz & Zeiger, 2009) e possuem mecanismo de concentração de carbono antes do ciclo de Calvin-Benson, com modificações bioquímicas, anatômicas e ultraestruturais quando comparadas à via fotossintética C_3 (Sage *et al.*, 2014). Os cloroplastos nas folhas de espécies com metabolismo C_4 podem ser encontrados em dois tipos de células, as células do mesofilo e da bainha perivascular, formando uma alteração estrutural em torno dos feixes vasculares conhecida como anatomia de Kranz (Edwards *et al.*, 2001). A anatomia Kranz, no entanto, não constitui estrutura essencial para a fotossíntese C_4. O mecanismo fotossintético dessas plantas consiste primariamente na hidratação da molécula de CO_2 atmosférico pela enzima anidrase carbônica e posterior

difusão do HCO_3^- para as células do mesofilo. Pela ação da enzima fosfoenolpiruvato carboxilase (PEPcase), compartimentalizada nas células mesofilo, o HCO_3^- é incorporado ao fosfoenol piruvato produzindo ácido oxalacético (AOA) (Ghannoum, 2009). O oxaloacetato é convertido a um ácido de 4 carbonos (malato ou aspartato) que será difundido para as células da bainha vascular onde será descarboxilado, liberando CO_2 (Edwars *et al.*, 2001). A enzima ribulose-1,5-bifosfato carboxilase-oxigenasse (RuBisCO), por sua vez, se concentra nas células da bainha vascular. Assim, as moléculas de CO_2 serão incorporadas ao ciclo de Calvin-Benson, enquanto que a molécula de piruvato, ao chegar aos cloroplastos das células do mesofilo, será fosforilada dando origem a uma molécula de PEP, proporcionando a regeneração do ciclo (Drincovich *et al.*, 2011; Hatch, 1988). Esse mecanismo resulta em alta eficiência no uso da água e redução da função oxigenasse da enzima RuBisCO, pela alta concentração de CO_2, em condições de alta temperatura, luminosidade e condições de estresse (Ghannoum, 2009).

As plantas de metabolismo C_4 são divididas em três subgrupos 1) enzima málica NADP dependente (NADP-ME); 2) enzima málica NAD dependentes (NAD-ME); e 3) fosfoenol piruvato carboxiquinase (PCK), de acordo com a enzima que catalisa o processo de descarboxilação e o ácido transportado entre as células do mesofilo e bainha. Em plantas do subtipo NADP-ME o oxaloacetato é convertido a malato pela NAD-malato desidrogenase. O malato é transportado para as células da bainha onde será descarboxilado, dando origem a moléculas de CO_2 e piruvato (Buchanan, 2000). Plantas pertencentes ao subtipo NAD-ME a enzima málica é dependente de NADH e são transportados aspartato/alanina. No terceiro grupo, PCK, a etapa de descarboxilação é realizada pela enzima fosfoenol piruvato carboxiquinase e são transportados aspartato/alanina, PEP ou piruvato (Ghannoum, 2009).

1.4. Fotossíntese, potássio e o estresse salino em glicófitas e halófitas

A limitação hídrica assim como a absorção e não compartimentalização de íons inorgânicos até níveis tóxicos pode gerar impactos diretos no processo fotossintético. Seja por meio de limitações estomáticas e/ou distúrbio do equilíbrio iônico nos cloroplastos (Chaves *et al.*, 2009; Bose *et al.*, 2014). Nesse contexto, retenção de K^+ e manutenção do equilíbrio iônico em condições de salinidade é fundamental (Pottosin & Shabala, 2016). A alteração da homeostase iônica do cloroplasto em espécies glicófitas foi relacionada com a inativação das

principais enzimas fotossintéticas, como a RuBisCo e outras enzimas do estroma como a frutose-1,6-bisfosfatase, a dissociação de proteínas fotossintéticas intrínsecas e extrínsecas que suportam as atividades FSII e FSI, redução da formação de grana, prejudicando a atividade do PSII, e a degradação de pigmentos (Bose *et al.*, 2017; Chaves *et al*., 2009; Gosh *et al*., 2001; Pan *et al.*, 2020; Rahman *et al.*, 2000).

Além disso, o papel do K^+ para manutenção do potencial de membrana e regulação de pH nos cloroplastos parece ser crucial para transdução de energia e fixação do CO_2 atmosférico. O efluxo de Cl^- do estroma ao lúmen concomitante ao influxo de K^+ do lúmen para o estroma são importantes balanceadores para manutenção do potencial de membrana e regulação de pH (Pottosin & Shabala, 2016). Dessa forma, em espécies glicófitas, com a alteração e desequilíbrio dos níveis de K^+ nos cloroplastos, causada pela exposição ao excesso de sal, espera-se que tanto o potencial de membrana quanto o pH nos cloroplastos sejam afetados, gerando distúrbios nos processos de transdução de energia e fixação de CO_2 (Robinson & Downton, 1984).

Espécies halófitas, embora capazes de acumular e requerer Na^+ em seu cloroplasto (cerca de 20 vezes mais alta quando comparadas com glicófitas), possuem mecanismo para evitar que as concentrações de Na^+ nos cloroplastos excedam determinado limite, exibindo concentrações de sal no tecido foliar cerca de quatro vezes mais altas do que nos cloroplastos (Flowers *et al.*, 2015). A deficiência de Na^+ nessas espécies, ainda que acompanhada de nutrição potássica adequada, gerou efeitos deletérios como clorose, redução da atividade do FSII e alteração ultraestrutural em células do mesofilo (Grof *et al.*, 1989; Brownell & Wood, 1957; Müller *et al.*, 2014). A essencialidade de Na^+ nessas espécies, por outro lado, não exclui a essencialidade do K^+, uma vez que o K^+ não pode ser substituído pelo Na^+ em uma série de processos essenciais para manutenção da fotossíntese, como a síntese de clorofila e da enzima RuBisCo (Hanikenne *et al.*, 2014).

O Na^+ é descrito como nutriente essencial, estimulando o crescimento e capacidade fotossintética de espécies halófitas de metabolismo fotossintético C_4, como *Panicum coloratum* L. (Matoh & Murata, 1990), *P. miliaceum* L. (Ohnishi, 1990) e *P. antidotale* Retz. (Hussain *et al*., 2020). O papel essencial do sódio parece estar ligado a especificidades das vias fotossintéticas C_4 dos subgrupos NAD-ME e PCK, através do sistema de co-transporte

Na^+/piruvato (Aoki & Kanai, 1997) necessário para a regeneração de fosfoenolpiruvato e fixação de CO_2 atmosférico (Ohnishi, 1990).

Além disso, a inibição de enzimas fotossintéticas parece ocorrer em menor extensão em espécies halófitas quando comparadas a espécies glicófitas (Gosh *et al.*, 2001). Adicionalmente, síntese de osmólitos compatíveis no cloroplasto, mais expressiva em espécies halófitas (Bose *et al.*, 2014), resultou na não-inibição dessas enzimas em ensaios *in-vitro* com halófitas expostas a altos níveis de NaCl (500 e 400 mM) (Chatterjee *et al.*, 2013; Incharoensadki, 1986).

É importante salientar, entretanto, que embora altamente adaptadas a ambientes com salinidade maior ou igual a 200 mM de NaCl, o requerimento de Na^+ nas espécies halófitas, que demandam essencialmente o nutriente para atividades específicas no metabolismo celular, ocorre na faixa de micronutriente (Brownell & Wood, 1957; Cheeseman, 2015). A grande maioria das espécies halófitas é capaz de viver e se reproduzir em condições não-salinas e seu crescimento em condições de estresse severo pode resultar em alta demanda energética com redução no crescimento (Flowers & Colmer, 2015; Shabala, 2013).

1.5. *Setaria viridis* como plataforma de estudo para estresses abióticos

O estudo de culturas de importância econômica, nas mais diversas condições ambientais, contribui para o entendimento dos mecanismos e processos que regulam as respostas das plantas frente a condições não ideais, o que pode ser essencial para manutenção da produtividade destas culturas. No entanto, a maioria das culturas de interesse comercial, como, milho, miscanthus e cana-de-açúcar, possui características como grande porte, genoma complexo e longo ciclo de vida que limitam seu estudo em laboratório, tornando-o laborioso e extenso (Brutnell *et al.*, 2010; Wang *et al.*, 2013).

Nesse contexto a utilização de organismos modelo que possuem características fundamentais na aceleração dos estudos e, ao mesmo tempo, mecanismos genéticos comuns a um grande grupo de organismos relacionados, assume amplo protagonismo (Brutnell *et al.*, 2010; Layton & Kellog, 2014; Verslues *et al.*, 2006). Há algumas décadas *A. thaliana,* uma eudicotiledônea, foi consolidada como principal organismo modelo na biologia vegetal para plantas com metabolismo fotossintético C_3 (Delatorre & Silva, 2008). No entanto, a extensa

utilização e grande impacto econômico, agronômico e ecológico de culturas monocotiledôneas da família Poaceae, bem como a necessidade de compreensão dos processos e mecanismos genéticos regulatórios relacionados ao metabolismo fotossintético C_4, gerou a necessidade de estabelecimento de um novo modelo genômico vegetal (Brutnell *et al.*, 2010; Petti *et al.*, 2013).

Setaria viridis (L.) Beauv. é uma Poaceae anual pertencente à subfamília Panicoideae com metabolismo fotossintético C_4, tipo NADP-ME clássico (Aliscioni *et al.*, 2016; Junqueira *et al.*, 2018). Com centro de origem na Eurásia, *S. viridis* possui inflorescência bissexual e sementes de genoma diploide (2n=18) (Dekker, 2003; Layton & Kellog, 2014). O grande potencial da espécie como modelo genético se justifica por características como: pequeno porte (10-15 cm), ciclo de vida curto (6 a 9 semanas), genoma relativamente pequeno (~ 510 Mb), morfologia semelhante à maioria das espécies da família Poaceae tais como milho, cana-de-açúcar, sorgo sacarino (*Sorghum bicolor* (L.) Moench) e capim elefante (*Pennisetum purpureum* Schum.), além de possuir requisitos de crescimento simples e um sistema de transformação estabelecido (Brutnell *et al.*, 2010; Doust *et al.*, 2009). A variedade de ambientes nos quais espécies do gênero *Setaria* podem ser encontradas indica que seu germoplasma pode constituir importante fonte de variação na expressão de genes de resposta a estresses abióticos (Diao, 2005) e *Setaria viridis* foi relatada como um excelente modelo para estudos em condições de salinidade (Doust *et al*., 2019).

Ao ser submetida à restrição hídrica, *S. viridis* apresenta mecanismos adaptativos e alta resistência ao estresse (Saha *et al.*, 2016). Após ciclos de reidratação, *S. viridis* possui grande capacidade de recuperação do estresse hidríco, fazendo de forma eficiente ajustes fisiológicos e bioquímicos (Luo *et al.*, 2011). Além disso, também mantém o crescimento e exibe a recuperação dos parâmetros fotossintéticos ao longo do tempo sob déficits osmótico prolongado (Valença *et al.*, 2020). A redução no crescimento decorrente de exposição a restrição hídrica de *S. viridis* foi associada igualmente a fatores estomáticos e não estomáticos, conforme mostrado por diminuições no rendimento quântico do FSII e parâmetros de trocas gasosas sob restrições hídricas de intensidades leve e severa (Burbulis *et al.*, 2017).

Da mesma forma, a exposição de *S. viridis* à ambiente salino desencadeou alta

capacidade de produção e acúmulo de aminoácidos totais, concomitante ao aumento nas concentrações de NaCl, especialmente na maior concentração de NaCl testada (100mM) (Kim *et al.*, 2000), indicando a capacidade da espécie de manter a absorção de água em tais condições. Em outros estudos com *S. viridis* em condições de estresse salino, foi observado que o aumento da concentração de 20 a 200 mM de uma mistura de 9:1 NaCl:Na_2SO_4 resultou em aumento de cerca de 10% no nível de sódio presente nas folhas com a aplicação de 200mM de NaCl:Na_2SO_4 e redução de aproximadamente 20% no conteúdo de potássio. No entanto, impactos na atividade do FSII só foram observados quando a concentração de NaCl foi igual ou superior a 120 mM de NaCl (Guo *et al.*, 2011), enquanto a fotossíntese líquida sofreu reduções de aproximadamente 30% 96h após a exposição a 100 mM de NaCl (Duarte *et al.*, 2019).

1.6. Rhodes Grass (*Chloris gayana*)

Rhodes grass (*Chloris gayana* Kunth) é uma Poaceae anual pertencente à subfamília Chloridoideae com metabolismo fotossintético C_4 tipo PCK (fosfoenolpiruvato carboxiquinase) (Omoto *et al.*, 2010). Originária da África, apresenta dois níveis de ploidia – diploide e tetraploide (Loch *et al.*, 2004; Ponsens *et al.*, 2010). É comumente utilizada como pastagem em áreas tropicais e subtropicais (Smith, 1974; Suttie, 2000). Mais de 50 espécies são relatadas dentro do gênero Chloris (Phillips, 1995), no entanto, apenas *C. gayana* possui relevância econômica (Bogdan, 1977). Morfológica e agronomicamente *C. gayana* é comumente descrita como uma espécie extremamente variável (Bogdan, 1977). A presença de glândulas de sal nas duas faces da lâmina foliar é o mecanismo de tolerância mais estudado da espécie, relatado como capaz de excluir quase o dobro da quantidade de sódio presente em suas folhas mesmo sob altos níveis de salinidade (Oi *et al.*, 2012).

A avaliação da correspondência da taxa de crescimento com o conteúdo de sódio e potássio indica que *C. gayana* pode ter a capacidade de usar outros cátions, como o sódio, no lugar do potássio para algumas funções fisiológicas e metabólicas (Smith, 1974). Em *C. gayana* cv. Pioneer, a quantidade de potássio para atingir o crescimento máximo foi progressivamente reduzida à medida que o nível de sódio aumentava de 0 a 400 mg por pote, uma vez que a concentração de potássio estava acima de valor crítico (0,5% da matéria seca) necessário para a realização de atividades específicas do íon (Smith, 1974). Além disso, o Na^+ também é descrito como um nutriente essencial no cloroplasto de algumas espécies C_4 dos

subgrupos da enzima NAD-málica e PCK (Ohnishi, 1990). O papel essencial do sódio nessas espécies parece estar ligado às especificidades das vias fotossintéticas dessas espécies, por meio de sistema de co-transporte Na^+/piruvato (Aoki e Kanai, 1997), necessárias para a regeneração de fosfoenolpiruvato e fixação de CO_2 atmosférico (Ohnishi, 1990).

A sobrevivência de *C. gayana* em uma ampla gama de solos, incluindo os salinos com condutividades maiores do que 10 dS m^{-1} (Cook *et al.*, 2005), assim como sua capacidade de resistir a longos períodos de seca (mais de 6 meses) (Cook *et al.*, 2005), apontam *C. gayana* como cultura auspiciosa em solos de baixa qualidade além de fundamental em programas de conservação considerando a dessalinização do solo. A tolerância ao sal pode ser aumentada explorando a variação dentro das culturas existentes ou por meio do estudo de estratégias de mitigação em plantas halófitas e/ou altamente tolerantes, que podem ser usadas como ferramenta para o desenvolvimentos e seleção de novas culturas (Colmer *et al.*, 2005; Munns *et al.*, 2006; Shabala, 2013).

2. JUSTIFICATIVA

Face à grande extensão de áreas agrícolas degradadas por salinização e/ou sodização e ao contínuo crescimento dessas áreas, há uma grande preocupação em relação aos impactos negativos no setor agrícola, caracterizado pela diminuição dos níveis de produtividade, além das limitações geográficas impostas às culturas. Com isso, tornam-se necessários estudos voltados para elucidação e análise de respostas que levam à tolerância de plantas submetidas a ambientes salinizados e/ou sódicos. Por possuir relação evolutiva com culturas de importância econômica, o estudo da resposta de *S. viridis* frente a condições de salinidade e o possível papel do K^+, como mitigador do estresse pode fornecer alternativas para a expansão e manutenção da agricultura em áreas salinizadas, reduzindo o abandono de áreas agrícolas. Como segunda parte deste estudo, a avaliação da associação entre as relações iônicas e fotossíntese e seus impactos no crescimento da espécie C_4 Rodes Grass (*Chloris gayana*), anteriormente relatada como altamente tolerante a ambientes salinos, pode auxiliar na compreensão de questões importantes relacionadas aos mecanismos de tolerância ao sal da espécie. A seletividade K^+/Na^+ e as estratégias para tolerar ambientes salinos, por outro lado, podem contribuir para a elucidação dos papéis fisiológicos e metabólicos do potássio em *C. gayana*, e a influência e essencialidade do sódio no metabolismo dessas plantas. No futuro,

esses resultados podem ajudar a desenvolver ferramentas importantes para a tolerância ao sal em espécies não halófitas.

3. OBJETIVO

Estabelecer as principais respostas fisiológicas à exposição ao sódio e investigar o potencial mitigador do potássio na espécie modelo *Setaria viridis* e na gramínea altamente tolerante ao sal, *C. gayana.*

CAPÍTULO 2 – MATERIAL E MÉTODOS

1. MATERIAL E MÉTODOS - ARTIGO I

a. Germinação e condições de crescimento

Os experimentos foram realizados com o acesso *Setaria viridis* A10.1 em hidroponia. Durante todo o período experimental, as plantas foram mantidas em câmara de crescimento no Fitotron® do Laboratório de Genética Molecular Vegetal (LGMV) sob temperatura média de 30 ± 2ºC (dia) e 25 ± 2ºC (noite), fotoperíodo de 16/8 h (claro / escuro) e intensidade de luz de 750 $\mu mol.m^{-2}$ s^{-1}. Uma combinação de lâmpadas LED azuis-vermelhas-brancas forneceu essa intensidade de luz. Para germinação, foram utilizados berçários montados artesanalmente com material de baixo custo desenvolvido pelo grupo de pesquisa do Laboratório de Fisiologia Vegetal (LFV) da UFRJ. Foram utilizados potes de sorvete com tampas furadas com serra copo, formando orifícios para encaixe de gargalos cortados de garrafas pet (Figura 6).

Figura 6. Berçário utilizado para germinação das sementes.

Para o suporte da semente, foi colocado um pequeno pedaço de tecido do tipo tule, preso com elástico e preenchido com areia até o topo (Figuras 7A e 7B). Para esterilização, a areia foi lavada com solução de hipoclorito de sódio 0,1% e posteriormente enxaguada exaustivamente com água deionizada. Após a lavagem, a areia foi seca em estufa a 60ºC por 48 horas.

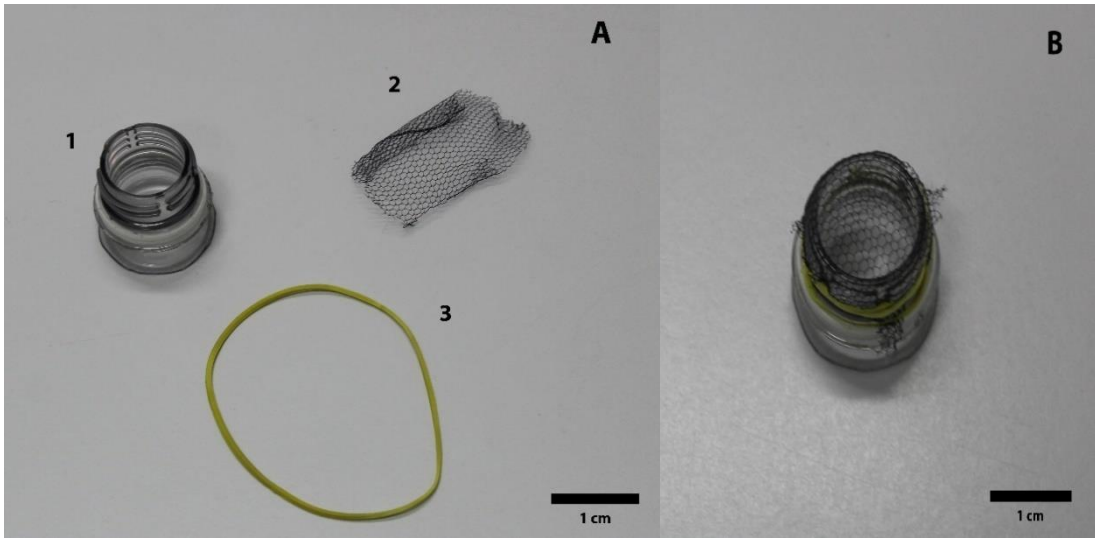

Figura 7. Material para construção do suporte utilizado para germinação das sementes. Aparato desmontado. 1- Gargalo de garrafa pet; 2- tecido do tipo tule; 3 – elástico (A) e aparato montado (B).

Sementes do acesso A10.1 de *S. viridis* foram cedidas pelo LGMV. As sementes foram colocadas diretamente na areia e o pote preenchido com água deionizada, sendo reabastecido quando necessário, até o estádio fenológico 1.1 de acordo com a escala BBCH, quando a primeira folha se encontrava totalmente expandida (Junqueira *et al.*, 2019). Foram colocadas três sementes por gargalo e, no caso de germinação de mais de uma semente, foi realizado o desbaste deixando uma plântula por gargalo. A utilização dos berçários dispensa a fase de transplante das plântulas, pois o gargalo da garrafa é transferido para o copo individual e encaixado na tampa dos copos individuais. Deste modo, o processo de transplante é facilitado, reduzindo o estresse decorrente do transplantio na fase inicial de estabelecimento da planta.

Após atingir o estádio 1.1, as plântulas foram transferidas para sistemas hidropônicos individuais sem aereação. O sistema hidropônico consistia em vasos de 0,2 L contendo solução nutritiva Hoagland a um quarto da força total (Hoagland & Arno, 1938; Caisson labs, nº 2), substituída a cada cinco dias.

A segunda etapa do cultivo das plantas também foi realizada em sistema montado artesanalmente com material de baixo custo, desenvolvido pelo grupo de pesquisa do LFV. O sistema consiste de um copo de acrílico transparente (0,2 L) dentro de um copo preto de plástico coberto com papel alumínio com tampa, a fim de evitar a passagem de luz e o aquecimento da solução nutritiva (Figura 8). O copo transparente é utilizado como reservatório de solução nutritiva. A tampa do copo é furada com a serra copo possibilitando, assim, a transferência do gargalo da garrafa pet do berçário para o copo. A grande vantagem da utilização do copo transparente é a possibilidade da observação e acompanhamento das raízes da planta sem que seja necessário retirá-la da solução, além de facilitar fotografá-las.

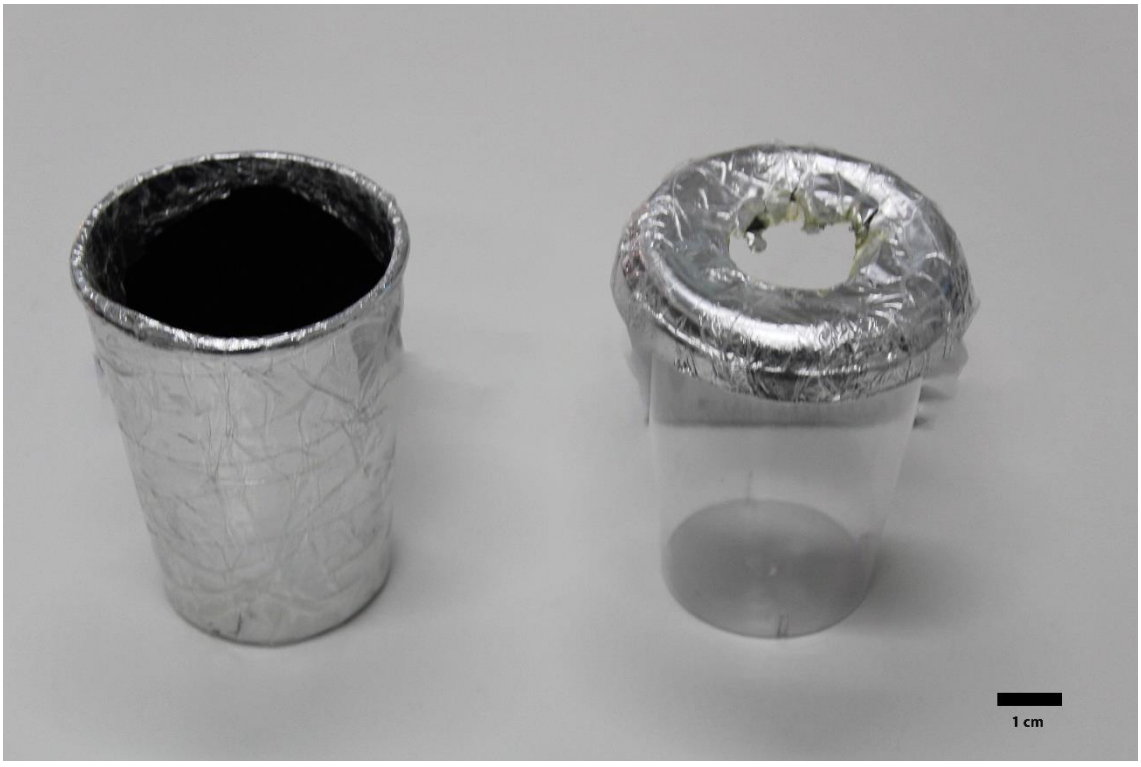

Figura 8. Copos utilizados para montagem do sistema hidropônico individual

Os tratamentos foram aplicados 15 dias após a germinação, quando a quinta folha se encontrava completamente expandida, estágio fenológico 1.5 de acordo com a escala BBCH (Junqueira *et al.*, 2019). Foi utilizado um esquema fatorial 3x3 com três níveis onde o fator A foi o tratamento com cloreto de sódio (NaCl; 0, 150 e 250 mM) e o fator B a aplicação de cloreto de potássio (KCl; 0, 5 e 9 mM) com 15 repetições, totalizando 135 unidades experimentais. Devido a observações anteriores, onde as panículas começaram a emergir 120 h após a imposição do tratamento, e observação previamente feita por Duarte *et al*. (2019) as plantas foram colhidas 96 h após a imposição do tratamento salino. Além disso, períodos de exposição mais longos provaram ser suficientes para ocasionar a morte das plantas de *S. viridis* expostas a níveis de NaCl maiores ou iguais a 250 mM, sem causar alterações significativas em níveis de NaCl menores ou iguais a 200 mM de NaCl (experimento piloto, dados não publicados).

b. Análises para coleta de dados.

b.1 Teores de K^+ e Na^+

Os conteúdos de K^+ e Na^+ foram aferidos conforme metodologia descrita em Munns *et al.* (2010) utilizando fotômetro de chama (Analyzer modelo 910 M, Comércio e Indústria Ltda, São Paulo, Brasil). Para extração, o material vegetal foi coletado, acondicionado em sacos de papel e alocado em estufa de circulação forçada à 60ºC por dois dias. A seguir, esse material foi triturado e 10 mg de tecido transferido para tubos plásticos de 10mL para realização de digestão com ácido nítrico 0,5 M. O material foi mantido em shaker no escuro por dois dias. Foi realizado ajuste nos dados mensurados a partir de curvas padrão para ambos os íons.

b.2 Fluorescência da clorofila a

As medições dos transientes de fluorescência da clorofila *a* foram realizadas com *Portable Chlorophyll Fluorimeter* (HandyPEA, Hansatech, King's Lynn, Norkfolk, UK). As leituras foram feitas em folhas totalmente expandidas do último nó desenvolvido pela manhã (das 10 às 11 da manhã) após adaptação ao escuro por pelo menos 20 min. As medições foram feitas em dez plantas para cada tratamento. A emissão de fluorescência foi induzida expondo a folha a um pulso de luz saturante (650 nm) a uma intensidade de 3.000 μmol fótons m^{-2} s^{-1}.

Os transientes de fluorescência OJIP são baseados no aumento rápido da fluorescência polifásica da intensidade mais baixa (F_O) para a mais alta (F_M) (Strasser *et al.*, 2004). O passo O é o nível de fluorescência inicial, F_O (50 μs), seguido pelos níveis intermediários J (2 ms) e I (30 ms), e o nível de pico P (500 ms), F_M. Transientes OJIP foram avaliados usando normalizações e subtrações para comparar os eventos refletidos nas etapas OJ, OI e IP. Os transientes foram normalizados como fluorescência variável relativa: $W_t = (F_t - F_0) / (F_J - F_0)$, $W_{OI} = (F_t - F_0) / (F_I - F_0)$ e $W_{IP} = (F_t - F_I) / (F_P - F_I)$. A diferença entre a cinética dos dados de fluorescência variável relativa foi calculada ($\Delta_W = W_{tratamento} - W_{controle}$), revelando bandas ocultas entre as etapas WOJ (banda K; 300 μs) e WOK (banda L; 150 μs) conforme descrito detalhadamente em Yusuf *et al.* (2010). Os parâmetros do teste JIP foram calculados usando o software Biolyzer (Bioenergetics Laboratory, University of Geneva, Switzerland) e as equações propostas por Strasser *et al.* (1995), Strasser *et al.* (2004), e Santos Júnior *et al.*

(2015).

b.3 Análises biométricas

O comprimento da parte aérea e raízes foi mensurado com auxílio de um paquímetro digital (Maxwell 150mm Digital Caliper, China). A determinação do peso fresco (biomassa) da raiz e parte aérea ocorreu imediatamente após a coleta com auxílio de balança analítica (Bioprecisa JA3003N, Curitiba, PR, Brazil). Para obtenção do peso seco, o material vegetal coletado foi acondicionado em sacos de papel e levado à estufa de circulação forçada (Olidef Medical CZ, SP, Brazil) a 70ºC, pelo período necessário à completa evaporação da água (peso constante). Posteriormente, o peso seco foi novamente aferido em balança analítica (Bioprecisa JA3003N, Curitiba, PR, Brazil) para a determinação da biomassa seca. O número de folhas do colmo principal foi obtido por meio de contagem manual das folhas.

b.4 Extravasamento de eletrólitos

O extravasamento de eletrólitos foi analisado segundo protocolo adaptado descrito por Liu *et al.* (2015), com a utilização de medidor de condutividade (modelo 3540, Jenway, Staffordshire, Reino Unido). Inicialmente, 200 mg de tecido foliar foi coletado e colocado em tubos do tipo Falcon contendo 20 mL de água deionizada. Após 24 h em shaker, foi medida a condutividade elétrica da solução (C1). As amostras foram, então, autoclavadas a 120°C por 30 min e quando os tubos atingiram novamente a temperatura ambiente, foi medida a condutividade da solução com o tecido morto (C2). O extravasamento eletrolítico foi calculado de acordo com a fórmula: $EL(\%) = \left(\frac{C1}{C2}\right) x100$.

b.5 Enzimas antioxidantes

O material vegetal de folhas (200 mg) foi coletado e armazenado imediatamente a -80 ºC para posterior análise. O extrato foi obtido por meio da maceração do material vegetal em nitrogênio líquido e a homogeneização com tampão de extração (fosfato de potássio 200 mM, pH 7,8; EDTA 0,1 mM; ácido ascórbico 20 mM; ditiotreitol 5 mM, β-mercaptoetanol 5 mM, Triton X-100 0,01% e água) completando volume final de 1500 µL. A mistura foi centrifugada por 20 min a 4ºC (Eppendorf 5424, Hauppauge, NY, EUA). O sobrenadante foi usado como extrato bruto de enzimas. A atividade das enzimas e a quantificação de proteína

foram determinadas em espectrofotômetro Thermo Scientific Multiskan GO (ThermoFisher Scientific, Vartaa, Finlândia).

- *Superóxido dismutase (EC 1.15.1.1)*

O protocolo de análise da enzima da superóxido dismutase (SOD; EC 1.15.1.1) foi adaptado ao descrito em Giannopolitis & Ries (1977). A mistura da reação consistiu de solução contendo 20 µL do material extraído no tópico *b.5*. A atividade da enzima foi avaliada monitorando a inibição da coloração de nitro azul-tetrazólio (NBT) a 560 nm após exposição à luz por cinco minutos.

- *Ascorbato peroxidase (EC 1.11.1.11)*

O protocolo adaptado de análise da enzima ascorbato peroxidase (APX; EC 1.11.1.11) foi realizado de acordo com metodologia descrita em Nakano & Asada (1981) em espectrofotômetro, com leituras a 290 nm. A mistura da reação consistiu de solução contendo 20 µL do material extraído no tópico *b.5*. A atividade da enzima foi avaliada pelo consumo de H_2O_2 medindo a diminuição da absorbância. As leituras foram realizadas de 10 em 10 segundos durante 2 min.

- *Catalase (EC 1.11.1.6)*

A mistura da reação para avaliação da atividade da enzima catalase (CAT; EC 1.11.1.6) consistiu de solução contendo 20 µL do material foliar extraído conforme descrição no tópico *b.5*. A análise da atividade da enzima seguiu protocolo semelhante ao da enzima ascorbato peroxidase, com avaliação de atividade pelo consumo de H_2O_2 e redução da absorbância. As leituras foram realizadas em espectrofotômetro a 240 nm de 10 em 10 segundos durante 2 min.

- *Glutationa redutase (EC 1.6.4.2)*

A atividade da glutationa redutase (GR; EC 1.6.4.2) foi medida como a oxidação do NADPH pela diminuição da absorbância a 340 nm por meio de leituras sucessivas por dois minutos (Foyer & Halliwell, 1976). A mistura da reação consistiu de solução contendo 20 µL do material extraído no tópico *b.5*.

- *Quantificação de proteína*

A quantificação de proteína em cada ensaio enzimático, para expressão da atividade específica (atividade por mg de proteína), utilizou albumina de soro bovino (BSA) como padrão. As amostras foram lidas a 595 nm a cinco minutos após a reação com a solução de Bradford.

b.6 Análises micromorfológicas

Para análise micromorfológica, as amostras foram coletadas em triplicata de seções transversais do terço médio de lâminas de folhas totalmente expandidas dos últimos nós desenvolvidos. Para a fixação, os fragmentos foliares foram imediatamente imersos em solução de Karnovsky (4% paraformaldeído, 2,5% glutaraldeído, 0,1 M tampão cacodilato de sódio) e colocados sob vácuo por duas horas. Os fragmentos foram lavados em solução tampão de cacodilato de sódio 0,1 M, pós-fixados em 1% de tetróxido de ósmio durante 2 h e, posteriormente, lavados três vezes com tampão cacodilato de sódio 0,1 M. A seguir, os fragmentos foram desidratados em séries etanólicas crescentes (15%, 30%, 50%, 70%, 90% e 100%) com intervalos de aproximadamente 30 minutos entre as trocas.

Para observações de microscopia óptica, os fragmentos foram incorporados em resina Spurr (Spurr, 1969) e polimerizados a 70°C por 12 h. Os blocos foram cortados em cortes transversais finos (1 µm) utilizando ultramicrótomo PowerTome-PC (RMC Products, Tucson, AZ, EUA), corados com azul de toluidina 0,5% e examinados usando microscópio óptico de campo claro (Leica DM 500-Wetzla, Alemanha).

Para análise micromorfológica de microscopia eletrônica de varredura (MEV) após a etapa de desidratação, os fragmentos foram secos até o ponto crítico (BAL-TEC, CPD-030, Principado de Liechtenstein) e alocados em tocos de pinos com fita de carbono, revestidos por pulverização catódica com ouro (Desk V Sample Preparation, Denton Vacuum), digitalizados e fotografados usando microscópio eletrônico de varredura a 20 kV (Vega 3LMU Tescan, Brno, República Tcheca).

b.7 Análise de dados

Os dados foram analisados por meio do software Sisvar (Universidade Federal de Lavras, Lavras, Brasil). Após a verificação da homogeneidade das variâncias pelo teste de

homogeneidade de Cochran, os resultados foram submetidos à análise de variância bifatorial (fatores: 'NaCl' e 'KCl'). Na presença de diferença significativa, o teste de Scott-Knott foi utilizado para determinar a significância para $p \leq 0,05$. A Análise de Componentes Principais (PCA) foi realizada para investigar agrupamentos de variáveis com o auxílio do software PAST 3 (PAleontological STatistics).

2. MATERIAL E MÉTODOS - ARTIGO II

a. Germinação e condições de crescimento

O experimento foi conduzido entre os meses de outubro e dezembro sob luz solar natural e temperatura média de 30ºC (dia) e 25ºC (noite) em uma casa de vegetação localizada na *University of Western Australia* (UWA), Perth WA, Austrália (31º57 'S, 115º47' E). Sementes de duas cultivares de *Chloris gayana*, Callide e Reclaimer, foram esterilizadas com solução de hipoclorito de sódio a 0,5% por 5 min e posteriormente lavadas 3 vezes com água deionizada. Foi utilizada solução nutritiva modificada adaptada de Kotula *et al.*, 2015, contendo os seguintes macro e micronutrientes (mM): $CaSO_4.2H_2O$ (1,5); $MgSO_4.7H_2O$ (0,4); Ca (NO_3) $2,4H_2O$ (1,5); KNO_3 (0,75); NH_4NO_3 (0,625); KH_2PO_4 (0,2); $Na_2O_3Si.9H_2O$ (0,1); Fe-EDTA (0,05); KCL (0,05); H_3BO_3 (0,025); $MnSO_4.H2O$ (0,002); $ZnSO_4.7H_2O$ (0,002); $CuSO_4.5H_2O$ (0,0005); $Na_2MoO_4.2H_2O$ (0,0005); $NiSO_4.7H_2O$ (0,001). A solução foi tamponada com 1,0 m de MES (ácido 2- [N-morfolino] etanossulfônico) e o pH foi ajustado para 6,5 usando NaOH.

O processo de germinação foi conduzido utilizando-se suportes flutuantes semelhantes a bandejas construídos artesanalmente (Figura 9A e 9B). O suporte possuía uma camada de tela na extremidade inferior de maneira a permitir que as sementes e plântulas tivessem contato com a solução nutritiva. Foram colocadas quatro sementes por subdivisão do suporte e durante os quatro dias iniciais as sementes foram mantidas no escuro e submetidas à solução nutritiva a 25% da concentração sob aeração. No quarto dia, a solução nutritiva foi alterada para dosagem de 50% e as sementes foram expostas à luz solar. O transplante ocorreu quando a quarta folha estava totalmente expandida (10 dias após a germinação). As plântulas, a partir de então, passaram a receber solução nutritiva a 100% da força, foram transferidas para vasos individuais de 5 L cobertos com papel alumínio e mantidas em sistema hidropônico continuamente aerado (Figura 10A e 10B).

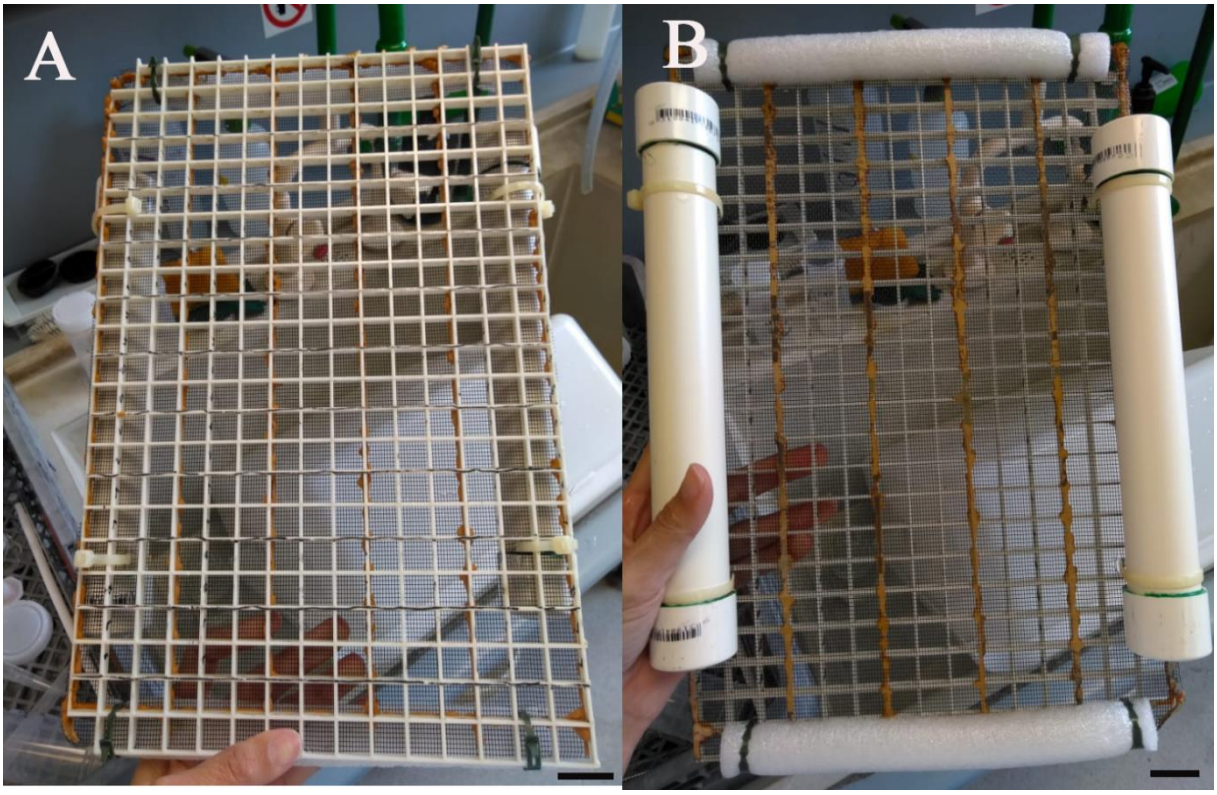

Figura 9. Suporte para germinação de sementes. A. parte superior com subdivisões; B. parte inferior com tela e estrutura para que o suporte possua capacidade de boiar. Barra de escala – 1,5 cm.

Os tratamentos de sal foram impostos após 7 dias do transplante. Em esquema fatorial, 4 vasos de plantas das cultivares Callide e Reclaimer foram expostos a combinações de cloreto de sódio (NaCl; 0, 200, 400 e 600 mM) e cloreto de potássio (KCl; 1 e 10 mM) (NaCl 0 mM + 1 KCl mM; NaCl 0 mM + KCl 10 mM; NaCl 200 mM + KCl 1 mM; NaCl 200 mM + KCl 10 mM; NaCl 400 mM + KCl 1 mM; NaCl 400 mM + KCl 10 mM; NaCl 600 mM + KCl 1 mM; 600 mM NaCl + 10 mM KCl) totalizando 64 unidades experimentais (2 cultivares × 4 tratamentos NaCl × 2 tratamentos KCl × 4 repetições). Cada vaso continha um total de 3 plantas. Os tratamentos de NaCl foram impostos pela adição de 100 mM de NaCl a cada 24 h até que as concentrações finais de NaCl fossem atingidas. A partir da primeira adição de NaCl, o experimento foi conduzido por ~ 25 dias e a solução nutritiva foi renovada a cada 7 dias. Antes da colheita, as amostras coletadas foram lavadas com água deionizada, enquanto as raízes das plantas tratadas com sal foram enxaguadas com solução de manitol com concentração equivalente aos níveis de NaCl para evitar choque osmótico. Medições não invasivas, como fluorescência da clorofila *a*, foram realizadas em mais de uma réplica por vaso.

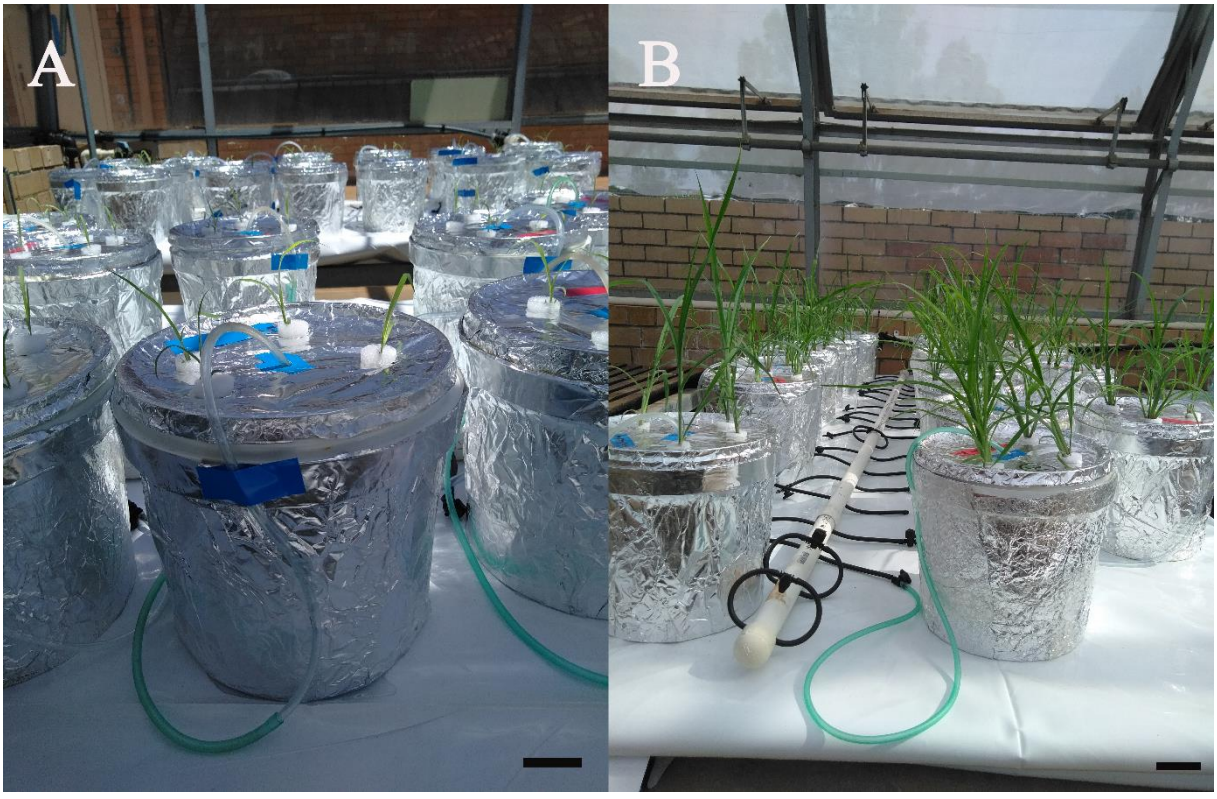

Figura 10. Vasos individuais utilizados para cultivo das plantas. A. vasos de 5 L utilizados para condução do experimento após transplante B. Bancada com tratamento aleatorizados e sistema hidropônico. Barra de escala – 1,5 cm.

b. Análises para coleta de dados.

b.1 Acúmulo de biomassa e taxa de crescimento relativo

Foram realizadas duas coletas de amostra: antes da aplicação dos tratamentos (DW_1; 7 dias após o transplante das mudas; 4ª folha totalmente expandida) e 25 dias após a aplicação dos tratamentos (DW_2; 32 dias após o transplante das mudas). Para avaliação do peso seco, a biomassa colhida foi seca em estufa (70ºC) por 72 horas até obtenção de peso constante. O conteúdo de água foi estimado usando dados de peso fresco e seco para calcular mL g^{-1} de massa seca. As taxas de crescimento relativo foram calculadas como $RGR = (\ln DW_2 - \ln DW_1\ )\ (t_2 - t_1)^{-1}$) (Hunt, 1982), onde: DW_1 é a massa seca total (parte aérea e raiz) antes da imposição dos tratamentos salinos; DW_2 é a massa seca total no momento da colheita final; t_1 é o tempo (em dias) em que a massa seca foi avaliada pela primeira vez e, t_2 é o tempo (em dias) da colheita final.

b.2 Teores de K^+ e Na^+

A análise dos teores dos íons K^+ e Na^+ nos tecidos de raiz e parte aérea das plantas foi realizada seguindo o mesmo procedimento utilizado no item b. do artigo I, conforme protocolo descrito por Munns *et al.* (2010). As amostras diluídas dos extratos foram analisadas para ambos os íons usando um fotômetro de chama (Flame Photometer 410, Sherwood, Cambridge, UK).

Adicionalmente, devido à presença de glândulas bicelulares excretoras de sal em ambas superfícies das folhas de *C. gayana*, foi realizada análise adicional com o objetivo de estimar a quantidade de íons K^+ e Na^+ extraídos e retidos pelas folhas. Dessa forma, a 3ª folha completamente expandida foi previamente lavada em água deionizada 24 horas antes da coleta. Após a realização desse procedimento, no momento da coleta, as mesmas folhas foram mergulhadas em tubo do tipo falcon contendo 10 mL de água deionizada. Após a lavagem, as folhas foram acondicionadas em sacos de papel e levadas à estufa a 60°C e moídas até um pó fino para análise dos teores de K^+ e Na^+ retidos no tecido foliar seguindo protocolo descrito em Munns et al. (2010) e no item b.1, artigo I. As concentrações de K^+ e Na^+ foram também avaliadas na solução de água deionizada contido no tubo do tipo falcon afim de estimar a quantidade dos íons excretados em um período de 24 horas. O procedimento foi realizado com fotômetro de chama (Flame Photometer 410, Sherwood, Cambridge, UK).

b.3 Potencial osmótico da seiva da folha

Para mensuração do potencial osmótico da seiva foliar, a lâmina foliar da quarta folha completamente expandida foi coletada e imediatamente alocada em um criotubo hermético de 2 mL, congelada em N_2 líquido e armazenada a –20ºC para análise posterior. Pequenos pedaços de tecido foliar foram usados para extração de seiva utilizando prensa manual simples. Cerca de 20 µL de seiva da folha foram coletados e as medições foram conduzidas utilizando osmômetro Fiske 210 de depressão de ponto de congelamento (Advanced Instruments Inc., Norwood, MA).

b.4 Estimativa da contribuição de íons (K^+ e Na^+) para o potencial osmótico da seiva foliar

A estimativa da contribuição dos íons K^+ e Na^+ para o potencial osmótico da seiva foliar foi calculada como: $\frac{([ion]\ pelo\ conteúdo\ de\ água\ da\ amostra)*100}{potencial\ osmótico}$ em mmol L^{-1} (Garthwaite *et al.*, 2005). Os valores do teor de água da amostra, referem-se à diferença entre peso fresco e

seco da parte aérea descritas no item b.1.

b.5 Medições de troca gasosa e fluorescência da clorofila a

Medições de trocas gasosas com obtenção de taxa fotossintética líquida (*A*), condutância estomática (*gs*), taxa de transpiração (*E*) e razão entre concentração interna e externa de CO_2 (*Ci/Ca*) foram realizadas na 2ª folha completamente expandida de *C. gayana* por meio da utilização sistema de troca gasosa aberto LI-6400XT (LI-COR, Lincoln, NB, EUA). A partir de tais medições, foi calculada a eficiência do uso da água (A/E). Foi utilizada radiação fotossinteticamente ativa de 1.500 µmol fótons m^{-2} s^{-1} (saturado com luz), temperatura da câmara foliar de 30º C, 60-70% de umidade relativa e concentrações de CO_2 de 400 (ambiente) e 800 (elevado) µmol mol^{-1}.

As medições dos transientes de fluorescência da clorofila *a* foram também realizadas na 2ª folha completamente expandidas, adaptadas ao escuro por pelo menos 20 minutos, usando fluorômetro portátil Pocket PEA (Hansatech Instruments, King's Lynn, Norfolk, Reino Unido). A fluorescência da clorofila *a* foi induzida por um pulso de luz saturante (3.500 µmol fótons m^{-2} s^{-1}) durante um segundo de iluminação (10 µs a 1 s). As intensidades de fluorescência nos momentos de 50 µs (fluorescência mínima, F_O), 100 µs, 300 µs, 2 e 30 ms até a intensidade mais alta de FM (fluorescência máxima) foram analisadas usando os parâmetros do teste JIP (Strasser *et al*., 1995; Strasser *et al*., 2004). A comparação de eventos refletidos nas fases OJ, OI e IP e cinética da diferença dos dados de fluorescência da variável relativa foi realizada da mesma forma descrita no artigo I (item b.2) (Yusuf *et al.*, 2010). Para traçar as curvas os dados foram normalizados com base nos valores de controle (W_{OJ}, W_{OK}, JIP radar). Afim de obter dados para comparação entre os tratamentos de NaCl e KCl para normalização das curvas de fluorescência, foi utilizado tratamento adicional sem alteração da solução nutritiva padrão usada pelo grupo de estudo (sem adição/alteração nos níveis de Na e K). Os valores plotados de fluorescência consistem na média de oito medições por cada tratamento.

b.6 Análises de dados

A distribuição normal de todos os dados e homogeneidade das variâncias foi previamente verificada pelo teste de homogeneidade de Cochran. Transformação Box-cox foi usada quando necessário. Os resultados foram submetidos à análise de variância - ANOVA

com três (fatores: ‘cultivar’, ‘NaCl’ e ‘KCl’) e dois fatores (fatores: ‘NaCl’ e ‘KCl’). Na presença de diferença significativa, foram utilizados teste de Scott-Knott e teste F para determinação da significância a $p \leq 0,05$. A análise foi realizada por meio do processamento dos dados experimentais nos softwares STATISTICA e Sisvar (Universidade Federal de Lavras, Lavras, Brasil). Para investigar os agrupamentos, a Análise de Componentes Principais (PCA) o software PAST 3 (PAleontological STatistics) foi utilizado.

REFERÊNCIAS BIBLIOGRÁFICAS

Abbasi, G.H.; *et al*. **Exogenous potassium differentially mitigates salt stress in tolerant and sensitive maize hybrids**. Pakistan Journal of Botany, v. 46, n. 1, p. 135-146, 2014.

Acosta-Motos, J.; *et al*. **Plant responses to salt stress: adaptive mechanisms**. Agronomy, v. 7, n. 1, p. 1-38, 2017.

Aliscioni, S., Ospina, J.C. & Gomiz, N.E. **Morphology and leaf anatomy of *Setaria s.l.* (Poaceae: Panicoideae: Paniceae) and its taxonomic significance**. Plant Systematics Evolution, v. 302, p. 173–185, 2016.

Aoki, N. & Kanai, R. **Reappraisal of the role of sodium in the light-dependent active transport of pyruvate into mesophyll chloroplasts of C_4 plants**. Plant and Cell Physiology, v. 38, p. 1217-1225, 1997.

Ashraf, M. Y.; Ahmad, A. & McNeilly, T. **Growth and photosynthetic characteristics in pearl millet under water stress and different potassium supply**. Photosynthetica, v. 39, n. 3, p. 389-394, 2001.

Assaha, D.V.M.; *et al*. **The Role of Na^+ and K^+ Transporters in Salt Stress Adaptation in Glycophytes**. Frontiers in Physiology, v. 8, n. 509, p. 1-19, 2017.

Baker, N.R. **Light-use efficiency and photoinhibition of photosynthesis in plants under environmental stress**. In: Smith JAC, Griffiths, H. (eds.), Water deficits plant responses from cell to community, pp.221-235. Bios Scientific Publisher, Oxford, 1993.

Barbosa, M.R.; *et al.* **Geração e desintoxicação enzimática de espécies reativas de oxigênio em plantas**. Ciência Rural, v. 44, n. 3, p. 453-460, 2014.

Bhandal, I.S. & Malik, C.P. **Potassium estimation, uptake and its role in the physiology and metabolism of flowering plants**. International Review of Cytology, v. 110, p. 205-254, 1988.

Bhattacharjee, S. **Sites of generation and physicochemical basis of formation of reactive oxygen species in plant cell**. In: Gupta, S.D. (ed.) Reactive oxygen species and antioxidants in higher plants. Enfield: Science Publishers, p. 1-30, 2010.

Blumwald, E.; Aharon, G.S. & Apse, M.P. **Sodium transport in plant cells**. Biochimica et Biophysica Acta, v. 1465, p. 140-151, 2000.

Bogdan, A.V. **Tropical Pasture and Fodder Plants**. Longman, London/New York, 1977.

Bose, J.; *et al*. **Chloroplast function and ion regulation in plants growing on saline soils: lessons from halophytes**. Journal of Experimental Botany, v. 68, n. 12, p. 3129–3143, 2017.

Bose, J.; Rodrigo-Moreno, A. & Shabala, S. **ROS homeostasis in halophytes in the context of salinity stress tolerance**. Journal of Experimental Botany, v. 65, p. 1241–1257, 2014.

Bray, E.A.; Bailey-Serres, J. & Weretilnyk, E. **Responses to abiotic stresses**. In: Buchanan, B.B.; Gruissem, W & Jones, R.L. (eds.) Biochemistry & Molecular Biology of Plants. Rockville. American Society of Plant Physiologists, p. 1158-1203, 2000.

Brownell, P.F. & Wood, J.G. **Sodium as an essential micronutrient element for *Atriplex vesicaria***. Heward. Nature, v. 179, p. 635–636, 1957.

Brutnell, T. P.; *et al*. ***Setaria viridis*: a model for C_4 photosynthesis**. The Plant cell, v. 22, n.8, p. 2537-2544, 2010.

Buchanan, B.B.; Gruissem, W. & Jones, R.L. **Biochemistry and molecular biology of plants**. Rockville: American Society of Plant Physiologists, p. 1158-1203, 2000.

Buege, J.A. & Aust, S.D. **Microsomal lipid peroxidation**. Methods in Enzymology, New York, v. 52, p. 302-310, 1978.

Burbulis, N.; *et al.* **Effect of potassium bicarbonate on photosynthetic parameters of *Setaria viridis* under drought conditions**. Zemdirbyste-Agriculture, v. 104, n. 1, p. 79-84, 2017.

Cakmak, I. **The role of potassium in alleviating detrimental effects of abiotic stresses in plants**. Journal of Plant Nutrition and Soil Science, v. 168, n. 4, p. 521-530, 2005.

Cavalcante, L.F.; *et al*. **Recuperação de solos afetados por sais**. In: Gheyi, H. R.; Dias, N. S.; Lacerda, C.F. (eds.) Manejo da Salinidade na Agricultura: Estudos Básicos e Aplicados, 2ª edição, INCTSal, Fortaleza, p. 423-448, 2016.

Chatterjee, J.; *et al*. **Cloning, characterization and expression of a chloroplastic fructose-1,6-bisphosphatase from *Porteresia coarctata* conferring salt-tolerance in transgenic tobacco**. Plant Cell, Tissue and Organ Culture, v. 114, p. 395–409, 2013.

Cha-Um, S. & Kirdmanee, C. **Effect of salt stress on proline accumulation, photosynthetic ability and growth characters in two maize cultivars**. Pakistan Journal of Botany, v. 41, n. 1, p. 87-98, 2009.

Cha-Um, S.; *et al*. **Water relations, pigment stabilization, photosynthetic abilities and growth improvement in salt stressed rice plants treated with exogenous potassium nitrate application**. International Journal of Plant Production, v. 4, n. 3, p. 187-198, 2010.

Chaves, M.M. & Oliveira, M.M. **Mechanisms underlying plant resilience to water deficits: Prospects for water-saving agriculture**. Journal of Experimental Botany, v. 55, n. 407, p. 2365-2384, 2004.

Chaves, M.M.; Flexas, J. & Pinheiro, C. **Photosynthesis under drought and salt stress: regulation mechanisms from whole plant to cell**. Annals of Botany, v. 103, n. 4, p. 551-560, 2009.

Cheeseman, J. M. **The evolution of halophytes, glycophytes and crops, and its implications for food security under saline conditions**. New Phytologist, v. 206, p. 557-570, 2015.

Chen, G-X. & Asada, K. **Ascorbate peroxidase in tea leaves: occurrence of two isoenzymes and the differences in their enzymatic and molecular properties**. Plant Cell Physiology, v. 30, p. 987-998, 1989.

Colmer, T.D., Munns, R. & Flowers, T.J. **Improving salt tolerance of wheat and barley: future prospects**. Australian Journal of Experimental Agriculture, v. 45, p. 1425-1443, 2005.

Cook, B.G.; *et al.* **Tropical Forages: an interactive selection tool**. CSIRO, DPI&F (Qld), CIAT and ILRI, Brisbane, Australia, 2005.

Cordeiro, G.G. **Salinidade e sodicidade de solos agrícolas. II Curso sobre manejo de solo e água em propriedades agrícolas do trópico semi-árido**. Embrapa, Petrolina, PE, 1983.

Cowan, I.R. **Transport of water in the soil-plant-atmosphere system**. The Journal of Applied Ecology, v.2, n. 1, p. 221, 1965.

Deinlen, U.; *et al*. **Plant salt-tolerance mechanisms**. Trends in Plant Science, v. 19, n. 6, p. 371-379, 2014.

Dekker, J. **The Foxtail (*Setaria*) Species-Group**. Weed Science, v. 51, p. 641–656, 2003.

Delatorre, C. A. & Silva, A. A. ***Arabidopsis thaliana*: uma pequena planta um grande papel**. Revista de Ciências Agrárias, v. 31, n. 2, p. 58-67, 2008.

Demidchik, V.; *et al.* **Calcium transport across plant membranes: mechanisms and functions**. New Phytologist, v. 220, p. 40-69, 2018.

Demidchik, V.; *et al*. **Stress-induced electrolyte leakage: The role of K^+-permeable channels and involvement in programmed cell death and metabolic adjustment**. Journal of Experimental Botany, v. 65, n. 5, p. 1259-1270, 2014.

Diao, X. **Advances in foxtail millet biotechnology and its future directions.** Journal of Hebei Agricultural Sciences, p. 61-68, 2005.

Dias, N.D.; *et al*. **Efeitos dos sais na planta e tolerância das culturas à salinidade.** In: GHEYI, H.R. *et al.* (*eds.)* Manejo da salinidade na agricultura: estudos básicos e aplicados. 2ª edição, INCTSal, Fortaleza, p. 151-161, 2016.

Doust, A.N.; *et al*. **Foxtail Millet: A Sequence-Driven Grass Model System.** Plant Physiology, v. 149, p. 137-141, 2009.

Doust, A.N.; *et al*. Editorial: ***Setaria* as a model genetic system to accelerate yield increases in cereals, forage crops, and bioenergy grasses**. Frontiers in Plant Science, v. 10, p. 1-2, 2019.

Drincovich, M.; *et al*. **C_4 decarboxylases: different solutions for the same biochemical problem, the provision of CO_2 to Rubisco in the bundle sheath cells**. Advances in Photosynthesis and Respiration, v. 32, chap. 14, 2011.

Duarte, K.E.; *et al.* **Identification and characterization of core abscisic acid (ABA) signaling components and their gene expression profile in response to abiotic stresses in *Setaria viridis***. Scientific Reports -UK, v. 9, p. 4028-4043, 2019.

Edwards, G.E.; *et al*. **What does it take to be C_4? Lessons from the evolution of C_4 photosynthesis.** Plant physiology, v. 125, n. 1, p. 46–49, 2001.

EMBRAPA SOLOS. **Sistema brasileiro de classificação de solos**. Embrapa. SPI, 2ª edição, 2006.

Flowers, T.J. & Colmer, T.D. **Plant salt tolerance: adaptations in halophytes.** Annals of Botany v. 115, p. 327–331, 2015.

Flowers, T.J. & Colmer, T.D. **Salinity tolerance in halophytes**. New Phytologist, v. 179, p. 945-963, 2008.

Flowers, T.J., Munns, R. & Colmer, T.D. **Sodium chloride toxicity and the cellular basis of salt tolerance in halophytes**. Annals of Botany, v. 115, p. 419-431, 2015.

Foyer, C.H. & Halliwell, B. **The presence of glutathione and glutathione reductase in chloroplasts: a proposed role in ascorbic acid metabolism**. Planta, v. 133, n. 1, p. 21–25, 1976.

Foyer, C.H.; *et al*. **Photosynthetic control of electron transport and the regulation of gene expression**. Journal of Experimental Botany, v. 63, p. 1637-1661, 2012.

Gadjev, I.; Stone, J.M. & Gechev, T.S. **Programmed cell death in plants: new insights into redox regulation and the role of hydrogen peroxide**. International Review of Cell and Molecular Biology, v. 270, p. 87-144, 2008.

Garcia-Mata, C.; *et al.* **A minimal cysteine motif required to activate the SKOR K^+ channel of Arabidopsis by the reactive oxygen species H_2O_2**. The Journal of Biological Chemistry, v. 285, n. 38, p. 29286-29294, 2010.

Garthwaite, A.J., Bothmer, R. von & Colmer, T.D. **Salt tolerance in wild *Hordeum* species is associated with restricted entry of Na^+ and Cl^- into the shoots**. Journal of Experimental Botany, v. 56, n. 419, p. 2365-2378, 2005.

Ghannoum, O. **C_4 photosynthesis and water stress**. Annals of Botany, v. 103, n. 4, p. 635–

644, 2009.

Giannopolitis, C.N. & Ries, S.K. **Superoxide dismutases. I. Occurrence in higher plants**. Plant Physiology, v. 59, p. 309–314, 1977.

Gill, S.S. & Tuteja, N. **Reactive oxygen species and antioxidant machinery in abiotic stress tolerance in crop plants**. Plant Physiology and Biochemistry, v. 48, n. 12, p. 909-930, 2010.

Gosh, S., Bagchi, S. & Lahiri Majumder, A. **Chloroplast fructose-1,6-bisphosphatase from *Oryza* differs in salt tolerance property from the *Porteresia* enzyme and is protected by osmolytes**. Plant Science, v.160, p. 1171–1181, 2001.

Grof, C.P.; Johnston, M. & Brownell, P.F. **Effect of sodium nutrition on the ultrastructure of chloroplasts of C_4 plants**. Plant Physiology, v. 89, p. 539–543, 1989.

Guan, L.M. & Scandalios, J.G. **Hydrogen peroxide-mediated catalase gene expression. In response to wounding**. Free Radical Biology and Medicine, v. 28, n. 8, p. 1182-1190, 2000.

Guo, R.; *et al*. **Germination, growth, photosynthesis and ionic balance in *Setaria viridis* seedlings subjected to saline and alkaline stress**. Canadian Journal of Plant Science, v. 91, n. 6, p. 1077-1088, 2011.

Gutteridge, J.M.C. & Halliwell, B. **The measurement and mechanism of lipid peroxidation in biological systems**. Trends in Biochemical Science., v. 15, p. 129-135, 1990.

Hanikenne, M.; Bernal, M. & Urzica, E-I. **Ion homeostasis in the chloroplast**. In: Theg, S.M.; Wollman, F-A (eds.). Plastid Biology. New York: Springer, p. 465–514, 2014.

Hasanuzzaman, M.; *et al.* **Plant response and tolerance to abiotic oxidative stress: antioxidant defense is a key factor**. In: Hasanuzzaman, M.; *et al.* (eds.) Crop Stress and its Management: Perspectives and Strategies. Springer, p. 261-315. 2012.

Hasanuzzaman, M.; *et al*. **Potassium: a vital regulator of plant responses and tolerance to abiotic stresses**. Agronomy, v. 8, n. 31, p. 1-29, 2018.

Hasewaga, P.M.; *et al.* **Plant cellular and molecular responses to high salinity**. Annual Review of Plant Physiology and Plant Molecular Biology, v. 51, p. 463-99, 2000.

Hatch, M.D. **C_4 photosynthesis: a unique mena of modified biochemistry, anatomy and ultrastructure**. In: Biochimica et Biophysica Acta, v. 895, p. 81–106, 1988.

Heldt, H.W. **Plant Biochemistry**. 3 ed. San Diego: Elsevier Academic Press, 630 p., 2005.

Hoagland, D.R. & Arnon, D.I. **The water culture method of groin plants without soil**. California Agriculture Experimental Station circular, v. 347, p. 1–39, 1938.

Hunt, R. **Plant growth curves. The functional approach to plant growth analysis**. London: Edward Arnold, 1982.

Hussain, T.; *et al*. **Low salinity improves photosynthetic performance in *Panicum antidotale* under drought stress**. Frontiers in Plant Science, v. 11, p. 481, 2020.

Incharoensakdi, A., Takabe, T. & Akazawa, T. **Effect of betaine on enzyme activity and subunit interaction of ribulose-1,5-bisphosphate carboxylase/oxygenase from *Aphanothece halophytica***. Plant Physiology, v. 81, p. 1044–1049, 1986.

Ivushkin, K.; *et al.* **Global mapping of soil salinity change**. Remote Sensing of Environment, v. 231, p. 111260, 2019.

Jackson, R.B.; Sperry, J.S. & Dawson, T.E. **Root water uptake and transport: Using physiological processes in global predictions**. Trends in Plant Science, v. 5, n. 11, p. 482-488, 2000.

Jiang, X.; Leidi, E. O.; Pardo, J. M. **How do vacuolar NHX exchangers function in plant salt tolerance?** Plant Signaling and Behavior, v. 5, n. 7, p. 792-795, 2010.

Junqueira, N. E. G.; *et al*. **Anatomy and ultrastructure of embryonic leaves of the C_4 species *Setaria Viridis***. Annals of Botany, v. 121, n. 6, p. 1163-1172, 2018.

Junqueira, N.E.G.; *et al.* **Phenology of the genetic model *Setaria viridis* (Poaceae) according to the BBCH-scale of development**. Botanical Journal of the Linnean Society, v. 192, n. 1, p. 1-18, 2019.

Kaddour, R.; *et al*. **Comparative effect of potassium on K and Na uptake and transport in two accessions of *Arabidopsis thaliana* during salinity stress**. Comptes Rendus – Biologies, v. 332, n. 9, p. 784-794, 2009.

Kataria S.; Baghel L. & Guruprasad, K. **Alleviation of adverse effects of ambient UV stress on growth and some potential physiological attributes in soybean (*Glycine max*) by seed pre-treatment with static magnetic field**. Journal Plant Growth, p. 1–16, 2017.

Kataria, S. & Verma, S.P. **Salinity stress responses and adaptive mechanisms in major glycophytic crops: The Story so far**. In: Kumar V.; *et al.* (eds.) Salinity Responses and Tolerance in Plants, Volume 1, Springer, p. 1-40, 2018.

Kim, Y.H.; *et al*. **Accumulation of amino acids and glycinebetaine by NaCl treatment and its relation to salt tolerance in three gramineous plants**. Journal of Weed Science and Technology, v. 45, n. 2, p. 96-103, 2000.

Kotula, L.; *et al.* 2015. **Oxygen deficiency and salinity affect cell-specific ion concentrations in adventitious roots of barley (*Hordeum vulgare*)**. New Phytologist, v. 208, n.4, p. 1114-1125, 2015.

Layton, D.J. & Kellogg, E.A. **Morphological, phylogenetic, and ecological diversity of the new model species *Setaria Viridis* (Poaceae: PANICEAE) and its close relatives**. American Journal of Botany, v. 101, n. 3, p. 539-557, 2014.

Liu, Y.; *et al*. **Assessment of drought tolerance of 49 switchgrass (*Panicum virgatum*) genotypes using physiological and morphological parameters**. Biotechnology for

Biofuels, v. 8, n. 1, p. 1-18, 2015.

Loch, D.S., Rethman, N.F.G. & van Niekerk, W.A. **Rhodes grass**. In: Moser, L. E., *et al.* (Eds.), Warm Season (C_4) Grasses. American Society of Agronomy/Crop Science Society of America/Soil Science Society of America, Madison, p. 833–872, 2004.

Luo, Y.; *et al*. **Physiological acclimation of two psammophytes to repeated soil drought and rewatering**. Acta Physiologiae Plantarum, v. 33, n. 1, p. 79–91, 2011.

Maathuis, F.J.M.; *et al*. **Roles of higher plant K^+ channels**. Plant Physiology, v. 114, n. 4, p.1141–1149, 1997.

Matoh, T. & Murata, S. **Sodium stimulates growth of *Panicum coloratum* through enhanced photosynthesis**. Plant Physiology, v. 92, p. 1169-1173, 1990.

Mitler, R. **ROS are good**. Trends in Plant Science, v. 22, n. 1, p. 11-19, 2017.

Müller, M.; *et al*. **Decreased capacity for sodium export out of *Arabidopsis* chloroplasts impairs salt tolerance, photosynthesis and plant performance**. The Plant Journal, v. 78, p. 646–658, 2014.

Munns, R. & Tester, M. **Mechanisms of salinity tolerance**. Annual Review of Plant Biology, v. 59, n. 1, p. 651-681, 2008.

Munns, R. **Comparative physiology of salt and water stress**. Plant, cell & environment, v. 25, n. 2, p. 239-250, 2002.

Munns, R., Goyal, S., & Passioura, J. **Salinity stress and its mitigation**. Plant Stress Website. Blum A. (*ed*), 2004.

Munns, R.; *et al*. **Measuring soluble ions concentrations (Na^+, K^+ e Cl^-) in salt treated plants**. In: Clifton, N.J. (*ed.*) Plant stress tolerance: methods and protocols. Humana Press. Springer, v. 639, p. 371-382, 2010.

Munns, R.; James, R.A. & Läuchli, A. **Approaches to increasing the salt tolerance of wheat and other cereals**. Journal of Experimental Botany, v. 57, p. 1025-1043, 2006.

Nakano, Y. & Asada, K. **Hydrogen peroxide is scavenged by ascorbate-specific peroxidases in spinach chloroplasts**. Plant and Cell Physiology, v. 22, p. 867–880, 1981.

Navrot, N.; *et al*. **Plant glutathione oeroxidases are functional peroxiredoxins distributed in several subcellular compartments and regulated during biotic and abiotic stresses**. Plant Physiology, v. 142, n. 4, p. 1364-1379, 2006.

Noctor, G.; Lelarge-Trouverie, C. & Mhamdi, A. **The metabolomics of oxidative stress**. Phytochemistry, v. 112, n. 1, p. 33-53, 2015.

Novák, V. **Soil-plant-atmosphere system**. In: Evapotranspiration in the soil-plant-atmosphere system. Springer, p. 1-253, 2012.

Ohnishi, J.; *et al*. **Involvement of Na^+/ in active uptake of pyruvate in mesophyll**

chloroplasts of some C_4 plants. Na^+/pyruvate cotransport. Plant Physiology, v.94, p. 950-959, 1990.

Oi, T., Taniguchi, M. & Miyake, H. **Morphology and ultrastructure of the salt glands on the leaf surface of Rhodes grass (*Chloris gayana* Kunth)**. International Journal of Plant Sciences, v. 173, n. 5, p. 454-463, 2012.

Omoto, E., Taniguchi, M. & Miyake, H. **Effects of salinity stress on the structure of bundle sheath and mesophyll chloroplasts in NAD-malic enzyme and PCK type C_4 plants.** Plant Production Science, v. 13, n. 2, p. 169-176, 2010.

Pan, T.; *et al*. **Non-stomatal limitation of photosynthesis by soil salinity**. Critical Reviews in Environmental Science and Technology, p. 1-35, 2020.

Passioura, J.B. **Water in the soil-plant-atmosphere continuum**. Physiological Plant Ecology II, Springer, p. 5-33, 1982.

Pedrotti, A.; *et al*. **Causas e consequências do processo de salinização dos solos**. Revista Eletrônica em Gestão, Educação e Tecnologia Ambiental, v. 19, n. 2, p. 1308-1324, 2015.

Petti, C.; *et al*. **Comparative feedstock analysis in *Setaria viridis* L. as a model for C_4 bioenergy grasses and Panicoid crop species**. Frontiers in plant science, v. 4, n. 181, p. 1-14, 2013.

Phillips, S. **Poaceae (Gramineae). Flora of Ethiopia and Eritrea**. Volume 7: The National Herbarium, Addis Ababa University, Addis Ababa/The Department of Systematic Botany, Uppsala University, Uppsala, 1995.

Ponsens, J.; *et al*. **Characterization of phenotypic diversity, yield and response to drought stress in a collection of Rhodes grass (*Chloris gayana* Kunth) accessions**. Field Crops Research, v. 118, p. 57–72, 2010.

Pottosin, I. & Shabala, S. **Transport across chloroplast membranes: optimizing photosynthesis for adverse environmental conditions**. Molecular Plant, v 9, p. 356–370, 2016.

Prisco, J.T.; Gomes-Filho, E. & Miranda, R. **Physiology and biochemistry of plants growing under salt stress**. In: Gheyi, H.R. *et al.* (eds.) Manejo da salinidade na agricultura: estudos básicos e aplicados. 2ª edição, INCTSal, p. 163-180, 2016.

Rahman, S.; *et al*. **Salinity induced ultrastructural alterations in leaf cells of rice (*Oryza sativa* L.)**. Plant Production Science, v. 3, p. 422–429, 2000.

Ribeiro, M.R.; *et al.* **Química e mineralogia do solo**. Viçosa: Sociedade Brasileira de Ciência do Solo, 2009. v.2., cap.19, p.449- 484, 2009.

Robinson, S.P. & Downton, W.J. **Potassium, sodium, and chloride content of isolated intact chloroplasts in relation to ionic compartmentation in leaves**. Archives of Biochemistry and Biophysics, v. 228, p. 197–206, 1984.

Sage, R.F. **The evolution of C_4 photosynthesis**. New Phytologist, v. 161, p. 341-370, 2004.

Sage, R.F.; Khoshravesh, R. & Sage, T.L. **From proto-Kranz to C_4 Kranz: building the bridge to C_4 photosynthesis**. Journal of Experimental Botany, v. 65, n. 13, p. 3341–3356, 2014.

Saha, P.; *et al*. **Effects of abiotic stress on physiological plasticity and water use of *Setaria viridis* (L.)**. Plant Science, v. 251, p. 128-138, 2016.

Saneoka, H.; *et al***. Salt tolerance of glycinebetaine-deficient and -containing maize lines**. Plant physiology, v. 107, n. 2, p. 631-638, 1995.

Sangakkara, U.R., Frehner, M. & Nösberger, J. **Effect of soil moisture and potassium fertilizer on shoot water potential, photosynthesis and partitioning of carbon in mungbean and cowpea**. Journal of Agronomy and Crop Science, v. 185, n. 3, p. 201-207, 2000.

Santos Júnior, U.M. dos; *et al.* **Flooding of tropical forests in central Amazonia: what do the effects on the photosynthetic apparatus of trees tell us about species suitability for reforestation in extreme environments created by hydroelectric dams?** Acta Physiologiae Plantarum, v. 37, n. 8, p. 166, 2015.

Shabala, S. & Pottosin, I. **Regulation of potassium transport in plants under hostile conditions: implications for abiotic and biotic stress tolerance**. Physiologia Plantarum, v. 151, n. 3, p. 257-279, 2014.

Shabala, S**. Ionic and osmotic components of salt stress specifically modulate net ion fluxes from bean leaf mesophyll**. Plant, Cell and Envinroment, v. 23, p. 825-837, 2000.

Shabala, S. **Learning from halophytes: physiological basis and strategies to improve abiotic stress tolerance in crops**. Annals of Botany, v. 112, p. 1209-1221, 2013.

Sharma, P.; *et al*. **Reactive oxygen species, oxidative damage, and antioxidative defense mechanism in plants under stressful conditions**. Journal of Botany, p. 1-26, 2012.

Silveira, J.A.G.; *et al*. **Mecanismos biomoleculares envolvidos com a resistência ao estresse salino em plantas.** In: Gheyi, H. R. *et al.* (eds.) Manejo da salinidade na agricultura: estudos básicos e aplicados. 2ª edição, INCTSal, p. 181-197, 2016.

Siringam, K.; *et al*. **Exogenous application of potassium nitrate to alleviate salt stress in rice seedlings.** Journal of Plant Nutrition, v. 36, n. 4, p. 607-616, 2013.

Smith, F.W. **The effect of sodium on potassium nutrition and ionic relations in Rhodes grass.** Australian Journal of Agricultural Research, v. 25, p. 407-414, 1974.

Spurr, A.R. **A low-viscosity epoxy resin embedding medium for electron microscopy**. Journal of Ultrastructure Research, v. 26, p. 31-43, 1969.

Sreenivasulu, N.; *et al*. **Differential response of antioxidant compounds to salinity stress in salt-tolerant and salt-sensitive seedlings of foxtail millet (*Setaria italica*).** Physiologia

Plantarum, v. 109, n. 4, p. 435-442, 2000.

Strasser, R.J., Srivastava, A. & Govindjee. **Polyphasic chlorophyll *a* fluorescence transient in plants and cyanobacteria.** Photochemistry and Photobiology, v. 61, n. 1, p. 32-42, 1995.

Strasser, R.J., Tsimilli-Michael, M. & Srivastava, A. **Analysis of the chlorophyll *a* fluorescence transient.** In: Papageorgiou, G.C., Govindjee (*eds.*) Advances in Photosynthesis and Respiration, Springer, v. 19, p. 321-362, 2004.

Studer, C., Hu, Y. & Schmidhalter, U. Interactive **Effects of N-, P- and K- nutrition and drought stress on the development of maize seedlings**. Agriculture, v. 7, n. 11, p. 1-12, 2017.

Suttie, J.M. **Hay and straw conservation– for small-scale farming and pastoral conditions**. FAO Plant Production and Protection Series 29. Food and Agriculture Organization, Rome, 2000.

Taiz, L. & Zeiger, E. **Fisiologia vegetal**. 4ª edição. Porto Alegre: Artmed, 2009. 819 p.

Tester, M. & Davenport, R. **Na^+ tolerance and Na^+ transport in higher plants**. Annals of Botany, v. 91, n. 5, p. 503-527, 2003.

V'ery, A.A. & Sentenac, H. **Molecular mechanisms and regulation of K^+ transport in higher plants**. Annual Review of Plant Biology, v. 54, p. 575-603, 2003.

Valença, D.C.; *et al.* **Physiological and molecular responses of *Setaria viridis* to osmotic stress**. Plant Physiology and Biochemistry, v. 155, p. 114-125, 2020.

Verslues P.E.; *et al.* **Methods and concepts in quantifying resistance to drought, salt and freezing, abiotic stresses that affect plant water status.** Plant Journal: for cell and molecular biology, v. 45, p. 523–539, 2006.

Wakeel, A. **Potassium-sodium interactions in soil and plant under saline sodic conditions.** Journal of Plant Nutrition and Soil Science, v. 176, p. 344-354, 2013.

Wang, Y. H.; *et al*. **Genetic structure and linkage disequilibrium in a diverse, representative collection of the C_4 model plant, *Sorghum bicolor***. Genes, Genomes, Genetics, v. 3, n. 5, p. 783-793, 2013.

Willadino, L. & Camara, T. R. **Aspectos fisiológicos do estresse salino em plantas**. In: Nogueira, R. J. M. C; *et al.* (eds). Estresses ambientais: danos e benefícios em plantas. Recife. MXM Gráfica e Editora, parte II, cap. 10, p. 118-126, 2005.

Willadino, L. & Camara, T.R. **Enciclopédia Biosfera.** Centro Científico Conhecer - Goiânia, vol.6, n.11, p.16, 2010.

Willadino, L.; *et al.* **Polyamines and free amino acid variation in NaCl-treated embryogenic maize callus from sensitive and resistant cultivars**. Journal of Plant Physiology, v. 149, p. 179- 185, 1996.

Xue, Z.Y.; *et al*. **Enhanced salt tolerance of transgenic wheat (*Tritivum aestivim* L.) expressing a vacuolar Na^+/H^+ antiporter gene with improved grain yields in saline soils in the field and a reduced level of leaf Na^+.** Plant Science, v. 167, n. 4, p. 849-859, 2004.

Yusuf, M.A.; *et al*. **Overexpression of y-tocopherol methyl transferase gene in transgenic *Brassica juncea* plants alleviates abiotic stress: Physiological and chlorophyll *a* fluorescence measurements**. Biochimica et Biophysica Acta, v. 1797, p. 1428-1438, 2010.

Zhao, C.; *et al*. **Mechanisms of plant responses and adaptation to soil salinity**. The innovation, v. 1, n.1, p. 100017, 2020.

CAPÍTULO 3 – ARTIGO I

Potassium supply promotes the mitigation of NaCl-induced effects on leaf photochemistry, metabolism and morphology of *Setaria viridis*

Artigo publicado no periódico "Plant Phisiology and Biochemistry"

https://doi.org/10.1016/j.plaphy.2021.01.021

Plant Physiology and Biochemistry 160 (2021) 193–210

Contents lists available at ScienceDirect

Plant Physiology and Biochemistry

journal homepage: www.elsevier.com/locate/plaphy

Research article

Potassium supply promotes the mitigation of NaCl-induced effects on leaf photochemistry, metabolism and morphology of *Setaria viridis*

Ana Carolina Mendes Bezerra [a,*], David da Cunha Valença [a], Nicia Eloísa da Gama Junqueira [a], Cristina Moll Hüther [b], Junior Borella [c], Camila Ferreira de Pinho [d], Marcio Alves Ferreira [e], Leonardo Oliveira Medici [f], Bianca Ortiz-Silva [g], Fernanda Reinert [a]

[a] Universidade Federal Do Rio de Janeiro/IB —Dept. of Botany, Av. Carlos Chagas Filho, 373 — Ilha Do Fundão —21941-902, Rio de Janeiro, RJ, Brazil
[b] Universidade Federal Fluminense – Dept. of Agricultural and Environmental Engineering, R. Passo da Pátria 156, São Domingos — 24210-240 — Niterói, RJ, Brazil
[c] Universidade Federal Do Rio Grande – Institute of Biological Sciences, Av. Itália, Km 8, Bairro Carreiros – 96203-900 – Rio Grande, RS, Brazil
[d] Universidade Federal Rural Do Rio de Janeiro — Dept. of Plant Sciences, Rod. BR 465, Km 7 — 23897-000, Seropédica, RJ, Brazil
[e] Universidade Federal Do Rio de Janeiro/IB — Dept. of Genetics, Av. Carlos Chagas Filho, 373 — Ilha Do Fundão — 21941-902, Rio de Janeiro, RJ, Brazil
[f] Universidade Federal Rural Do Rio de Janeiro — Dept. of Physiological Sciences, Rod. BR 465, Km 7 — 23897-000, Seropédica, RJ, Brazil
[g] Universidade Federal Do Rio de Janeiro- NUMPEX-Bio, Estrada de Xerém, 27- Duque de Caxias — 25245-390, Rio de Janeiro, RJ, Brazil

ARTICLE INFO

Keywords:
A10.1
Abiotic stress
Chlorophyll fluorescence
K^+ fertilization
Model plant
Salinity

ABSTRACT

Soil salinity has the potential to severely affect crop performance. To maintain cell functioning and improve salt tolerance, the maintenance of K^+ homeostasis is crucial in several plant metabolism processes. Besides, potassium fertilization can efficiently alleviate the perilous effects of salinity. We characterized impacts in *Setaria viridis* exposed to NaCl and KCl to underlying photochemistry mechanisms, K^+ and Na^+ shoot contents, enzymatic activity, electrolytic leakage, and morphological responses focusing on non-stomatal limitation of photosynthesis. Plants were exposed to sodium chloride (NaCl; 0, 150 and 250 mM) and potassium chloride (KCl; 0, 5, 9 mM). The exposure to NaCl affected *S. viridis* leaves morphological and physiologically. Plants submitted to 150 mM showed reductions in performance indexes (PI_{abs} and PI_{total}; JIP-test), and the presence of positive K- and L-bands. Plants exposed to 250 mM exhibited blockage in electron flow further than Q_A within 48h and permanent photoinhibition at 96 h. The presence of 9 and 5 mM of KCl counteracted the effects of NaCl on plants submitted to 150 mM, concomitant with increases in K^+ accumulation and cell turgidity conservation, causing positive effects in plant growth and metabolism. Neither KCl concentrations were effective in reducing NaCl-induced effects on plants exposed to 250 mM of NaCl. Our results support the conclusion that greater availability of K^+ alleviates the harmful effects of salinity in *S. viridis* under moderate stress and that application of KCl as means of lightning saline stress has a concentration and a salt level limit that must be experimentally determined.

1. Introduction

Agricultural production is greatly affected by soil salinity (Munns and Tester, 2008; Yan et al., 2013). It is estimated more than 1 billion hectares of salt-affected land worldwide, with increasing trend (Ivushkin et al., 2019). Salinity impacts on crops are often described as having two specific components, osmotic and ionic (Deinlein et al., 2014). Osmotic stress refers to the reduction of water potential in soil solution as result of excess salt in the root environment affecting water availability to plants. Ionic imbalance is associated with the accumulation of sodium (Na^+) and chloride (Cl^-) interfering with ionic homeostasis, generating ion toxicity and nutritional disorders (Zhao et al., 2020).

The impact of osmotic and ionic components can lead to severe oxidative stress depending on plant species, stage of development and, responses and mechanisms of adaptation (Deinlein et al., 2014; Kataria and Verma, 2018). Moreover, photosynthesis is very sensitive to

* Corresponding author.
E-mail addresses: anacarolina_mb@yahoo.com.br, anacarolinamb.ufrj@gmail.com (A.C. Mendes Bezerra), davidcunha@id.uff.br (D. da Cunha Valença), nicia.junqueira@gmail.com (N.E. da Gama Junqueira), cristinahuther@gmail.com (C. Moll Hüther), borellaj@gmail.com (J. Borella), camilafepi@hotmail.com (C. Ferreira de Pinho), marcioaf@ufrj.br (M. Alves Ferreira), lmedici@gmail.com (L. Oliveira Medici), bianca.ortix@gmail.com (B. Ortiz-Silva), freinert@biologia.ufrj.br (F. Reinert).
https://doi.org/10.1016/j.plaphy.2021.01.021
Received 20 December 2020; Accepted 15 January 2021. Available online 21 January 2021 0981-9428/

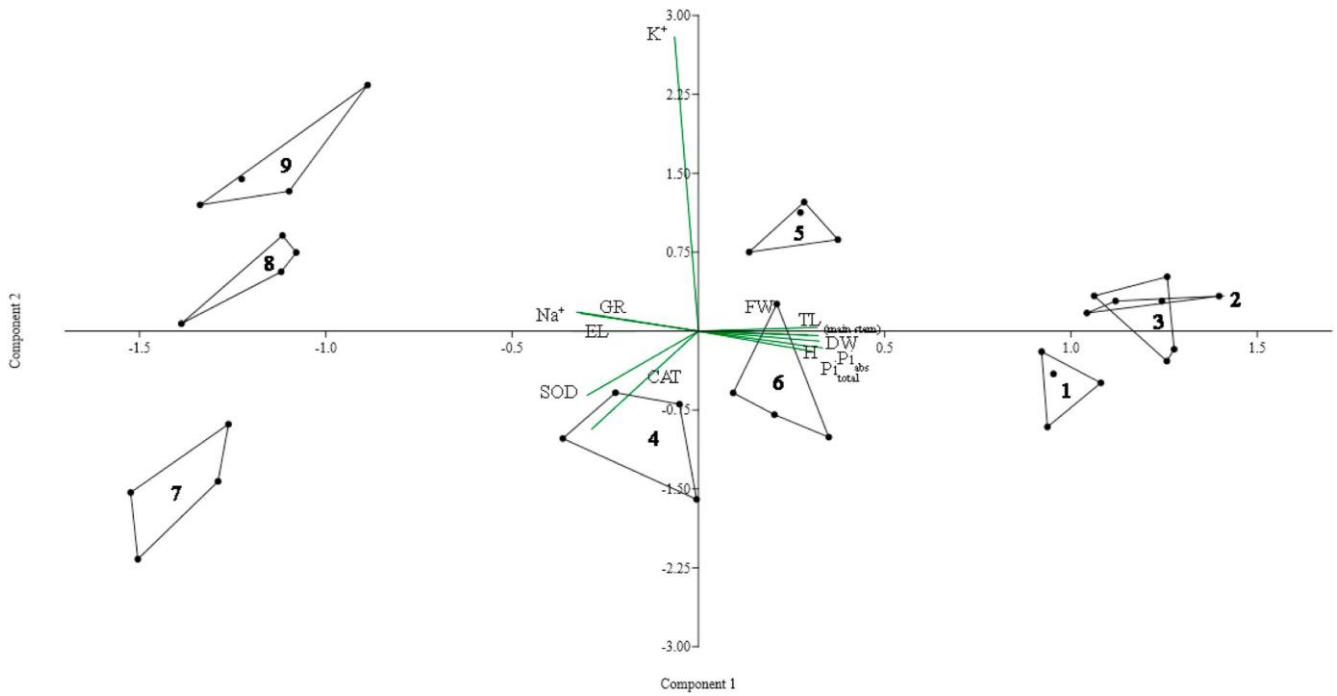

Fig. 1. Principal component analysis (PCA) of *S. viridis* leaves exposed to NaCl with and without KCl application. Axes is in eigenvalue scale. 1 - 0 mM of NaCl; 2 - 0 mM of NaCl +5 mM of KCl; 3 - 0 mM of NaCl +9 mM of KCl; 4–150 mM of NaCl; 5–150 mM of NaCl +5 mM of KCl; 6–150 mM of NaCl +9 mM of KCl; 7–250 mM of NaCl; 8–250 mM of NaCl +5 mM of KCl; 9–250 mM of NaCl +9 mM of KCl. GR: Glutathione Reductase activity; SOD: Superoxide dismutase activity; CAT: catalase activity; EL: electrolytic leakage; Na+: shoot Na+ content; K+: shoot K+ content; FW: shoot fresh weight; DW: shoot dry weight; H: height; TL: total number of leaves of the main stem; PIabs and PItotal: performance indexes of chlorophyll *a* fluorescence (JIP-test).

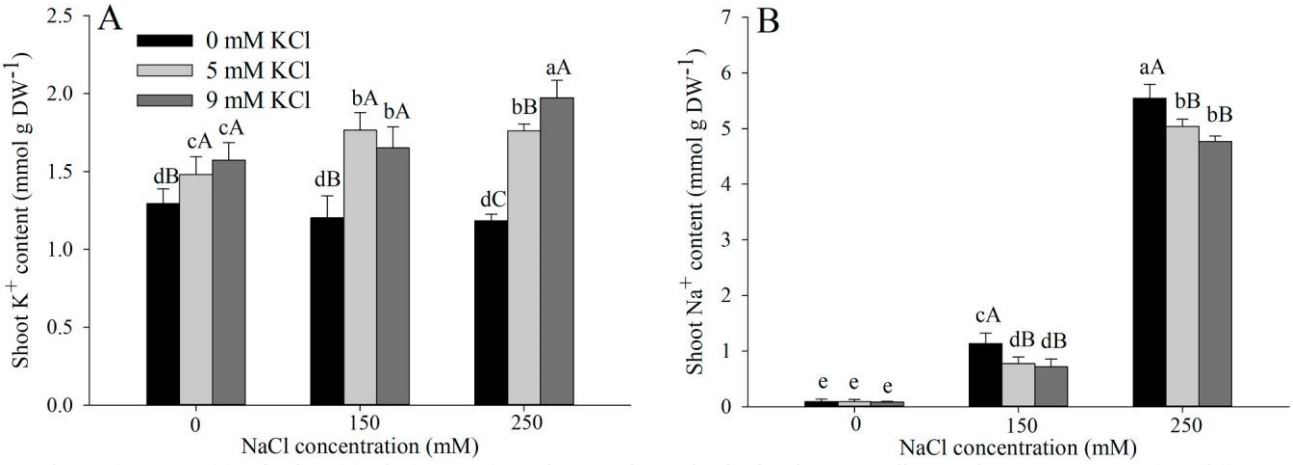

Fig. 2. Accumulation of potassium (A) and sodium (B) in leaf tissues of S. viridis exposed to NaCl and KCl application. Small caption letters represent significant differences using the Scott-Knott test at $p < 0.05$ and upper case letters represent significant differences of KCl mitigation within level of salt using the Scott-Knott test at $p < 0.05$ (means ± standard deviation; n = 4).

environmental stresses and shows a robust relationship with crop biomass and yield (Bussotti et al., 2010; Yan et al., 2013). Negative regulation of photosynthesis might be related to stomatal and diffusive limitation of CO_2 influx to the Rubisco (Ribulose-1,5-Bisphosphate Carboxylase/Oxygenase; EC 4.1.1.39) site, which promotes the consequent saturation and imbalance of the electron transport chain (ETC), causing excessive production of reactive oxygen species (ROS) (Acos-ta-Motos et al., 2017; Chaves et al., 2009). When ROS formation exceeds plants antioxidant capacity it causes alterations to the activity of various ion channels affecting plant ionic homeostasis (Demidchik, 2018) and damaging biological molecules such as lipids, proteins, and nucleic acids (Sharma et al., 2012).

The accumulation of ions in the cytoplasm, as an attempt to adjust osmotically, and the degradation of cellular membranes caused by ROS, generates ion leakage and, therefore, increases the passage of toxic ions into the chloroplast (Pan et al., 2020). Disturbance of ionic homeostasis in chloroplast may cause inactivation of key photosynthetic enzymes, dissociation of photosynthetic intrinsic and extrinsic proteins supporting PSII and PSI activities, accelerates damage to photosystems complexes, and degradation of pigments. Such circumstance characterizes the non-stomatal limitation of the photosynthetic process (Chaves et al., 2009; Kan et al., 2017; Pan et al., 2020; Sasi et al., 2018).

Even though the influence of both stomatal and non-stomatal limitations will jointly impact plants' photosynthetic capacity, the major

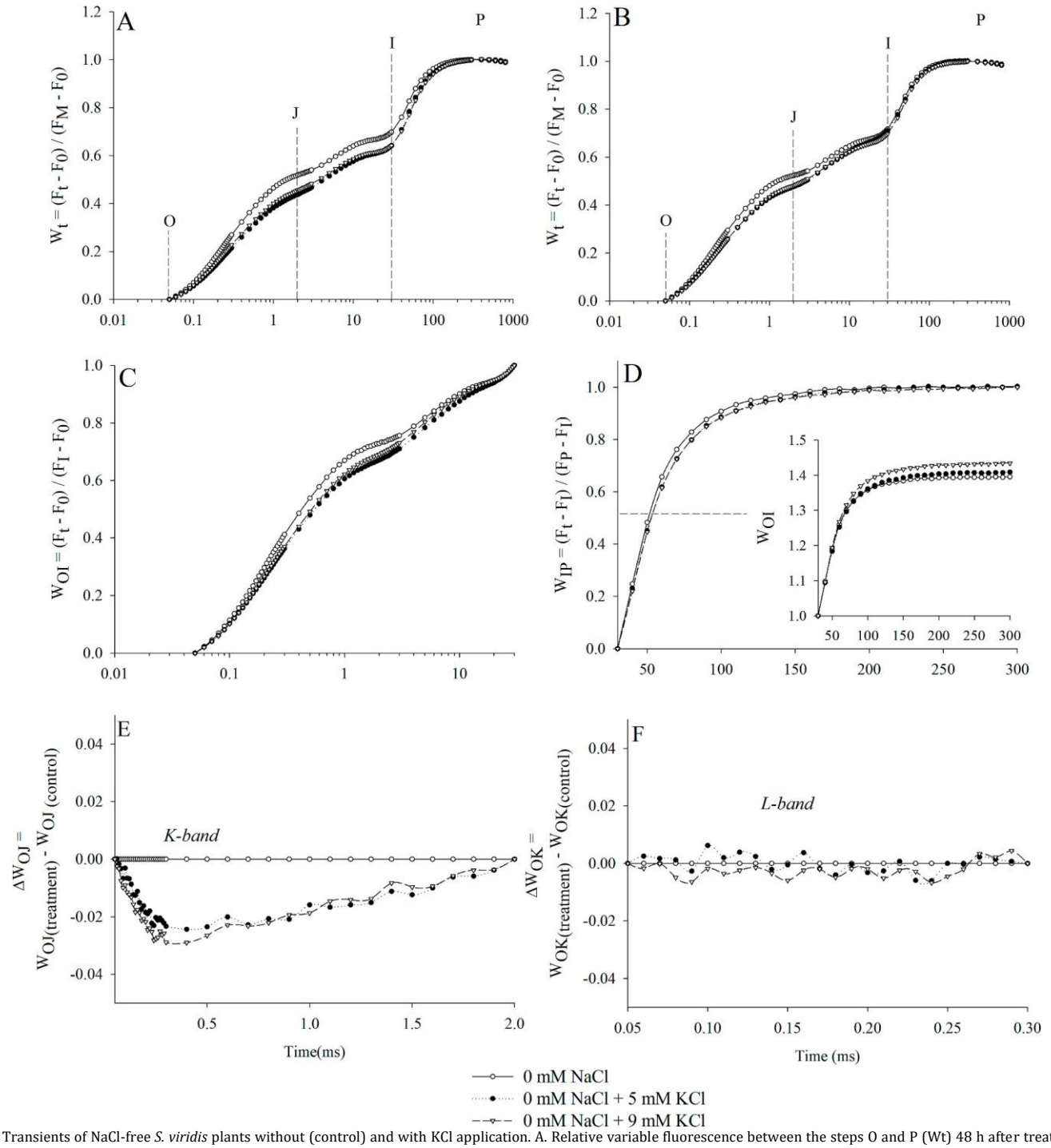

Fig. 3. Transients of NaCl-free *S. viridis* plants without (control) and with KCl application. A. Relative variable fluorescence between the steps O and P (Wt) 48 h after treatments application; B. Relative variable fluorescence between the steps O and P (Wt) 96 h after treatments application; C. Relative variable fluorescence between the steps O and I (WOI) 96 h after treatments application; D. Relative variable fluorescence between the steps I and P (WIP) and WOI in the insert 96 h after treatments application; E. The PF transient curves normalized between Fo and FJ, expressed as WOJ = [(Ft-Fo)/(FJ-Fo)] 96 h after treatments application; F. The PF transient curves normalized between FO and FK, presented as WOK = [(Ft-FO)/(FK-FO)] 96 h after treatment application. The signals were plotted on a logarithmic time scale. Each curve is the average of 10 replicates.

limiting factor to photosynthesis of plants coping with salinity was suggested to be dependent on the severity of the stress (Hussain et al., 2020; Rivelli et al., 2002). Non-stomatal effects are described as predominant at higher levels of salinity (Hussain et al., 2020; Maricle and Maricle, 2018). Accordingly, under mild stress, PSII photoinhibition was described as a secondary cause in photosynthesis restriction in two corn varieties (Hichem et al., 2009), while reductions in PSII integrity and carboxylation capacity are the major factors limiting photosynthesis under high levels of salt in sorghum (Netondo et al., 2004), and in the high-tolerant C_4 grasses *Panicum antidotale* Retz. (Hussain et al., 2020), *Panicum turgidum* Forssk (Koyro et al., 2013), *Spartina pectinate* Link and, *Distichlis spicata* (L.) Greene (Maricle and Maricle, 2018).

High levels of salt in soil solution negatively affect potassium (K^+) absorption and homeostasis in leaves (Hasanuzzaman et al., 2018; Percey et al., 2016; Shabala and Pottosin, 2014). Among the macronutrients, K^+ performs several fundamental functions in plant metabolism,

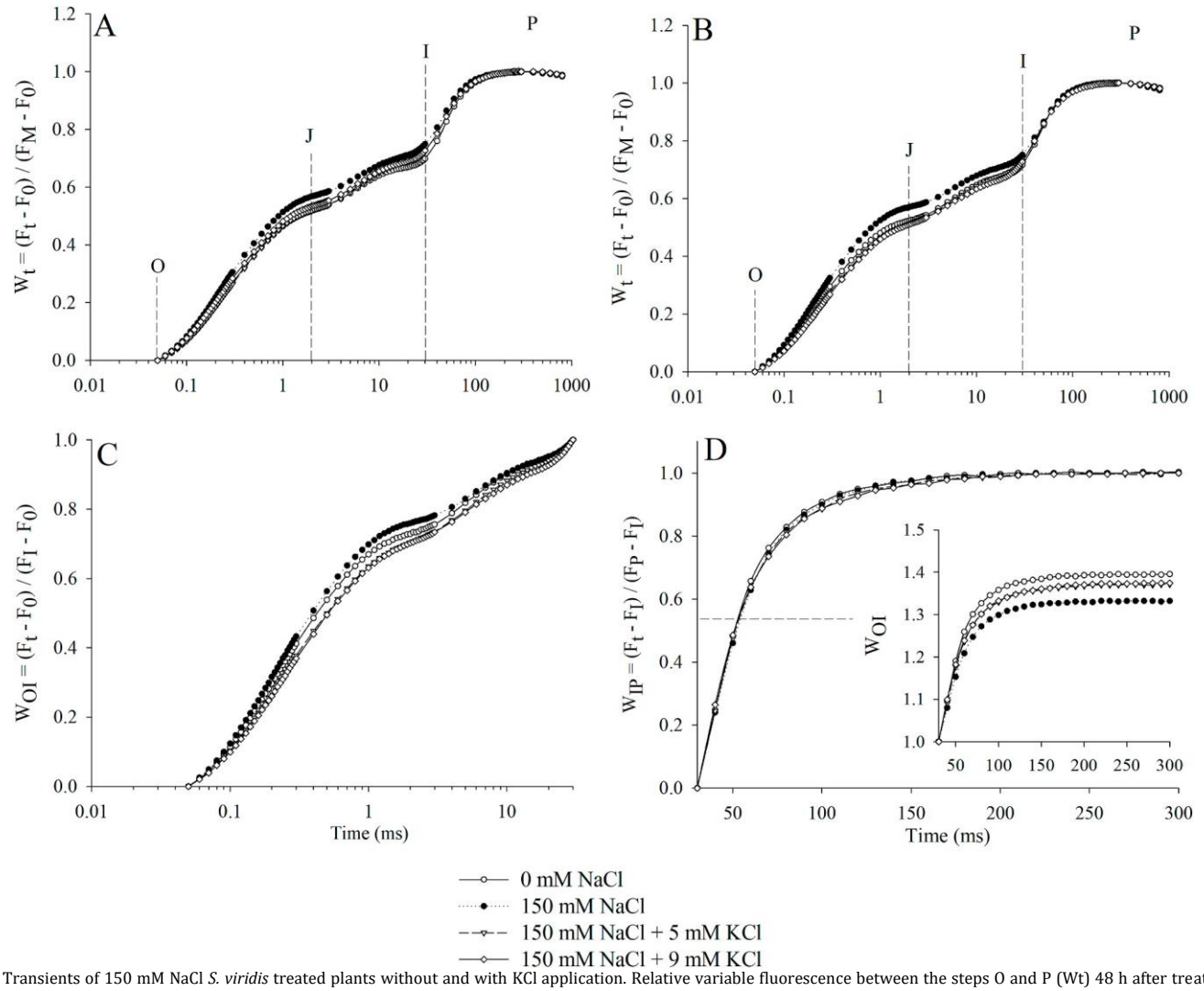

Fig. 4. Transients of 150 mM NaCl *S. viridis* treated plants without and with KCl application. Relative variable fluorescence between the steps O and P (Wt) 48 h after treatments application; B. Relative variable fluorescence between the steps O and P (Wt) 96 h after treatments application; C. Relative variable fluorescence between the steps O and I (WOI) 96 h after treatment application; D. Relative variable fluorescence between the steps I and P (WIP) and WOI in the insert 96 h after treatments application. The signals were plotted on a logarithmic time scale. Each curve is the average of 10 replicates.

besides having a fundamental role in stress tolerance capacity (Cakmak, 2005; Hasanuzzaman et al., 2018). Alternatively, the ability to retain K^+ ions in crop plants is often described as a crucial strategy to enable plants to better survive under abiotic and biotic stresses (Zhao et al., 2001; Zörb et al., 2014). The effect of adequate K^+ homeostasis on plants' photosynthesis is associated with both stomatal and non-stomatal effects and its role on the activation of photosynthetic enzymes and, protein and ATP synthesis were reported as more injurious to the photosynthetic process than its effects on CO_2 diffusion due to stomatal limitations (Murata et al., 2012). Exogenous K^+ application has been shown as an efficient alternative to alleviate toxic NaCl effects in several studies, with positive effects in photosynthetic parameters (Abbasi et al., 2015; Burbulis et al., 2017; Jan et al., 2017; Kaddour et al., 2009; Siringam et al., 2013).

The use of model organisms to accelerate abiotic stress studies is mandatory (Brutnell et al., 2010; Doust et al., 2019). *Setaria viridis* (L.) Beauv. is an annual Poaceae with C_4 photosynthetic metabolism (Aliscioni et al., 2016; Junqueira et al., 2018) described as an excellent vehicle for salinity stress studies (Doust et al., 2019). *S. viridis* possesses a great capacity of recovery from osmotic stress efficiently making physiological and biochemical adjustments under such conditions after rehydration cycles (Luo et al., 2011). In addition, also maintain the growth and display recovery of photosynthetic parameters over time under prolonged water deficits (Valença et al., 2020). Reduction in growth coupled with drought-stress of *S. viridis* was associated equally to stomatal and non-stomatal factors as shown by decreases in PSII quantum yield and gas exchange parameters under mild and severe water restriction (Burbulis et al., 2017). However, exposure to NaCl only had significant impact on PSII activity from 120 mM of NaCl (Guo et al., 2011), whereas net photosynthesis suffered reductions of ~30% and 60% under 100 and 200 mM of NaCl, respectively, 96h after the exposure to stress (Duarte et al., 2019).

Although studies of the impacts of the excess of salts on plants are quite evolved, their effects on non-stomatal limitation of photosynthesis are still little explored (Pan et al., 2020). The impacts of salinity on the quality of soil represents a major concern for food production and conservation programs. Plant production in salt impacted soils represents one of the primary demands. The use of model organisms is the key to improve our capacity to test alternative and remediation approaches. We present data from chlorophyll *a* fluorescence, K^+ and Na^+ content, antioxidant enzyme activities, and electrolytic leakage (EL) along with macro and micromorphological analysis. This study aimed to characterize the simultaneous influence of saline components on specific blockages and interferences in leaf photochemistry (if any), metabolism

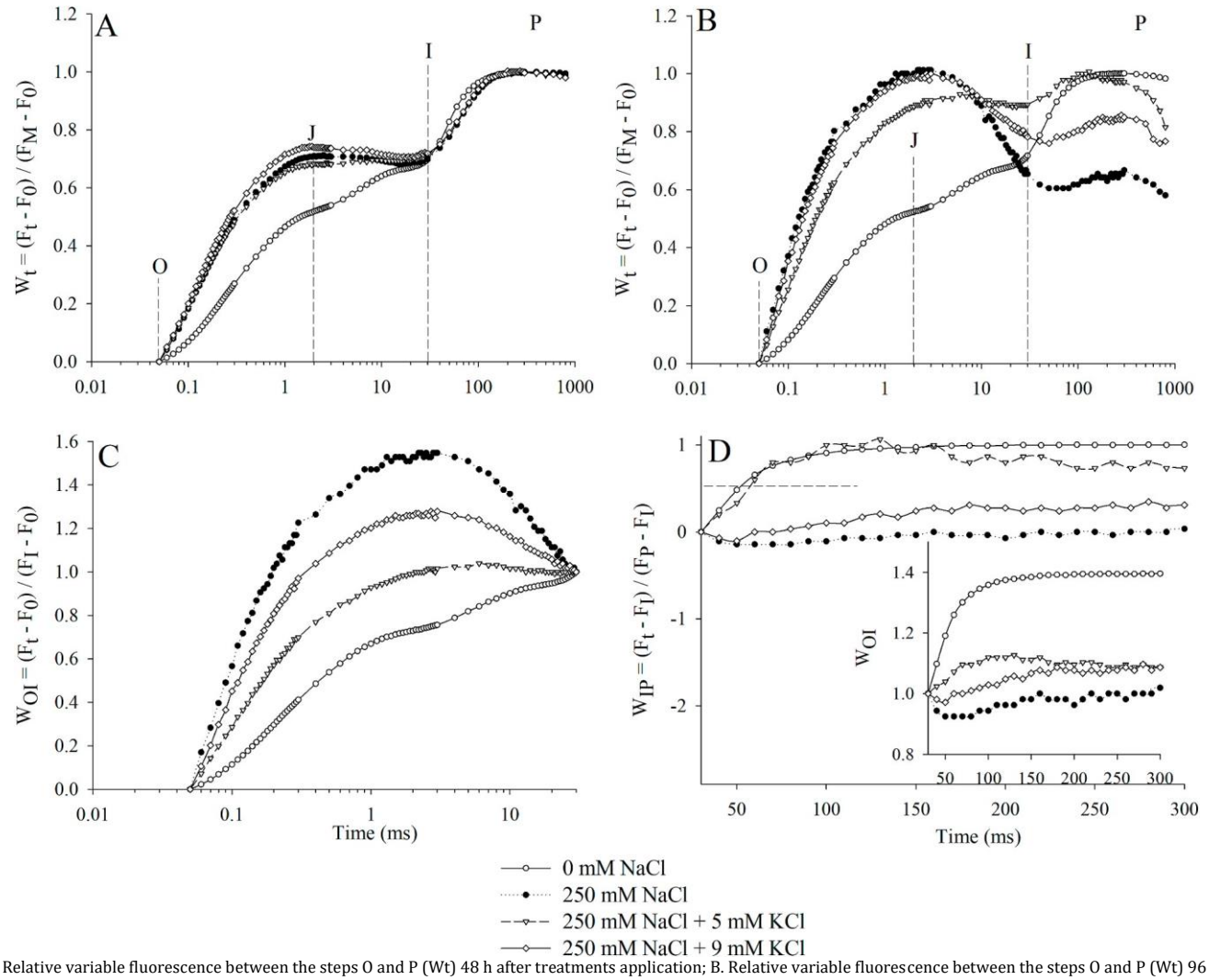

Fig. 5. Relative variable fluorescence between the steps O and P (Wt) 48 h after treatments application; B. Relative variable fluorescence between the steps O and P (Wt) 96 h after treatments application; C. Relative variable fluorescence between the steps O and I (WOI) 96 h after treatment application; D. Relative variable fluorescence between the steps I and P (WIP) and WOI in the insert 96 h after treatments application. The signals were plotted on a logarithmic time scale. Each curve is the average of 10 replicates.

and morphology of *S. viridis,* and the effectiveness of K^+ supply in alleviating saline stress-related symptoms. Data described in this study can be used to identify specific sites of blockages and alterations in photosynthetic electron transport as response to different levels of salinity and its reflection on plants' metabolism and morphology. Our results can contribute to research on crop improvement and also indicate a promising effect of extra potassium fertilization in mitigating stress-responses by maintaining equilibrated K^+/Na^+ ratios in *S. viridis* leaves moderately salt-stressed.

2. Materials and methods

2.1. Plant material and growth conditions

The experiment was carried out with the *Setaria viridis* A10.1 accession in hydroponics. During the entire experimental period, plants were kept in a growth chamber under an average temperature of 30 ± 2 °C (day) and 25 ±2 °C (night), photoperiod of 16/8 h (light/dark), and light intensity of 750 μmol m^{-2} s^{-1}. A combination of blue-red-white LED lamps provided this light intensity. Plant pots were randomized every two days to avoid discrepancies related to the position on the shelves.

Seeds were germinated and kept in hand-assembled nurseries filled with deionized water until the phenological state 1.1 according to the BBCH scale, when the first leave was fully expanded (Junqueira et al., 2019). After that, seedlings were transferred to individual hydroponic systems. The hydroponic system consisted of 0.2 L pots containing Hoagland nutrient solution at one-fourth of full strength (Hoagland and Arno, 1938; Caisson labs, nº 2) replaced every five days.

Treatments were applied when the fifth leave was fully expanded (phenological stage 1.5 according to the BBCH scale, Junqueira et al., 2019) ~ 15 days after germination. We used a factorial scheme 3x3, where factor A was the sodium chloride treatment (NaCl; 0, 150, and 250 mM) and factor B the application potassium chloride (KCl; 0, 5, and 9 mM) with 15 replicates, totaling 135 experimental units. Due to previous observations, where panicles began to emerge 120 h after treatment imposition, plants were harvested 96 h after salt treatment imposition. Also, longer exposure periods proved to be sufficient to cause the death of *S. viridis* plants exposed to levels of NaCl greater or equal to 250 mM NaCl, without causing further significant changes at lower NaCl levels tested (100, 150, and 200 mM of NaCl) (data not published). All analyses and measurements, except chlorophyll *a* fluorescence, relate to the time of harvesting.

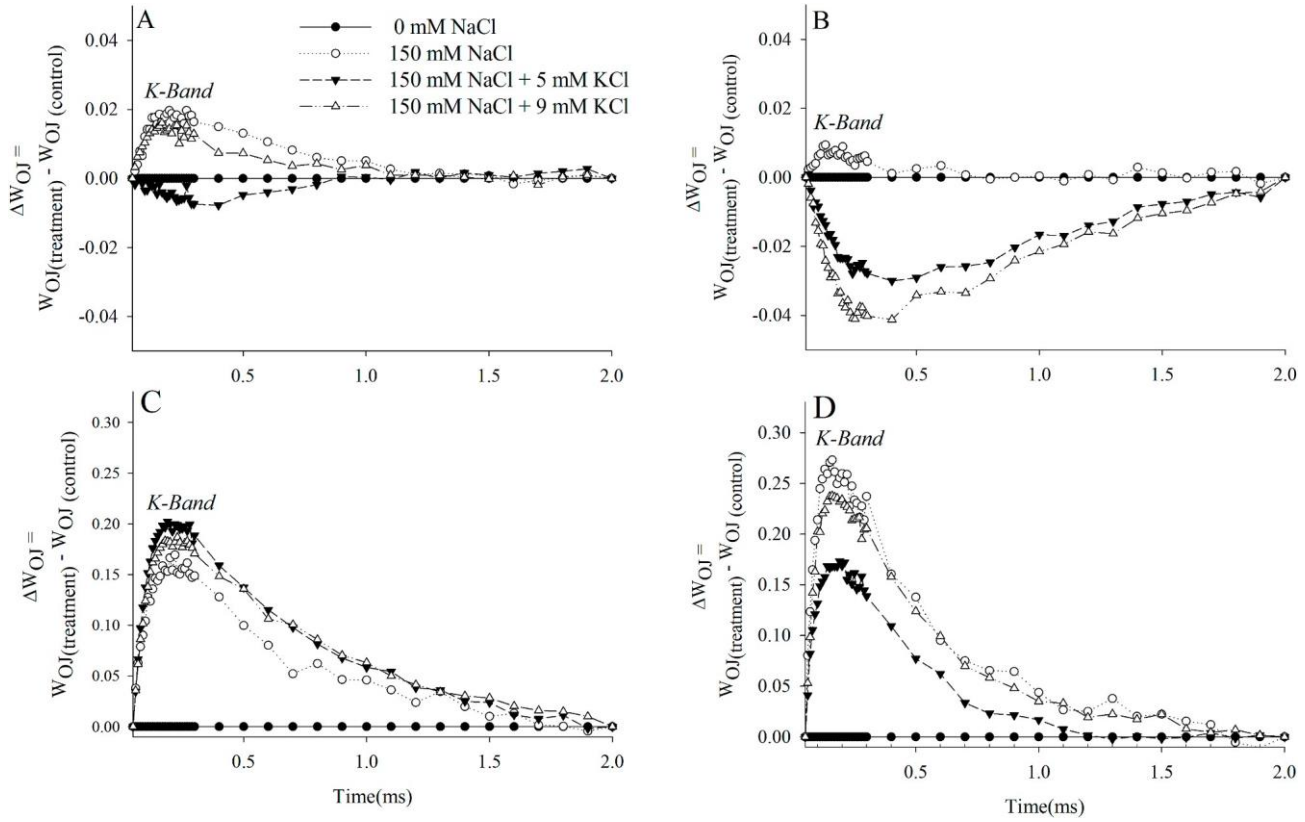

Fig. 6. K-bands of 150 and 250 mM NaCl *S. viridis* treated plants without and with KCl application 48 and 96 h after treatments application. A. The PF transient curves normalized between Fo and FJ, expressed as WOJ = [(Ft-Fo)/(FJ-Fo)] of 150 mM plants 48 h after treatment application; B. The PF transient curves normalized between Fo and FJ, expressed as WOJ = [(Ft-Fo)/(FJ-Fo)] of 150 mM plants 96 h after treatments application; C. The PF transient curves normalized between Fo and FJ, expressed as WOJ = [(Ft-Fo)/(FJ-Fo)] of 250 mM plants 48 h after treatment application; D. The PF transient curves normalized between Fo and FJ, expressed as WOJ = [(Ft-Fo)/(FJ-Fo)] of 250 mM plants 96 h after treatments application. The signals were plotted on a logarithmic time scale. Each curve is the average of 10 replicates.

2.2. K^+ and Na^+ content

K^+ and Na^+ contents were analyzed as described by Munns et al. (2010). For extraction, plant material was collected, moved to paper bags, and placed in a forced circulation oven at 70 °C for two days. Samples were grounded and 0.2 g of shoot tissue was transferred to 5 mL digestion with 0.5 M nitric acid. The material was kept in a shaker for two days. After that, readings were done using a flame photometer (Analyzer 910 M model, Comércio e Indústria Ltda, São Paulo, Brazil).

2.3. Chlorophyll *a* fluorescence transient

Measurements of chlorophyll *a* fluorescence transients were performed with a Portable Chlorophyll Fluorimeter (HandyPEA, Hansatech, King's Lynn, Norfolk, UK). The readings were done in fully expanded leaves from the last developed node in the mornings (from 10 to 11 a.m.) after dark adaptation for at least 20 min. Measurements were done in ten plants for each treatment. Fluorescence emission was induced by exposing the leaf to a pulse of saturating red-light flash (peak at 650 nm) at an intensity of 3000 μmol photons m^{-2} s^{-1}. The OJIP fluorescence transients are based on the polyphasic fast fluorescence rise from the lowest (F_O) to the highest (F_M) intensity of fluorescence (Strasser et al., 2004). The O-step is the initial fluorescence level (50 μs), followed by intermediate levels J (2 ms) and I (30 ms), and the peak level P (500 ms). OJIP transients were evaluated by using normalizations and subtractions to compare the events reflected in the OJ, OI, and IP steps. Transients were normalized as relative variable fluorescence: $W_t = (F_t - F_O)/(F_J - F_O)$, $W_{OI} = (F_t - F_O)/(F_I - F_O)$ and $W_{IP} = (F_t - F_I)/(F_P - F_I)$. Difference between kinetics from relative variable fluorescence data were calculated ($\Delta W = W_{treatment} - W_{control}$), revealing two hidden bands between the steps W_{OJ} (K-band; 300 μs) and W_{OK} (L-band; 150 μs) following Yusuf et al. (2010). JIP-test parameters were calculated using the software Biolyzer (Bioenergetics Laboratory, University of Geneva, Switzerland) and the equations proposed by Strasser et al. (2004) and Santos Júnior et al. (2015).

2.4. Biometric traits

Plant height, shoot fresh and dry weight were measured using a digital caliper (Maxwell 150 mM Digital Caliper, China) and an analytical laboratory balance (Bioprecisa JA3003N, Curitiba, PR, Brazil), respectively. To obtain dry weight, plants were oven-dried at 70 °C (Olidef Medical CZ, SP, Brazil) until constant weight. The number of leaves of the main stem was counted.

2.5. Electrolytic leakage

Electrolytic Leakage was analyzed according to Liu et al. (2015) using a conductivity meter (3540 model, Jenway, Staffordshire, UK). Initially, 0.2 g of leaf tissue was collected and placed in Falcon-type tubes containing 20 mL of deionized water. After 24 h in a shaker, the electrical conductivity of the solution was measured (C1). Samples were, then, autoclaved at 120 °C for 30 min, and when the tubes reached ambient temperature again, the conductivity of the solution with the dead tissue was measured (C2). Electrolytic leakage was calculated according to the formula: *EL* (%) = (C1/C2) x 100.

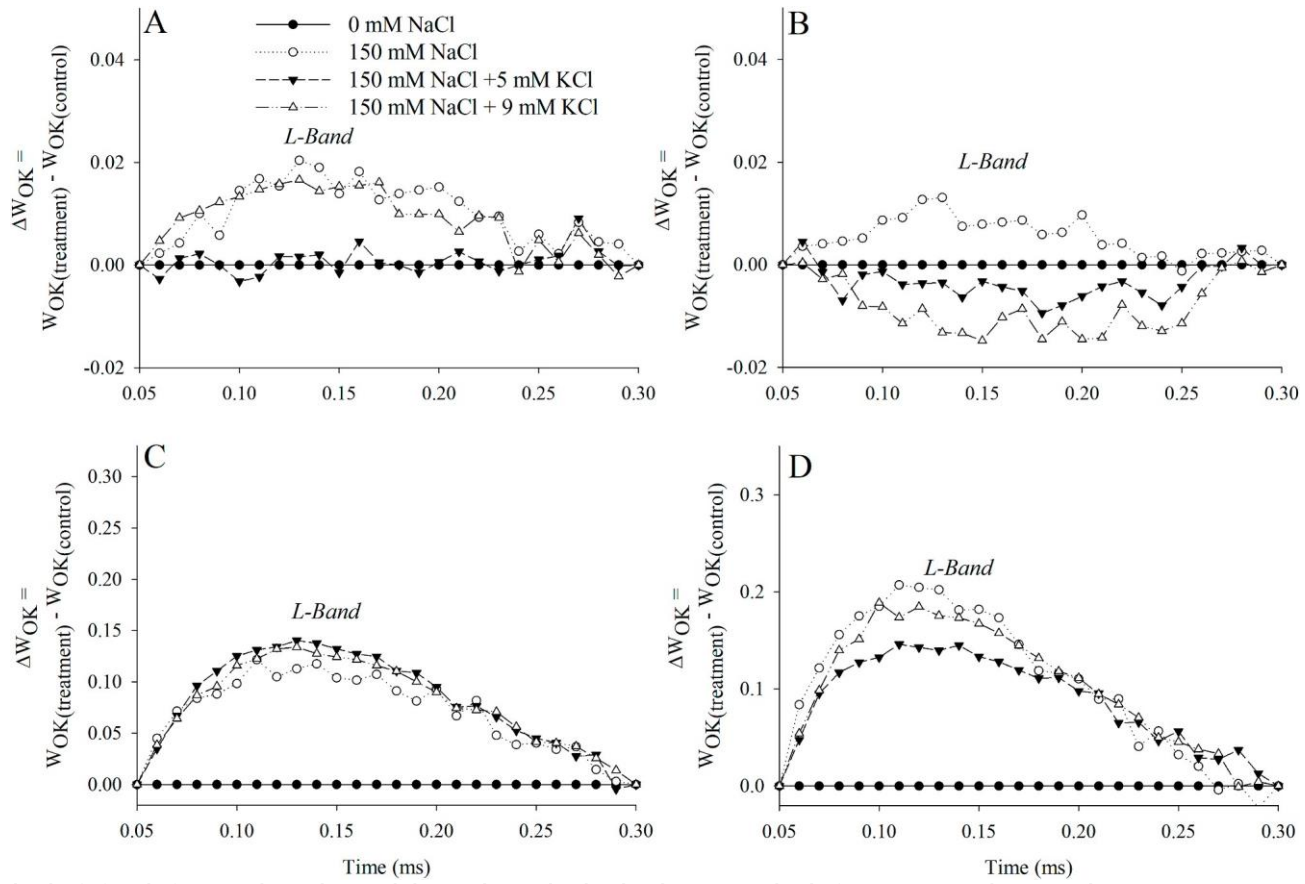

Fig. 7. L-bands of 150 and 250 mM NaCl *S. viridis* treated plants without and with KCl application 48 and 96 h after treatments application. A. The PF transient curves normalized between FO and FK, presented as WOK = [(Ft-FO)/(FK-FO)] of 150 mM plants 48 h after treatment application; B. The PF transient curves normalized between FO and FK, presented as WOK = [(Ft-FO)/(FK-FO)] of 150 mM plants 96 h after treatments application; D. The PF transient curves normalized between FO and FK, presented as WOK = [(Ft-FO)/(FK-FO)] of 250 mM plants 48 h after treatments application; E. The PF transient curves normalized between FO and FK, presented as WOK = [(Ft-FO)/(FK-FO)] of 250 mM plants 96 h after treatment application. The signals were plotted on a logarithmic time scale. Each curve is the average of 10 replicates.

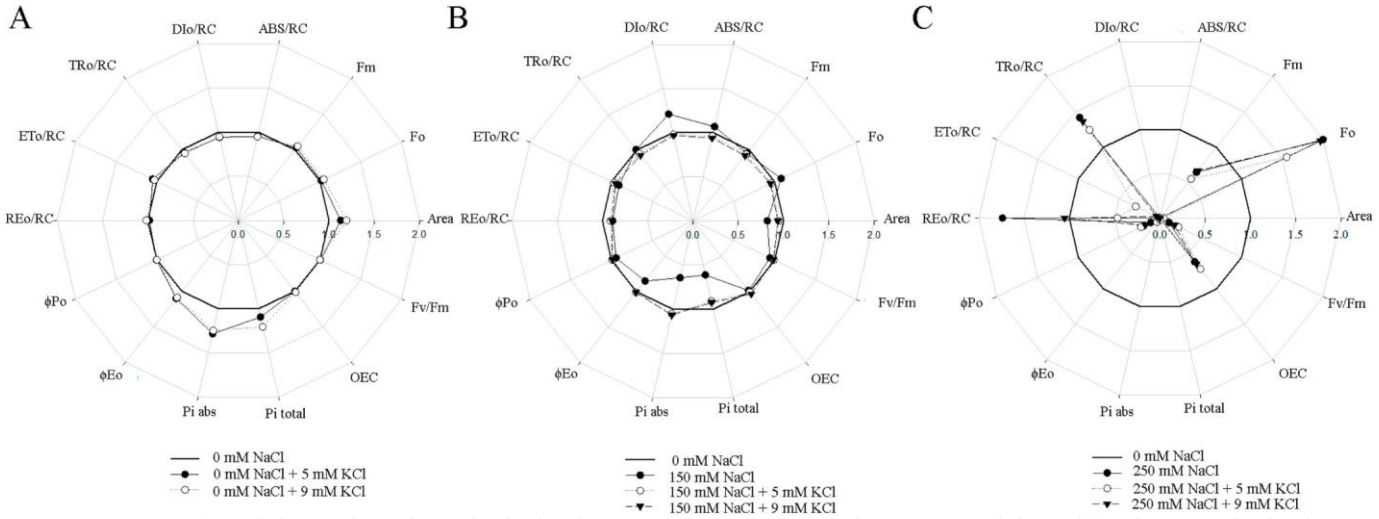

Fig. 8. JIP test parameters of *S. viridis* leaves submitted to NaCl and KCl application at 96 h after treatment application. A. Control plus NaCl-free plants treated with KCl; B. Control plants plus plants treated with 150 mM of NaCl; C. Control plants plus plants treated with 250 mM of NaCl (n = 10).

2.6. Antioxidant enzyme and protein-specific activity assays

Shoots were collected (0.2 g) and immediately stored at −80 ˚C for further analysis. Samples were ground to powder after frozen in liquid nitrogen, homogenized with extraction buffer (Potassium Phosphate 200 mM, pH 7.8; EDTA 0.1 mM; ascorbic acid 20 mM; Dithiothreitol 5 mM, β-mercaptoethanol 5 mM, Triton X-100 0.01% and water) and centrifuged at 12,000 *g* for 20 min at 4 ˚C (Eppendorf centrifuge 5424,

Table 1
JIP parameters of chlorophyll *a* fluorescence of *Setaria viridis* exposed to NaCl and KCl application.

		Fo			Fo/Fm			OEC		
		NaCl (mM)								
		0	150	250	0	150	250	0	150	250
KCl (mM)	0	474 ± 34a	512 ± 53a	948 ± 46 aB	0.30 ± 0.01c	0.34 ± 0.04c	0.92 ± 0.02a	0.43 ± 0.02a	0.39 ± 0.03a	0.21 ± 0.05b
	5	481 ± 38a	456 ± 39a	736 ± 45bA	0.29 ± 0.02c	0.31 ± 0.01c	0.83 ± 0.1b	0.46 ± 0.03a	0.46 ± 0.03a	0.27 ± 0.05b
	9	496 ± 36a	450 ± 39a	932 ± 44 aB	0.30 ± 0.02c	0.31 ± 0.1c	0.87 ± 0.2b	0.47 ± 0.03a	0.48 ± 0.03a	0.21 ± 0.05b

		PIabs			PItotal			ϕEO		
		NaCl (mM)								
		0	150	250	0	150	250	0	150	250
KCl (mM)	0	0.68 ± 0.14b	0.44 ± 0.14c	–	1.01 ± 0.22a	0.62 ± 0.25c	–	0.34 ± 0.03b	0.28 ± 0.04c	–
	5	0.90 ± 0.24a	0.70 ± 0.10b	–	1.11 ± 0.27a	0.89 ± 0.18b	–	0.37 ± 0.03a	0.34 ± 0.02b	–
	9	0.85 ± 0.24a	0.72 ± 0.13b	–	1.23 ± 0.24a	0.92 ± 0.20b	–	0.36 ± 0.03a	0.34 ± 0.02b	–

Small case letters represent significant differences using Scott-Knott test at $p < 0.05$ (means ± standard deviation; n = 10). Data related to 96 h after exposition to treatment. Values replaced by (—) were very close to zero.

Hauppauge, NY, USA). The supernatant was used as crude enzymes extract. Enzymes and protein-specific activity were determined in a Thermo Scientific Multiskan GO spectrophotometer (ThermoFisher Scientific, Vartaa, Finland).

Superoxide dismutase (SOD; EC 1.15.1.1) activity was assessed by monitoring the inhibition of the nitro blue-tetrazolium (NBT) coloration at 560 nm after exposure to light for 5 min. Ascorbate peroxidase (APX; EC 1.11.1.11) and catalase (CAT; EC 1.11.1.6) activities were evaluated by the decomposition of H_2O_2 at 290 and 240 nm, respectively, by measuring decreasing in absorbance during 2 min. Glutathione reductase (GR; EC 1.6.4.2) activity was measured as the oxidation of NADPH by the decrease of absorbance at 340 nm through successive readings for 2 min. Protein-specific activity quantification used bovine serum albumin (BSA) as standard. Samples were read at 595 nm at 5 min after reaction with Bradford's solution.

2.7. Anatomical and ultrastructural analysis

Samplings for micromorphological analysis were taken in triplicates from mid-third cross-sections of fully expanded leaf blades from the last developed nodes. For fixation, shoot fragments were immediately immersed in Karnovsky's solution (4% paraformaldehyde, 2.5% glutaraldehyde, 0.1 M sodium cacodylate buffer) and placed under vacuum for 2 h. Fragments were washed in 0.1 M sodium cacodylate buffer solution, post-fixed in 1% of tetroxide osmium during 2 h, and washed three times with sodium cacodylate 0.1 M buffer. Next, the fragments were dehydrated in increasing ethanolic series (15%, 30%, 50%, 70%, 90%, and 100%) with intervals of approximately 30 min between the exchanges.

For optical observations, fragments were embedded in Spurr's resin (Spurr, 1969) and polymerized at 70 °C for 12 h. Blocks were cut in transversal thin sections (1 μm) using an ultramicrotome PowerTome-PC (RMC Products, Tucson, AZ, USA), stained with 0.5% toluidine blue, and examined using a bright-field optical microscope (Leica DM 500-Wetzlar, Germany).

For micromorphological analysis (scanning electron microscopy; SEM) after the dehydration step, fragments were dried to the critical point (BAL-TEC, CPD-030, Principality of Liechtenstein). Fragments were placed in pin stubs with carbon tape, sputter-coated with gold (Desk V Sample Preparation, Denton Vacuum), scanned, and photographed using a scanning electron microscope at 20 kV (Vega 3LMU Tescan, Brno, Czech Republic).

2.8. Data analysis

Data were analyzed using Sisvar (Federal University of Lavras, Lavras, Brazil) software. After the verification of the homogeneity of variances using the Cochran homogeneity test, the results were submitted to analysis of variance ($p \leq 0.05$). In the presence of significant difference, Scott-Knott's test was used to determine the significance at $p \leq 0.05$. Principal Component Analysis (PCA) was carried out to investigate variable groupings with the aid of PAST 3 software (PAleontological STatistics).

3. Results

3.1. Principal component analysis

Principal component analysis showed a comprehensive understanding of the influence treatments had on the analyzed parameters and identified groupings (Fig. 1). The first and second components (PC1 and PC2) explained, respectively, 73.5 and 10.8% of the total variation among individuals. The main characteristics responsible for separating the individuals exposed to NaCl were shoot Na^+ content, shoot electrolytic leakage, and enzymatic activity, while NaCl-free plants were divided by biometric traits and photosynthetic performance indexes of the JIP-test. Shoot K^+ content was mainly responsible for separations among NaCl treated plants and plants that received KCl, bringing groups with additional K^+ closer to control groups (Fig. 1). This result was especially true for plants treated with 150 mM of NaCl.

3.2. K^+ and Na^+ content

NaCl addition caused a significant increase in shoot Na^+ concentration while K^+ concentration remained constant among all plants without KCl application (Fig. 2A and B). The increase of KCl supply led to a rise in K^+ content in shoots of both NaCl-treated and NaCl-free plants (Fig. 2A). Na^+ accumulation was reduced with the addition of KCl, especially in the highest salt treatment (Fig. 2B).

3.3. Chlorophyll a fluorescence transients

Curves of transient relative fluorescence (OJIP) normalized between the steps F_o and F_m at 48 h (Figs. 3A, 4A and 5A) and 96 h (Figs. 3B, 4B and 5B), OI- and IP-phases (Fig. 3C and D, 4C-D, and 5C-D) and the hidden K and L-bands (Fig. 3E and F) are shown in Figs. 3–5. In 48 h, the curves of control plants exhibited a typical polyphasic format OJIP (Fig. 3A). The application of 150 mM of NaCl slightly increased fluorescence peaks while maintaining the polyphasic curve format (Fig. 4A). Curves of plants exposed to 250 mM of NaCl exhibited a high sensitivity to salt as evidenced by the loss of the O–I curve shape, irrespective of K^+ application (Fig. 5A). Fluorescence peaks were reduced by KCl application in NaCl-free and plants treated with150 mM of NaCl (Figs. 3A and 5A).

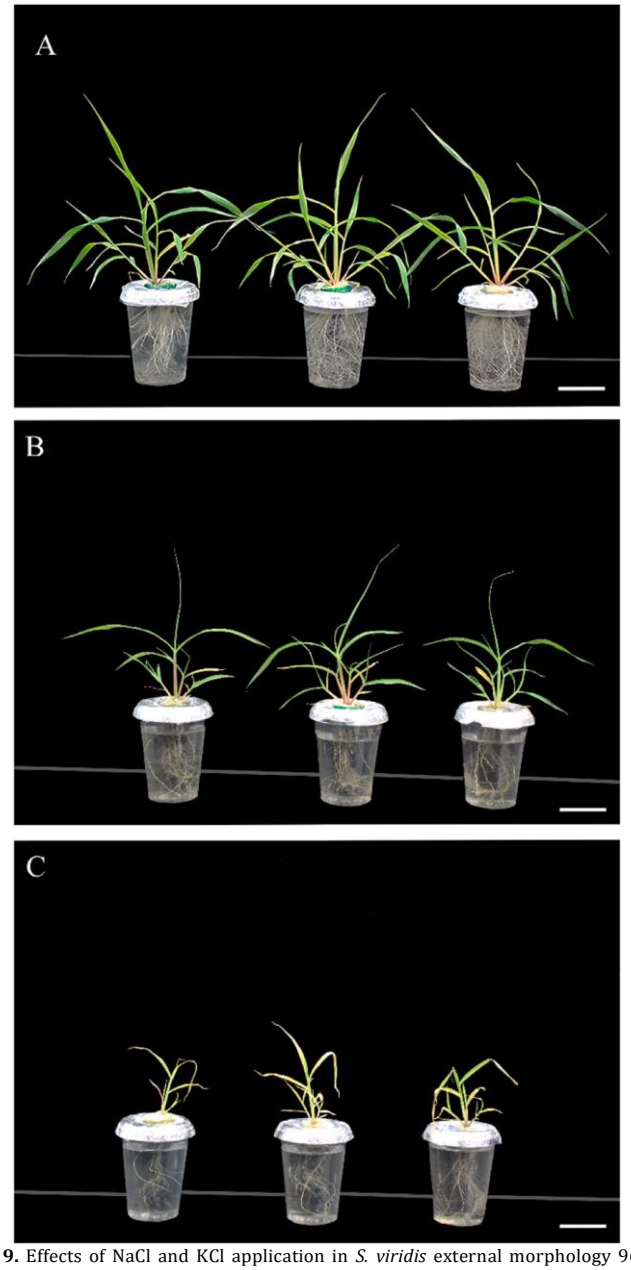

Fig. 9. Effects of NaCl and KCl application in *S. viridis* external morphology 96 h after exposure to the treatments. A. Non-salt treated plants with 0, 5 and 9 mM of KCl, respectively; B. Plants treated with 150 mM of NaCl and 0, 5 and 9 mM of KCl, respectively; C. Plants treated with 250 mM of NaCl and 0, 5 and 9 mM of KCl, respectively; Scale bars: 5 cm.

In 96 h the OJIP curve shape remained similar among control, NaCl-free, and plants exposed to 150 mM of NaCl (Figs. 3B and 4B). Fluorescence peaks of all salt-treated plants increased between O–I steps and were slightly reduced by the addition of KCl (Figs. 3C and 4C), while I–P steps were only affected in the highest NaCl concentration (Fig. 5D). The differences between transients made the K- and L-bands visible with peaks indicatives of stress for both salt treatments 48 h after exposure to the treatments (Fig. 6A and C; 7A and 7C). Application of KCl led to positive effects for all treatments, including NaCl-free (Fig. 3E and F), as shown by the negative K- and L-bands in 96 h (Fig. 6B and D; 7B and 7D) (see Fig. 7).

Several parameters deduced from the JIP-test were affected by both NaCl and KCl (Fig. 8). Photosynthetic performance index PI_{abs} (energy conservation from the exciton until the reduction of the final acceptors of the intersystem) showed a reduction of ~35 and 100% in the salt treatments of 150 and 250 mM, respectively (Table 1). However, the application of KCl increased PI_{abs} of 150 mM NaCl-treated plants, achieving values equivalent to those presented by control plants (Fig. 8B and Table 1). Similarly, PI_{abs} of NaCl-free plants with the addition of KCl improved compared to control plants (Fig. 8A; Table 1).

The performance index PI_{total}, which describes the total photosynthetic performances up to the final acceptors of photosystem I (PSI), also showed a salt-dependent reduction in plants treated with 150 mM (~39%) and 250 mM (~100%) of NaCl (Fig. 8B and C; Table 1). Application of KCl (5 and 9 mM) increased PI_{total} among the plants under the concentration of 150 mM of NaCl, although these values were still ~10% lower than that of control plants. Similarly, the area between the OJIP curve and the line F_o ∓ F_M, energy yield ϕ_{Eo} (quantum yield of electron transport) were also sensitive to both NaCl and KCl treatment (Fig. 8C; Table 1).

Specific energy fluxes per reaction center for absorption (ABS/RC), energy trapping (TR_o/RC), dissipation (DI_o/RC), electron transport (ET_o/RC), and reduction of the final electron acceptor on the acceptor side of photosystem I (RE_o/RC) were severely affected by 250 mM of NaCl (Fig. 8C; Table 1). KCl application induced slight reductions in specific fluxes for absorption and dissipation energy, however, it had no effect in the other fluorescence parameters at the highest level of NaCl. The fraction of the oxygen-evolving complex (OEC) was also reduced by exposure to 250 mM of NaCl. Rises in minimal fluorescence values (F_o) were observed (Fig. 8C; Table 1).

3.4. Biometric traits

Exposure to NaCl had a direct impact on biometric traits, reducing plant growth by affecting its morphological characteristics (Figs. 9 and 10). Nevertheless, plants with additional KCl developed more tillers (Fig. 9A and B), which can be confirmed by the increase in fresh and dry weights of these plants. Plants exposed to 250 mM of salt showed a severe reduction of biomass accumulation as well as chlorotic discolorations with curled necrotic areas in the leaf tips (Fig. 9C). Salt treatments of 150 and 250 mM led to reductions of ~70% and ~86% in shoot fresh weight (SFW) and ~60% and ~86% in shoot dry weight (SDW), respectively (Fig. 10A and B). The addition of K^+ favored biomass accumulation even in the NaCl-free plants: FW was ~21% and ~31% higher and SDW improved 28 and 14% with the addition of 5 and 9 mM of K^+, respectively (Fig. 10A and B).

In contrast with the 150 mM of NaCl, in the highest concentration of salt (250 mM) KCl effect was not sufficient to avoid severe reductions in shoot fresh and dry weights at the end of the experiment, although shoot fresh weight of 250 mM NaCl + 5 mM KCl treated plants increased. No new leaves developed after the application of 250 mM of NaCl (Fig. 10C) but both KCl concentrations mitigated that effect (Fig. 10C). Height was reduced by salt application, but the presence of KCl in plants exposed to 150 (9 mM) and 250 mM (5 mM) of NaCl treated plants reduced the negative effect on height (Fig. 10D).

3.5. Electrolytic leakage

Electrolytic leakage increased 6 and 10 times with exposure to 150 and 250 mM of NaCl, respectively (Fig. 11A). Application of KCl reduced EL close to 30% in plants submitted to 150 mM NaCl concentration. There was a decrease in EL for 250 mM salt-treated, from ~95 to ~85 with KCl application, which was not sufficient to allow the continuity ofplant development.

3.6. Antioxidant enzyme assays

Levels of SOD, CAT, and GR activities progressively increased with NaCl application (Fig. 11B, C, and D). Application of KCl in both NaCl-free plants and plants exposed to 150 mM of NaCl did not change

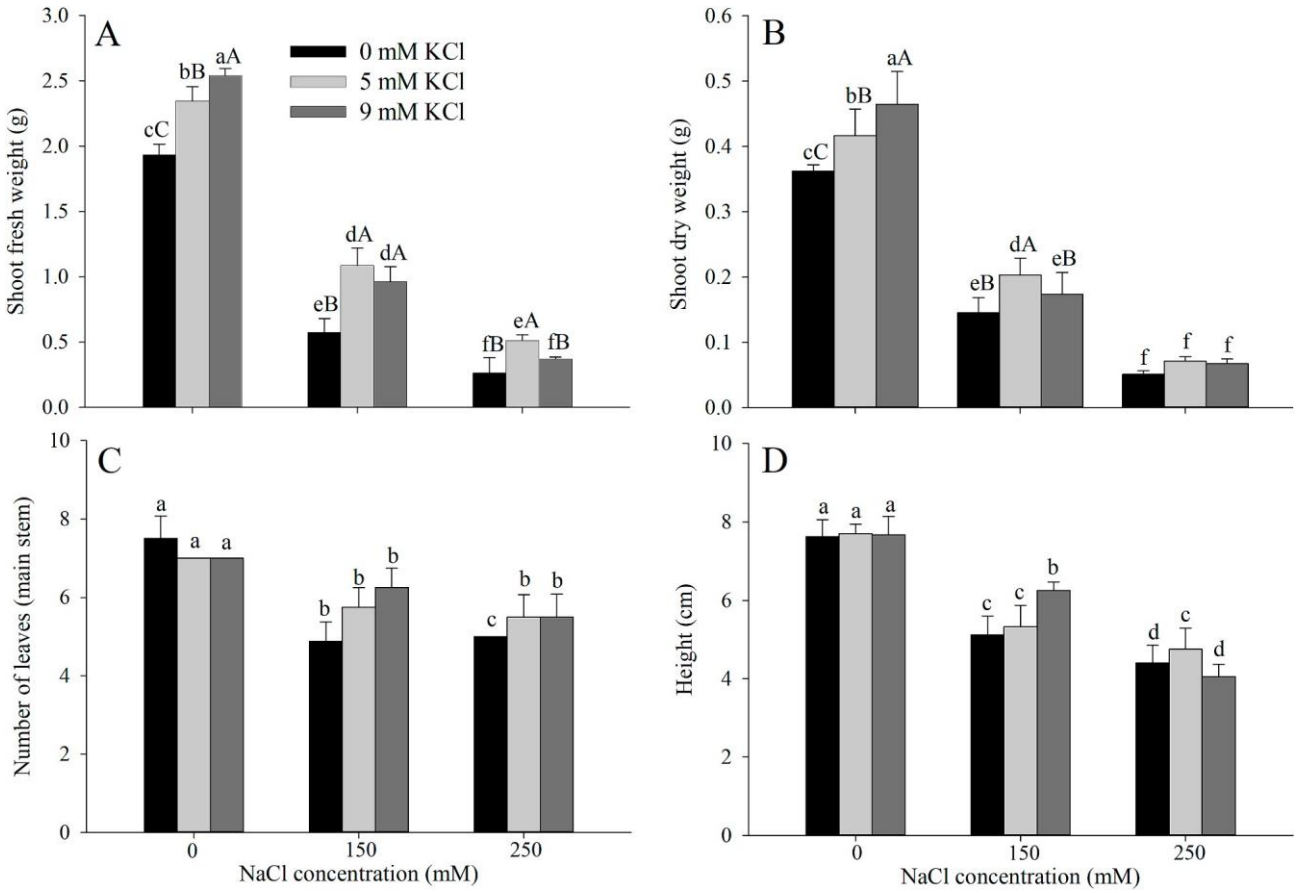

Fig. 10. Effects of NaCl and KCl application in *S. viridis* biometric traits. A. shoot fresh weight; B. shoot dry weight; C. number of leaves of the main stem; D. height. Small caption letters represent significant differences using the Scott-Knott test at $p < 0.05$ and upper case letters represent significant differences of KCl mitigation within level of salt using the Scott-Knott test at $p < 0.05$ (means ± standard deviation; n = 4).

enzyme activity (Fig. 11B, C, and D), except for an increase in catalase activity due to the presence of 9 mM in plants treated with 150 mM of NaCl. At the highest NaCl concentration SOD activity was enhanced ~20% by KCl application at both concentrations, while CAT activity was only improved by the application of 5 mM of KCl (Fig. 11B and D). APX showed no activity in any of the plants (data not showed).

3.7. Anatomical and ultrastructural analysis

Leaf transections of *S. viridis* exhibited Kranz architecture characteristic of the majority of plants with C_4 photosynthesis, one layer of bundle sheath cells (BSC) surrounded by three layers of mesophyll cells (MC) (Fig. 12). Leaves were amphistomatic, with stomata situated on the same level as the other epidermal cells (EC), presenting substomatic chambers at both epidermal surfaces and large bulliform cells in the adaxial epidermis of leaf lamina. Transverse sections showed prickle trichomes distributed in the coastal area, few intercellular spaces between MC, and numerous chloroplasts in both MC and BSC (Fig. 12A). Exposure to NaCl led to some changes in the anatomical pattern. In the 150 mM of NaCl plants, the abaxial epidermis surface exhibited flattening of epidermal cells (Fig. 12B). Chloroplast numbers in MC and BSC, as well as general anatomical characteristics, remained similar to control plants (Fig. 12B). Exposure to 250 mM of NaCl, however, triggered drastic changes. Qualitative anatomical analysis showed apparent increase in leaf blade thickness, intercellular spaces and, expressive reduction in chloroplast number in both MC and BSC (Fig. 12C, F, and I).

Supplementation with KCl induced alterations in the anatomical structure irrespective of exposure to NaCl (Fig. 12D and G). Application of KCl 5 mM and 9 mM promoted similar results in both NaCl-free and plants treated with 150 mM of NaCl. Cell organization was maintained, although, intercellular spaces between MC and volume of BSC increased (Fig. 12D, G, E, and H). Moreover, KCl application restored epidermal cells round shape in plants treated with 150 mM of NaCl (Fig. 12E and H). Application of 5 mM of KCl favored leaf blade thickness (Fig. 12E), while 9 mM appeared to reduce it (Fig. 12H). In the highest concentration of NaCl, application of KCl caused changes in the cellular organization with increasing cell flattening, leaf blade thickness (Fig. 12F and I), and some EC exhibited invaginations in the adaxial surface of the external periclinal walls (Fig. 12F).

Comparative analysis of scanning electron microscopy (SEM) of the adaxial surface of *S. viridis* leaves indicated an alteration in the morphology of epidermal cells with apparent changes in turgor pressure in the response to NaCl application. This effect was more severe as NaCl concentration rise (Fig. 13). In general, plants showed uniserial EC with three types of trichomes, called prickles, hooks, and microhairs. Microhairs and prickles were in the coastal zone and hooks in the intercoastal zone (Fig. 13A). The addition of 150 mM of NaCl triggered a progressive change characterized by the loss of turgor of epidermal cells situated in the intercoastal zone and epidermal cells of coastal zones were preserved (Fig. 13B). In 250 mM of NaCl areas of EC destruction were observed among areas of healthy tissue (Fig. 13C).

Application of KCl in NaCl-free plants did not lead to obvious changes in SEM images (data not showed). However, for salt-treated plants KCl application increased EC turgidity, visually restoring non-salt conditions in the plants treated with 150 mM of NaCl (Fig. 13D). In the concentration of 250 mM of NaCl, exogenous application of 5 mM of KCl was more efficient in preserve the foliar surface and turgidity in the intercostal zone. Nevertheless, some epidermal cells were still

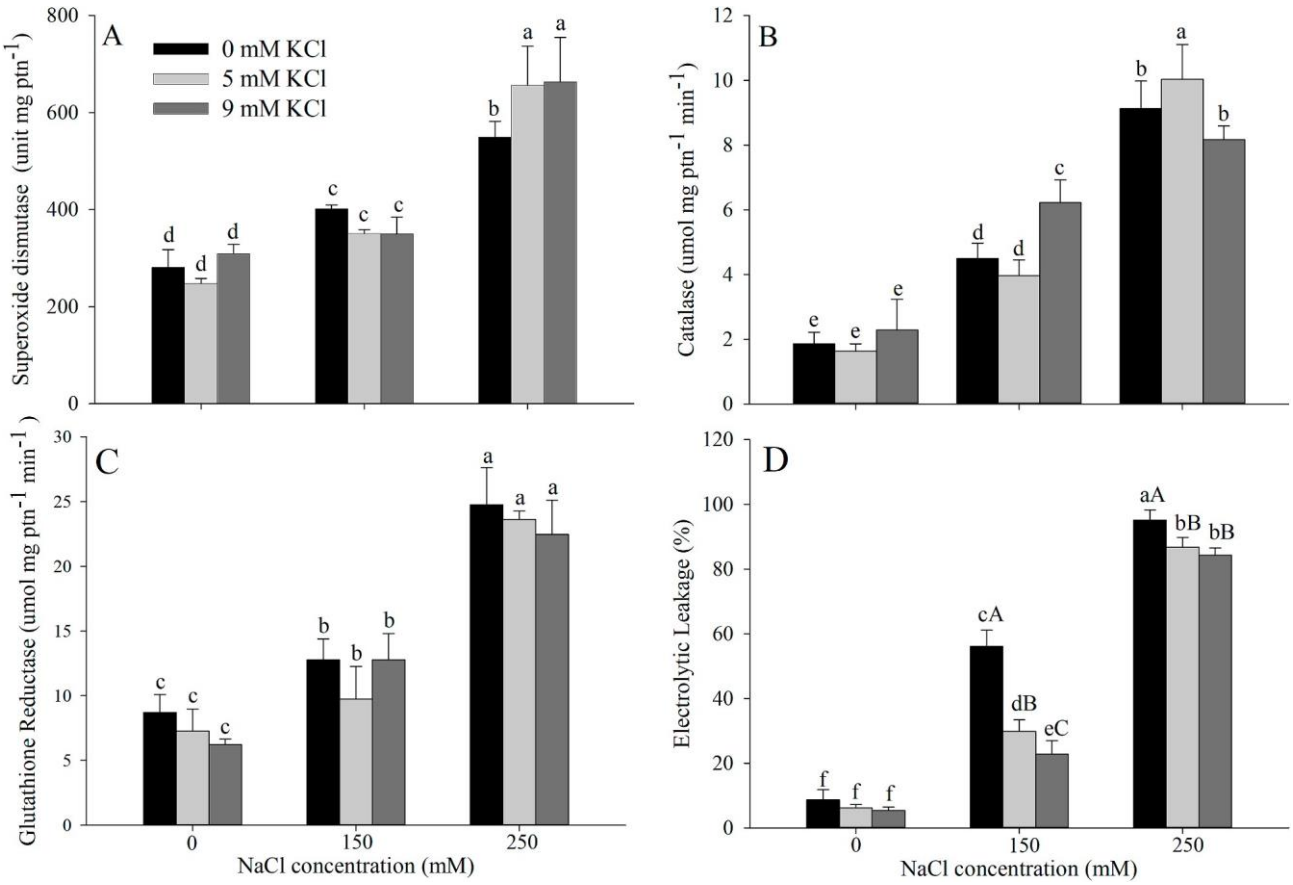

Fig. 11. Electrolytic leakage and antioxidant activity of *S. viridis* leaf tissues exposed to NaCl and KCl application. A. Electrolytic Leakage; B. Superoxide dismutase activity; C. Glutathione Reductase activity; D. Catalase activity. Small caption letters represent significant differences using the Sc ott-Knott test at $p < 0.05$ and upper case letters represent significant differences of KCl mitigation within level of salt using the Scott-Knott test at $p < 0.05$ (means ± standard deviation; n = 4).

bulging and control conditions were not restored (Fig. 13E). Plants that received 9 mM of KCl, however, also exhibited areas of leaf tissue destruction (Fig. 13F).

The adaxial foliar surface was covered with a high density of plate-type epicuticular wax over ordinary epidermal cells and stomatal complexes in all the treatments, including control (Fig. 14A, B, C) differently from the abaxial surface where almost no wax deposition was observed (Fig. 14D, E, F). The halter shape of the guard cells was not altered by NaCl application. However, NaCl changed stomata conformation, characterized by increase in stomatal width and length in the adaxial and abaxial surfaces, respectively (Fig. 14A, B, C, D, E, F, and Table 2) and flattening of subsidiary cells (Table 2). In the highest NaCl treatment, stomata situated in the salt-affected areas exhibited complete loss of subsidiary cell turgidity (Fig. 14C), whereas subsidiary cells of stomata placed in the non-destroyed areas were preserved avoiding drastic losses width of those structures (Table 2).

The number of stomata per area increased with KCl application considering the adaxial surface (Table 2). In the adaxial surface stomata density of 150 mM of NaCl treated plants reached values equal to control plants with the application of KCl, while for the abaxial surface such improvements were only observed with the application of 9 mM of KCl.

4. Discussion

Adequate ionic balance in the cytosol and chloroplasts is critical in regulating biochemical machinery and many of the reactions involved in the primary processes of photosynthesis (Pan et al., 2020). *Setaria viridis* was capable of maintaining net growth and photosynthetic electron flow for as long as it was capable of preventing most salt from reaching the shoot, i.e. treatment of 150 mM of NaCl. Extra potassium supply was effective in mitigating negative effects resulting from the exposure to 150 mM of NaCl. Conversely, the concentration of 250 mM resulted in severe photoinhibition after 96 h and potassium did very little to protect photosynthetic apparatus. Similar behavior was found in rice (Cha-um et al., 2010) in opposition to pearl millet (Ashraf et al., 2001), where K^+ supra-optimum fertilization did not prove to be beneficial in alleviating stress-induced effects at moderate levels of salinity. Additionally, potassium supplementation enhanced K^+ net uptake on *Arabidopsis thaliana* (L.) Heynh accession NOK2 while had no effects on Columbia-0 in the presence of 50 mM of salt. This illustrates that plants' K^+ and Na^+ transport systems depend on both inter and intra-specific variations (Kaddour et al., 2009).

Higher accumulation of K^+ ions in leaves concomitant with reduced Na^+ levels as a response to external KCl levels indicates selectivity of the accession A10.1 for K^+ over Na^+. Transport systems with high selectivity for K^+ are strongly associated with salt tolerance (Kaddour et al., 2009). The specific mechanism of selectivity and transport of K^+ over Na^+ is complex and not completely clear, yet it is known to be linked to 1) the regulation of high and low affinity selective and non-selective cation channels favoring K^+ root uptake, as HTK and AKT transporters; 2) the activity of H^+-ATPases, like PM Na^+/H^+ antiporter SOS1, inhibiting membrane depolarization and favoring Na^+ efflux; 3) transport systems controlling xylem K^+-loading and long-distance K^+ transport; 4) activity of NHXs catalyzing the vacuolar sequestration of Na^+ into vacuoles and mediating K^+ influx to the cytoplasm (Assaha et al., 2017; Kaddour et al., 2009; V'ery and Sentenac, 2003). Additionally, K^+/Na^+ homeostasis has an important relation with ROS and Ca^{2+} nutrition under salt stress, via regulation of ROS-activated mineral influx and efflux

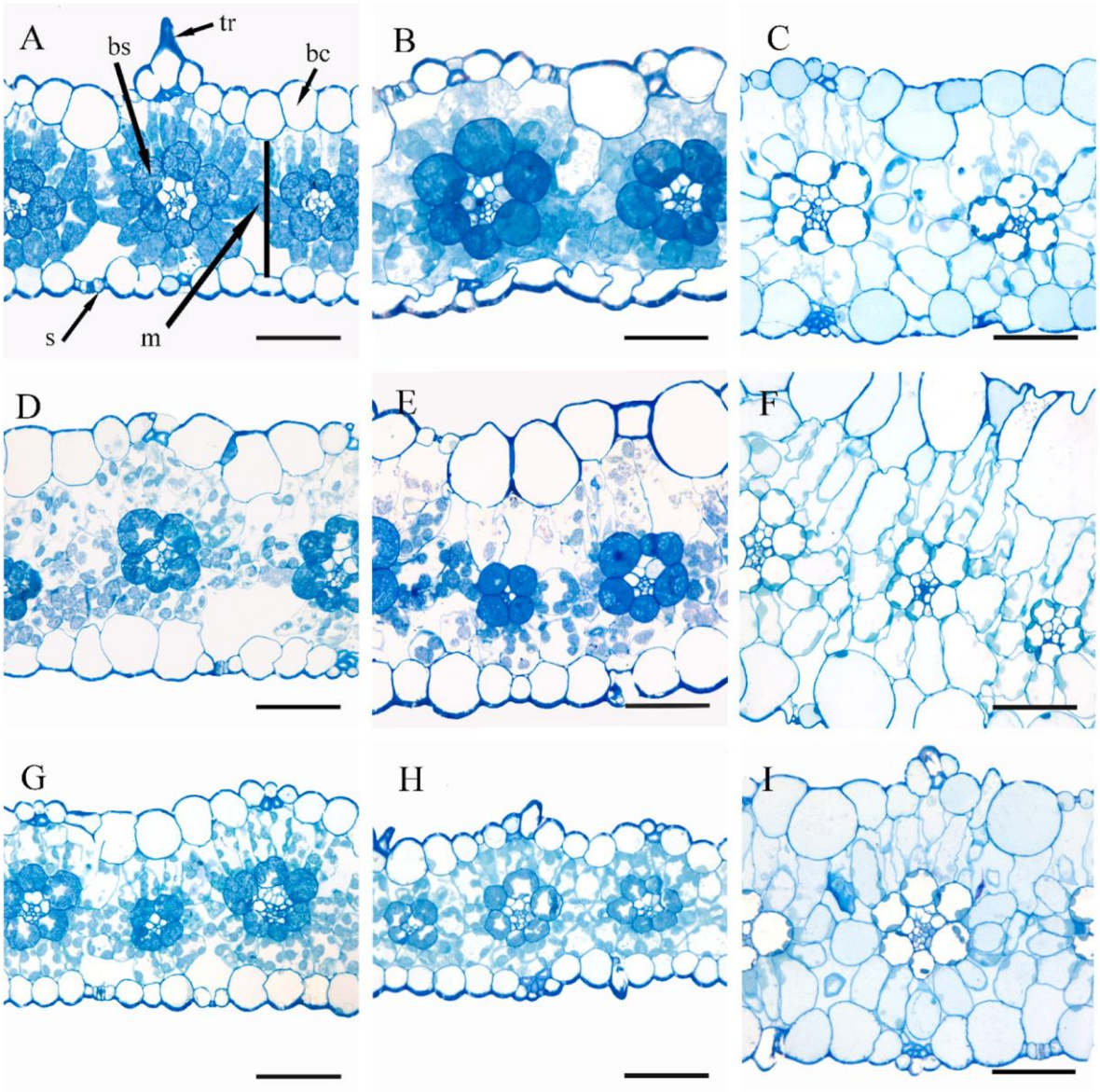

Fig. 12. Effects of NaCl and KCl application in the anatomical pattern of *S. viridis* leaves. A. NaCl-free plants without KCl application (control); B. Plants exposed to 150 mM of NaCl; C. Plants exposed to 250 mM of NaCl; D. NaCl-free plants with 5 mM of KCl; E. Plant exposed to 150 mM of NaCl treated with 5 mM of KCl; F. Plant exposed to 250 mM of NaCl treated with 5 mM of KCl; G. NaCl-free plants with 9 mM of KCl; H. Plant exposed to 150 mM of NaCl treated with 9 mM of KCl; I. Plant exposed to 250 mM of NaCl treated with 9 mM of KCl. Scale bars: 50 μm. s-stomata; tr-trichome; bc-bulliform cells; m-mesophyll cells; bs-bundle sheath cells.

channels and ion partitioning (Demidchik et al., 2018; Garcia-Mata, 2010; V'ery and Sentenac, 2003).

Previous results of our research group showed that *S. viridis* avoids accumulation of high amounts of Na^+ by restricting its transport to the shoots to a threshold of 200 mM of NaCl (supplementing material). Here, we confirmed this behavior. Our results suggest that this ability was crucial to conserve ionic homeostasis and prevent permanent damages to ETC guaranteeing the continuousness of the primary processes of photosynthesis. Accumulation of Na^+ in the cytosol is deleterious to the cellular metabolism limiting intercellular K^+ homeostasis, by reducing its uptake and inducing its efflux through the depolarization of the plasma membrane, and inhibiting metabolic processes depending on K^+ (Kataria and Verma, 2018; Sharma et al., 2012). The capacity to prevent Na^+ ions from reaching the xylem might be related to factors as the presence of mechanisms limiting radial movement of Na^+ in the roots and the regulation of transporters mediating intake, retrieving and, loading of Na^+, like SOS and HKT (Assaha et al., 2017; Munns and Tester, 2008; Shi et al., 2002). Maize seedlings and hybrids at different stages of development as well as barley present a similar strategy by progressively reducing the movement of Na^+ from roots to shoots avoiding the impairment of metabolic processes due to ion toxicity in the leaves (Abbasi et al., 2015; Shone et al., 1969).

The effect of NaCl and KCl on PSII activity and photosynthetic electron transfer capacity was studied using chlorophyll *a* fluorescence analysis. The results showed that both NaCl and KCl augment in the growth medium affected photosynthetic ETC. The OJIP curves, L and K-bands, and the JIP parameters were indicatives of ETC limitation and preservation due to NaCl and KCl supplementation, respectively. Reduction of the performance indexes, energy yields, specific fluxes per reaction center, and exhibition of a higher J-step in the OJIP-curves with application of 150 mM of NaCl indicate negative impacts of salt on electron transport at the PSII acceptor side. NaCl induced a decrease in the size of the pool of electron acceptors on the PSI acceptor side ($W_{0I}>1$; insert) while the rates of the end electron acceptors' pool (I–P steps) remained very similar and with very close half-times and similar maximum variable fluorescence in the plants submitted to 150 mM of

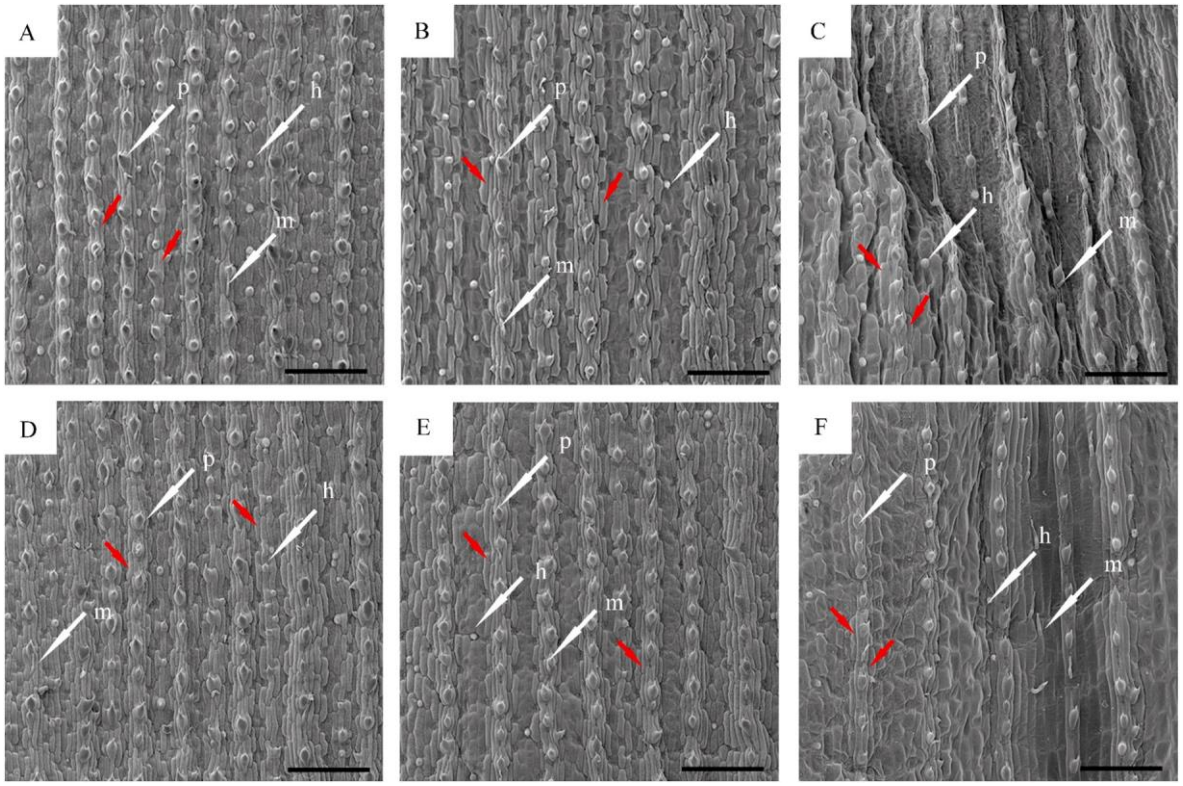

Fig. 13. Effects of NaCl and KCl application on the adaxial surface of *S. viridis* leaves. A. NaCl-free plants without KCl application (control); B. Plant exposed to 150 mM of NaCl; C. Plant exposed to 250 mM of NaCl; D. Plant exposed to150 mM of NaCl treated with 5 mM of KCl; E. Plant exposed to 250 mM of NaCl treated with 5 mM of KCl; F. Plant exposed to 250 mM of NaCl treated with 9 mM of KCl. Scale bars: 200 μm. Red arrows indicate patterns of epidermal cells; p-prickles; h-hooks; m- microhairs. (For interpretation of the references to color in this figure legend, the reader is referred to the Web version of this article.)

NaCl. These results show an independency of the regulation of the pool size and the overall rate constant for reduction of the end electron acceptor pool (Yusuf et al., 2010).

Both concentrations of KCl proved to be efficient in preserving photosystems activity under the applied moderate level of NaCl, especially among the functional PSII units as evidenced by OJIP-W_{OI} curves, the quantum yield for electron transport (JIP-test), and the performance indexes (PI_{abs} and PI_{total}). Photosynthetic indexes PI_{abs} and PI_{total} are sensitive and responsive to several stress conditions besides providing an overview of energy absorption and transfer state through ETC (Bussotti et al., 2010).

To further analyze the damaged sites of the photosynthetic apparatus in *S. viridis* leaves, we calculated difference kinetics from relative variable fluorescence to identify bands that are frequently hidden between OJIP-steps. The presence of K- and L-bands result from variations in the OJIP curves due to exposure to stress conditions (Yusuf et al., 2010). In 48h, the presence of NaCl in both concentrations induced positive K- and L-bands of different amplitudes according to the level of NaCl, with more severe outcomes in plants exposed to 250 mM of salt. Positive K-bands are sign of OEC inactivation, leading to incomplete cleavage of water and production of H_2O_2, and/or increase in PSII functional antenna size (Yusuf et al., 2010; Zhang et al., 2018). Positive L-bands are indicative of dissociation of PSII units, usually characterized by increase in the number of closed PSII reaction centers and loss of stability of energy changes (Kan et al., 2017; Strasser et al., 2004). Likewise, limitation on PSII activity on both donor and acceptor sides in response to NaCl was reported in sorghum as a result of damages to both the donor and the acceptor sides of PSII (Zhang et al., 2018). PSII inhibition can be associated with the inactivation and/or dissociation of intrinsic and extrinsic proteins due to Na^+ leak through the thylakoid membrane (Sasi et al., 2018; Sudhir et al., 2005). Over time, both concentrations of KCl in the nutrient solution annulled the effects of 150 mM of NaCl, not only reducing K- and L-bands, but also optimizing plants' performance by demonstrating higher efficiency of the OEC transfer capacity and recovery of photodamaged PSII centers, as indicated by the presence of negative bands. Under 250 mM of NaCl, however, potassium failed to protect PSII activity.

The influence of excessive Na^+ to the ETC of leaves exposed to the highest NaCl concentration induced severe changes in the OJIP curves between 48 and 96 h. After 48h, amplitude increase of the OJIP curve between steps O-J indicates expressive damage in the acceptor side of PSII. This suggests a decrease in the ability of PSII to transfer electrons beyond the primary quinone acceptor (Q_A) to the secondary quinone acceptor (Q_B), interrupting the flow of electrons between the two photosystems (Yusuf et al., 2010). The occurrence of damages to the acceptor side of PSII is also implied by the initial inclination of the fluorescence curve in step J and ϕ_{Eo} (JIP-test), indicative of accumulation of reduced Q_A (Yusuf et al., 2010). The behavior of PSII as DCMU-treated centers was previously reported as a response to 200 mM of NaCl in chickpea (Çicek et al., 2017) and sorghum under the exposure to 100 mM of Na_2CO_3 and $NaHCO_3$ (Zhang et al., 2018). It was hypothesized that a higher J-step associated with a smaller I–P amplitude in severely salt-stressed leaves may be related to reducing the binding constant of PQ for the Q_B site, inhibiting the transport of electrons beyond Q_A (Çicek et al., 2017).

After 96 h, the complete loss of shape of the OJIP-curve under 250 mM od NaCl points to limited capacity for PSII electron transport, and with time the entire ETC was compromised, as verified by the reduction of I–P steps. High levels of EL, demonstrating membrane peroxidation and blockages on PSII acceptor side in 48 h are strong signs of oxidative stress and, therefore, high ROS production (Demidchik et al., 2014). Excessive production of ROS, in its turn, affects photosynthetic-proteins biosynthesis, like D1 repair, putting extra strain on the inhibition of PSII centers (Murata et al., 2012). The complete inhibition of the ETC under

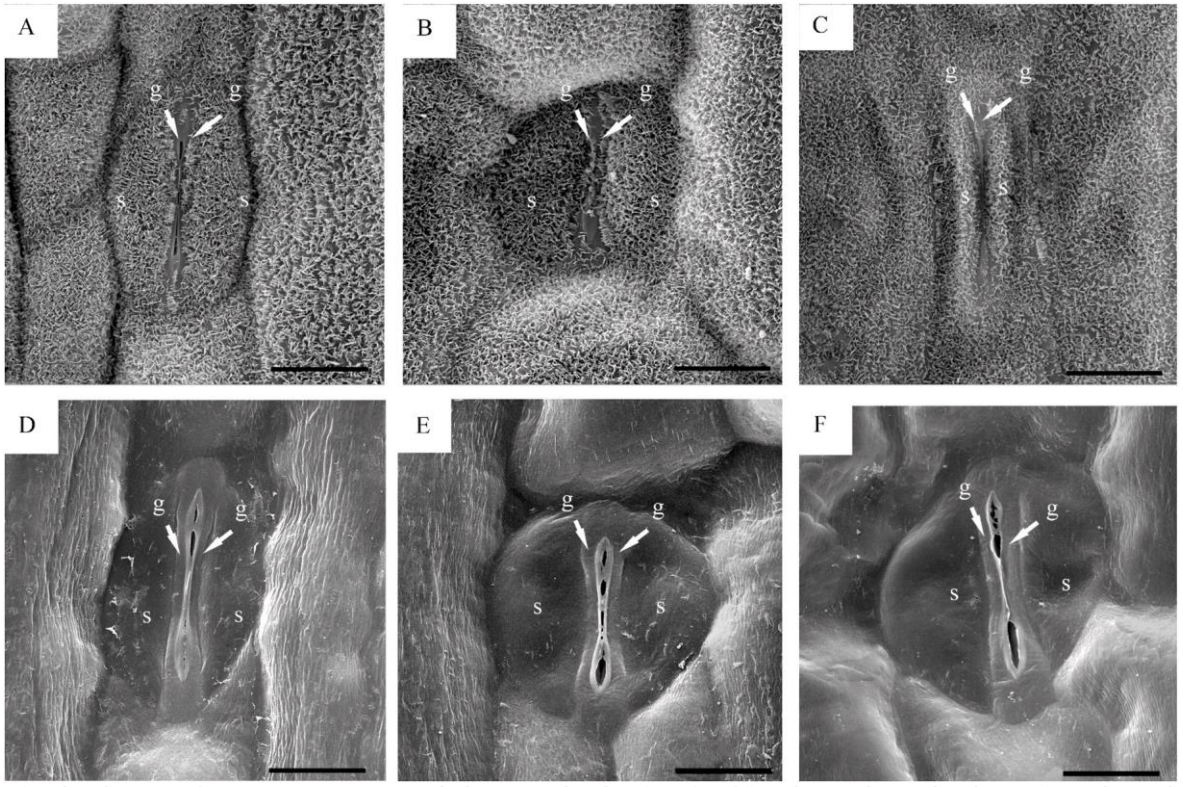

Fig. 14. Effects of NaCl application in the stomata pattern on *S. viridis* leaves. A. Adaxial surface of NaCl-free plants without KCl application (control); B. Adaxial surface of plants exposed to 150 mM of NaCl; C. Adaxial surface of plants exposed to 250 mM of NaCl; D. Abaxial surface of NaCl-free plants without KCl application (control); E. Abaxial surface of plants exposed to 150 mM of NaCl; F. Abaxial surface of plants exposed to 250 mM of NaCl. Scale bars: 10 μm. g-guard cells; s-subsidiary cells.

250 mM of NaCl after 96 h was evidenced by JIP-parameters. Rises in ABS/RC and DI_o/RC signify, respectively, a rise in the antenna complex size and loss of photochemical efficiency by energy dissipation (Strasser et al., 2004), while degradation of D1 protein with damages in electron transfer on PSII was implied by the increase in F_0 (Calatayud et al., 2006; Strasser et al., 2000; Yamane et al., 2008).

The impairment of electron transport between the photosystems will reduce the rates of ATP and NADPH production, generating productivity losses in the photochemical step and affecting carbon assimilation process via the Calvin-Benson Cycle (Chaves et al., 2009). Indirectly, a drop in ATP production will reduce chemical energy for ATP-dependent processes, such as H^+-ATPase activity (Assaha et al., 2017). Membrane H^+-ATPase have a crucial role in energy supply for the active secondary transport of nutrients and vacuolar sequestration of Na^+, fundamental for the protection of cytosolic functioning (Falhof et al., 2016; Shabala and Pottosin, 2014). Additionally, H^+-ATPase activity is fundamental to maintain negative membrane potential and K^+ retention under the influence of salt (Demidchik et al., 2014). Thus, this lack of energy leads to a decrease in other molecules or nutrients, disrupting cellular ionic homeostasis, increasing the entropy of the system, and consequently worsening oxidative damage (Foyer, 2018; Demidchik et al., 2014).

Antioxidative enzymes play a vital role in protecting cell structures against excessive ROS (Gill and Tuteja, 2010). Superoxide dismutase is the key enzyme in the active oxygen scavenger system and is considered the first line of defense against ROS damages responsible for rapid dismutation of O^{2-} radicals. Low cellular level of H_2O_2 is maintained by other enzymes, like CAT and GR (Acosta-Motos et al., 2017; Kataria and Verma, 2018; Sharma et al., 2012). Salt increased the levels of oxidative stress and naturally raised enzymatic activity. Although the enhancement of K^+ nutritional status of plants is often associated with improvements in antioxidant capacity (Abbasi et al., 2015), KCl addition did not have this effect on antioxidant enzyme activity in plants under 150 mM NaCl and salt-free plants, except for CAT (9 mM - KCl). Maintenance of enzymatic activity in these plants might be related to reduction in ROS formation in the first place, as showed by reductions in EL, a well-known indicator of oxidative stress (Demidchik et al., 2014). In rice, salinity induced excessive H_2O_2 production in leaves (Yamane et al., 2012), therefore intensification in CAT activity might be crucial to protect photosynthetic machinery. Increase in CAT activity due to K^+ fertilization was also reported for maize hybrids, inducing a protective effect on growth and photosynthesis against salt-induced oxidative stress (Abbasi et al., 2014).

Despite being cytotoxic and highly reactive, formation of ROS at early stages derived from the activity of NADP oxidases and rises in cytosolic Ca^{2+} is involved in stress-signaling and regulation pathways, critical for stress-tolerance and ionic homeostasis (Demidchik, 2018; Garcia-Mata, 2010). Under moderate stress (150 mM), extra KCl improved ionic homeostasis and reduced the excessive levels of oxidative stress, promoting stress-alleviation, and optimizing plant performance probably by stimulating cellular stress responses. Higher K^+ accumulation favors the maintenance of water flow and carbon assimilation through its well-described roles in osmotic adjustment and stomatal control (Cakmak, 2005; Hasanuzzaman et al., 2018; Shabala and Pottosin, 2014). Potassium's role reflected in the maintenance of photosynthetic energy dissipation and improved biomass accumulation by generating turgor and driving cell expansion. In accordance, preservation of leaf turgidity in the intercoastal zones with KCl supplementation in both concentrations in plants treated with 150 mM of NaCl was observed in SEM microscopy. Cell turgidity is achieved by vacuolar K^+ pools and positively linked with variable chlorophyll fluorescence recovery during salt stress, preventing damages to PSII (Downton and Millhouse, 1983; Latz et al., 2013).

Setaria viridis short life cycle is key for its use as a model plant and

Table 2

Density and stomatal diameters of the adaxial and abaxial surfaces of *S. viridis* leaves exposed to NaCl and KCl application.

		Stomata width (μm)			Stomata length (μm)			Nº of stomata area^{-1} (unit mm^{-2})		
		NaCl (mM)								
		0	150	250	0	150	250	0	150	250
KCl (mM)	0	14.29 ± 1.9^{cB}	19.39 ± 2.53^{bA}	ND*	22.25 ± 2.6^{aA}	20.71 ± 2.16^{bA}	ND*	192.0 ± 20.6^{bA}	145.60 ± 20.8^{cB}	ND*
	5	16.99 ± 2.8^{bA}	16.09 ± 2.8^{cB}	17.00 ± 2.30^{bB}	20.03 ± 1.85^{bB}	22.08 ± 2.3^{aA}	21.03 ± 2.0^{b}	129.1 ± 22.5^{cB}	178.9 ± 22.0^{bA}	137.2 ± 19.3^{cA}
	9	15.58 ± 2.4^{bB}	14.20 ± 2.1^{cC}	21.25 ± 3.1^{aA}	20.07 ± 2.6^{bB}	19.22 ± 2.3^{bB}	22.52 ± 2.2^{a}	210.6 ± 18.0^{aA}	193.4 ± 14.0^{bA}	151.93 ± 11.5^{cA}
		Abaxial surface								
		Stomata width (μm)			Stomata length (μm)			Nº of stomata area^{-1} (unit mm^{-2})		
		NaCl (mM)								
		0	150	250	0	150	250	0	150	250
KCl (mM)	0	27.03 ± 4.0^{aA}	24.69 ± 2.3^{b}	ND*	17.25 ± 3.0^{bB}	19.43 ± 3.8^{a}	ND*	201.1 ± 9.4^{aA}	133.81 ± 13.1^{cB}	ND*
	5	25.58 ± 2.6^{bB}	25.18 ± 2.6^{b}	26.80 ± 2.5^{a}	17.74 ± 3.8^{bB}	18.44 ± 2.9^{b}	19.37 ± 2.9^{a}	135.24 ± 15.1^{cB}	145.37 ± 8.1^{cB}	105.4 ± 9.3^{d}
	9	24.97 ± 2.1^{bB}	26.34 ± 2.4^{a}	26.85 ± 2.7^{a}	19.82 ± 2.5^{aA}	17.50 ± 3.1^{b}	20.01 ± 3.2^{a}	154.67 ± 11.2^{bB}	197.27 ± 7.9^{aA}	89.82 ± 4.4^{d}

Small case letters represent significant differences using Scott-Knott test at $p < 0.05$ and at upper case letters represent significant differences of KCl mitigation within level of salt using Scott-Knott test at $p < 0.05$ (means ± standard deviation; n = 7 for number of stomata area^{-1} and n = 20 for equatorial and polar diameters). ND = not defined. *as no new leaves emerged after stress induction in the highest salt treatment, measurements of stomatal length, width and density were not defined for this treatment.

optimization of biological studies (Brutnell et al., 2010). The period between the development of the 5th and the 8th leaf of *S. viridis* is approximately four days (Junqueira et al., 2019). Consistently, this study was carried out for four days during which three to four new leaves developed. We observed reduction of ~24 and 33% of stomatal density in the adaxial and abaxial surfaces, respectively, in response to 150 mM of NaCl. Both concentrations of KCl reflected in the conservation (to control values) or enhancement of the number of stomata per area in new-born leaves. Reduction in stomatal density in response to salt was reported in quinoa (Shabala et al., 2012) and can be an efficient strategy to optimize water use efficiency during limited water absorption (Bray and Reid, 2002).

Exposure to NaCl altered *S. viridis* micromorphological characteristics by increasing lamina thickness and bulliform cell size in most treatments irrespective of additional potassium. Bulliform cells play a key role in leaf curling and avoidance of excessive water loss in grasses (Grigori et al., 2010). Our data show that bulliform cells did not shrink nor leaves curled in response to salt, which may result from a thick layer of epicuticular wax on the adaxial surface limiting water loss under physiological drought conditions (Hameed et al., 2009; Kerstiens, 1996). The species also presented larger cells, resembling the shape of a bulliform cell, in the abaxial epidermis. Although less common, the presence of bulliform-like cells in the abaxial epidermal surface occurs in some grasses (Metcalfe, 1960). Under hydroponic cultivation, the area of bulliform cells of the C_4 grasses *Cynodon dactylon* (L.) Pers. and *Imperata cylindrica* (L.) Raeuschel, also exhibited larger bulliform cells as a response to increasing NaCl concentrations, however, contrary to our results, the expansion was followed by extensive shrinking and leaf rolling (Hameed et al., 2009, 2013).

Although not typical for monocots, the tendency to increase lamina thickness in response to high salinity is often described in eudicot species (Borochov-Neori and Borochov, 1991; Hameed et al., 2009; Yermanos et al., 1967) and was also reported for ecotypes collected from both high and non-saline environments of *I. cylindrica* (Hameed et al., 2009). Leaf succulence was positively linked with Na^+ accumulation for the natural accession of *Arabidopsis thaliana* NOK2, indicating the contribution of imported Na^+ ions to leaves in water retention in leaf cells (Kaddour et al., 2009). Thus, the increase in leaf thickness in response to NaCl might be related to the abrupt increase in Na^+ accumulation in these leaves as an attempt to adjust osmotically at a low energetic cost and retain water under physiological drought (Hussain et al., 2020). Excessive intake, however, might become inhibitory to cytosolic biochemical machinery and cell functioning depending on the location of the ions (Munns and Tester, 2008; Assaha et al., 2017).

Sodium accumulation is central to most studies under saline environments, nevertheless the combined effect of the ions Na^+ and Cl^- appears to be more deleterious than their individual outcomes in glycophytes (Khare et al., 2015). Even though Na^+ is metabolically more toxic than Cl^- (Shelke et al., 2019), the uptake of toxic levels of Cl^- ions may restrict nitrates (NO_3^-) absorption diminishing ETC efficiency and plant overall photosynthetic capacity via chlorophyll degradation (Shelke et al., 2019; Tavakkoli et al., 2010). Leaf external morphology of all plants exposed to 250 mM of NaCl, irrespective of the presence of KCl, displayed chlorosis with leaf-tip necrosis, symptoms that may be attributed to Cl^- toxicity (Geilfus, 2018). Further understand of toxic concentration of Cl^- as well as synergetic effect with Na^+ is an open venue.

NaCl reduced *S. viridis* growth by altering plant external and internal morphology, impairing or damaging ETC, changing K^+ and Na^+ homeostasis, and increasing EL. This response was more severe as NaCl concentration increased. Evaluation of alleviation of stress symptoms because of KCl application revealed that under moderate stress (150 mM) application of 5 and 9 mM of KCl was equally effective in maintaining adequate ETC operation as indicated by chlorophyll *a* fluorescence parameters and derived curves, as well as for sustaining growth, turgidity maintenance, maintenance of stomata density, and reduced

levels of EL. These responses may be correlated to a larger K^+/Na^+ ratio in the leaves achieved by a possible K^+ vs. Na^+ selectivity in *S. viridis*. The capacity to maintain K^+ homeostasis in saline environments is associated with adequate chloroplast operation and PSII activity (Pottosin and Shabala, 2016), regulation of stomatal conductance (Hatam et al., 2020), protein synthesis (Murata et al., 2012), enzyme activation (Shabala and Pottosin, 2014), phloem loading and transport (Wang et al., 2015), improvement of antioxidant capacity and, reduction of ROS production (Abbasi et al., 2015; Jan et al., 2017; Pottosin and Shabala, 2016). The same, however, was not valid for the highest NaCl concentration, where leaves probably accumulated excessive amounts of Na^+ and were not capable of coping with salt stress even with increments in K^+ levels. This points to the fact that stress-severity is determinant on the ability to reverse damages on leaf photochemistry of *S. viridis*.

5. Conclusions

The evaluation of the ETC behavior under moderate and high levels of salinity provided relevant information on the effects of NaCl in the state of electron acceptors as well as induction of blockages in electron transfer within ETC, predominantly in the PSII donor and acceptor sides. The highest level of salt severely affected photosynthetic ETC in at least three sites: as evidenced by alterations and impairments at both sides of PSII and reduced I–P amplitudes. Performance indexes (PI_{abs} and PI_{total}) were responsive to both NaCl and KCl in conditions of salinity and can be a key for quickly monitoring mitigation strategies to plants submitted to salinity. Data described here might provide data for future research in Panicoideae C_4 crops and their growth under conditions of salinity.

Our results also demonstrated the fundamental role of supplemental K^+ in guaranteeing adequate time and physiological conditions to better support plant acclimation therefore sustaining plant growth under moderate salinity. Under the highest level of NaCl, however, not all plant traits were sensitive to KCl, and alleviation of harmful effects was not sufficient to avoid photoinhibition, severe metabolic and, morphologic changes. Our results support the conclusion that KCl application can be an efficient strategy to counteract the harmful effects of salinity, but it has limitations depending on the level of stress applied. Additionally, application of KCl has a concentration optimum that must be experimentally determined.

Author's contributions

Conceptualization: Bezerra, A.C.M., Medici, L.O., Reinert, F., Silva-Ortiz, B; data acquisition: Bezerra, A.C.M., Valença, D.C., Silva-Ortiz, B.; data Analysis: Bezerra, A.C.M., Valença, D.C., Junqueira, N.E.G.; design of methodology: Bezerra, A.C.M., Medici, L.O., Silva-Ortiz, B., Reinert, F.; writing and Editing: Bezerra, A.C.M., Hüther, C.M., Borella, J., Pinho, C.F., Ferreira, M.A., Medici, L.O., Silva-Ortiz, B., Reinert, F.

Declaration of competing interest

The authors declare that they have no known competing financial interests or personal relationships that could have appeared to influence the work reported in this paper.

Acknowledgments

This work is part of the thesis of Bezerra, A.C.M., supported by a scholarship from Conselho Nacional de Desenvolvimento Científico e Tecnológico (CNPq, Brazil). This study was financed in part by Coordenação de Aperfeiçoamento de Pessoal de Nível Superior - Brasil (CAPES) - Finance Code 001. The authors thank the Nucleus of Multidisciplinary Research (Numpex-Bio) at Federal University of Rio de Janeiro.

References

Abbasi, G.H., Akhtar, J., Anwar-Ul-Haq, M., Ali, S., Chen, Z.-H., Malik, W., 2014. Exogenous potassium differentially mitigates salt stress in tolerant and sensitive maize hybrids. Pakistan J. Bot. 46 (1), 135–146.

Abbasi, G.H., Aktar, J., Ahmad, R., Jamil, M., Anwar-Ul-Haq, M., Shafaqat, A., Ali, S., Ijaz, M., 2015. Potassium application mitigates salt stress differentially at different growth stages in tolerant and sensitive maize hybrids. Plant Growth Regul. 76, 111. https://doi.org/10.1007/s10725-015-0050-1.

Acosta-Motos, J.R., Ortuñõ, M.F., Bernal-Vicente, A., Diaz-Vivancos, P., Sanchez-Blanco, M.J., Hernandez, J.A., 2017. Plant responses to salt stress: adaptive mechanisms. Agronomy 7 (1), 1–38. https://doi.org/10.3390/agronomy7010018.

Aliscioni, S., Ospina, J.C., Gomiz, N.E., 2016. Morphology and leaf anatomy of *Setaria s.l. (*Poaceae: Panicoideae: Paniceae) and its taxonomic significance. Plant Systemat. Evol. 302, 173–185. https://doi.org/10.1007/s00606-015-1251-9.

Ashraf, M.Y., Ahmad, A., Mcneilly, T., 2001. Growth and photosynthetic characteristics in pearl millet under water stress and different potassium supply. Photosynthetica 39 (3), 389–394. https://doi.org/10.1023/A:1015182310754.

Assaha, D.V.M., Ueda, A., Saneoka, H., Al-Yahyai, R., Yaish, M.W., 2017. The role of Na^+ and K^+ transporters in salt stress adaptation in glycophytes. Front. Physiol. 8, 509. https://doi.org/10.3389/fphys.2017.00509.

Borochov-Neori, H., Borochov, A., 1991. Response of melon plants to salt: 1. Growth, morphology and root membrane properties. J. Plant Physiol. 139, 100–105. https://doi.org/10.1016/S0176-1617(11)80173-2.

Bray, S., Reid, D.M., 2002. The effect of salinity and CO_2 enrichment on the growth and anatomy of the second trifoliate leaf of *Phaseolus vulgaris*. Can. J. Bot. 80 (4), 349–359. https://doi.org/10.1139/b02-018.

Brutnell, T.P., Wang, L., Swartwood, K., Goldschmidt, A., Jackson, D., Zhu, X., Kellog, E., Van Eck, J., 2010. *Setaria viridis*: a model for C_4 photosynthesis. Plant Cell 22 (8), 2537–2544. https://doi.org/10.1105/tpc.110.075309.

Burbulis, N., Vainoriene, R., Blinstrubiene, A., Jonytiene, V., Liakas, V., 2017. Effect of potassium bicarbonate on photosynthetic parameters of *Setaria viridis* under drought conditions. Zemdirbyste-Agriculture 104 (1), 79–84. https://doi.org/10.13080/z-a.2017.104.011.

Bussotti, F., Desotgiu, R., Pollastrini, M., Cascio, C., 2010. The JIP test: a tool to screen the capacity of plant adaptation to climate change. Scand. J. For. Res. 25 (8), 43–50. https://doi.org/10.1080/02827581.2010.485777.

Cakmak, I., 2005. The role of potassium in alleviating detrimental effects of abiotic stresses in plants. J. Plant Nutr. Soil Sci. 168 (4), 521–530. https://doi.org/10.1002/jpln.200420485.

Calatayud, A., Roca, D., Martínez, P.F., 2006. Spatial-temporal variations in rose leaves under water stress conditions studied by chlorophyll fluorescence imaging. Plant Physiol. Biochem. 44, 564–573. https://doi.org/10.1016/j.plaphy.2006.09.015.

Cha-um, S., Siringam, K., Juntawong, N., Kirdmanee, C., 2010. Water relations, pigment stabilization, photosynthetic abilities and growth improvement in salt stressed rice plants treated with exogenous potassium nitrate application. Int. J. Plant Prod. 4 (3), 187–198.

Chaves, M.M., Flexas, J., Pinheiro, C., 2009. Photosynthesis under drought and salt stress: regulation mechanisms from whole plant to cell. Ann. Bot. 103, 551–560. https://doi.org/10.1093/aob/mcn125.

Çicek, N., Oukarroum, A., Strasser, R.J., Schansker, G., 2017. Salt stress effects on the photosynthetic electron transport chain in two chickpea lines differing in their salt stress tolerance. Photosynth. Res. 136, 291–301. https://doi.org/10.1007/s11120-017-0463-y.

Deinlein, U., Stephan, A.B., Horie, T., Luo, W., Xu, G., Schroeder, J.I., 2014. Plant salt-tolerance mechanisms. Trends Plant Sci. 19 (6), 371–379. https://doi.org/10.1016/j.tplants.2014.02.001.

Demidchik, V., 2018. ROS-activated ion channels in plants: biophysical characteristics, physiological functions and molecular nature. Int. J. Mol. Sci. 19, 1263. https://doi.org/10.3390/ijms19041263.

Demidchik, V., Straltsova, D., Medvedev, S.S., Pozhvanov, G.A., Sokolik, A., Yurin, V., 2014. Stress-induced electrolyte leakage: the role of K^+-permeable channels and involvement in programmed cell death and metabolic adjustment. J. Exp. Bot. 65 (5), 1259–1270. https://doi.org/10.1093/jxb/eru004.

Demidchik, V., Shabala, S., Isayenkov, S., Cuin, T.A., Pottosin, I., 2018. Calcium transport across plant membranes: mechanisms and functions. New Phytol. 220, 40–69. https://doi.org/10.1111/nph.15266.

Doust, A.N., Brutnell, T.P., Upadhyaya, H.D., Eck, J.V., 2019. Editorial: *Setaria* as a model genetic system to accelerate yield increases in cereals, forage crops, and bioenergy grasses. Front. Plant Sci. 10, 1–2. https://doi.org/10.3389/fpls.2019.01211.

Downton, W.J.S., Millhouse, J., 1983. Turgor maintenance during salt stress prevents loss of variable fluorescence in grapevine leaves. Plant Sci. Lett. 31, 1–7. https://doi.org/10.1016/0304-4211(83)90124-4.

Duarte, K.E., de Souza, W.R., Santiago, T.R., Sampaio, B.L., Ribeiro, A.P., Cotta, M.G., da Cunha, B.A.D.B., Marraccini, P.R.R., Kobayashi, A.K., Molinari, H.C., 2019. Identification and characterization of core abscisic acid (ABA) signaling components and their gene expression profile in response to abiotic stresses in *Setaria viridis*. Scientific Reports -UK 9, 4028–4043. https://doi.org/10.1038/s41598-019-40623-5.

Falhof, J., Pedersen, J.T., Fuglsang, A.T., Palmgren, M., 2016. Plasma membrane H^+-ATPase regulation in the center of plant physiology. Mol. Plant 9, 323–337. https://doi.org/10.1016/j.molp.2015.11.002.

Foyer, C.H., 2018. Reactive oxygen species, oxidative signaling and the regulation of photosynthesis. Environ. Exp. Bot. 154, 134–142. https://doi.org/10.1016/j.envexpbot.2018.05.003.

Garcia-Mata, C., Wang, J., Gajdanowicz, P., Gonzalez, W., Hills, A., Donald, N., Riedelsberger, J., Amtmann, A., Dreyer, I., Blatt, M.R., 2010. A minimal cysteine motif required to activate the SKOR K^+ channel of Arabidopsis by the reactive oxygen species H_2O_2. J. Biol. Chem. 285 (38), 29286–29294. https://doi.org/10.1074/jbc.m110.141176.

Geilfus, C.-M., 2018. Chloride: from nutrient to toxicant. Plant Cell Physiol. 59 (5), 877–886. https://doi.org/10.1093/pcp/pcy071.

Gill, S.S., Tuteja, N., 2010. Reactive oxygen species and antioxidant machinery in abiotic stress tolerance in crop plants. Plant Physiol. Biochem. 48 (12), 909–930. https://doi.org/10.1016/j.plaphy.2010.08.016.

Grigori, M.-N., Toma, C., Boscaiu, M., 2010. Ecological implications of bulliform cells on halophytes, in salt and water stress natural conditions. Analele Stiintifice ale Universitatii "Alexandru Ioan Cuza" din Iasi. Biologie Vegetala 56 (2), 5–15. http://hdl.handle.net/10251/101713.

Guo, R., Zhou, J., Hao, W., Gong, D., Zhong, X., Gu, F., Li, Q., Xia, X., Tian, J., Li, H., 2011. Germination, growth, photosynthesis and ionic balance in *Setaria viridis* seedlings subjected to saline and alkaline stress. Can. J. Plant Sci. 91 (6), 1077–1088. https://doi.org/10.4141/cjps10167.

Hameed, M., Ashraf, M., Naz, N., 2009. Anatomical adaptations to salinity in cogon grass [*Imperata cylindrica* (L.) Raeuschel] from the Salt Range, Pakistan. Plant Soil 322, 229–238. https://doi.org/10.1007/s11104-009-9911-6.

Hameed, M., Ashraf, M., Naz, N., Nawaz, T., Batool, R., Ahmad, M.S.A., Ahmad, F., Hussan, M., 2013. Anatomical adaptations of *Cynodon dactylon* (L.) Pers. From the salt range (Pakistan) to salinity stress. II. Leaf anatomy. Pakistan J. Bot. 45 (1), 133–142.

Hasanuzzaman, M., Bhuyan, M.H.M., Nahar, K., Hossain, M.S., Mahmud, J.A., Hossen, M.S., Masud, A.A.C., Moumita, Fujita, M., 2018. Potassium: a vital regulator of plant responses and tolerance to abiotic stresses. Agronomy 8 (31), 1–29. https://doi.org/10.3390/agronomy8030031.

Hatam, Z., Sabet, M.S., Malakoutim, M.J., Mokhtassi-Bidgoli, A., Homaee, M., 2020. Zinc and potassium fertilizer recommendation for cotton seedlings under salinity stress based in gas exchange and chlorophyll fluorescence responses. South Afr. J. Bot. 130, 155–164. https://doi.org/10.1016/j.sajb.2019.11.032.

Hichem, H., Naceur, E.A., Mounir, D., 2009. Effects of salt stress on photosynthesis, PSII photochemistry and thermal energy dissipation in leaves of two corn (*Zea mays* L.) varieties. Photosynthetica 47 (4), 517–526. https://doi.org/10.1007/s11099-009-0077-5.

Hoagland, D.R., Arnon, D.I., 1938. The water culture method of groin plants without soil. Calif. Agric. Ext. Serv. Circ. 347, 1–39. http://hdl.handle.net/2027/uc2.ark:/13960/t51g1sb8j.

Hussain, T., Koyro, H.-W., Zhang, W., Liu, X., Gul, B., Liu, X., 2020. Low salinity improves photosynthetic performance in *Panicum antidotale* under drought stress. Front. Plant Sci. 11, 481. https://doi.org/10.3389/fpls.2020.00481.

Ivushkin, K., Bartholomeusa, H., Bregta, A.K., Pulatovb, A., Kempenc, B., Sousac, L., 2019. Global mapping of soil salinity change. Remote Sensing of Environment 231, 111260. https://doi.org/10.1016/j.rse.2019.111260.

Jan, A.U., Hadi, F., Midrarullah, Nawaz, M.A., Rahman, K., 2017. Potassium and zinc increase tolerance to salt stress in wheat (*Triticum aestivum L.*). Plant Physiol. Biochem. 116, 139–149. https://doi.org/10.1016/j.plaphy.2017.05.008.

Junqueira, N.E.G., Bezerra, A.C.M., Cattem, M.V.O., Medici, L.O., Alves-Ferreira, M., Macrae, A., Ortiz-Silva, B., Reinert, F., 2019. Phenology of the genetic model *Setaria viridis* (Poaceae) according to the BBCH-scale of development. Bot. J. Linn. Soc. 192 (1), 1–18. https://doi.org/10.1093/botlinnean/boz070.

Junqueira, N.E.G., Ortiz-Silva, B., Leal-Costa, M.V., Alves-Ferreira, M., Dickinson, H.G., Langdale, J.A., Reinert, F., 2018. Anatomy and ultrastructure of embryonic leaves of the C_4 species *Setaria viridis*. Ann. Bot. 121 (6), 1163–1172. https://doi.org/10.1093/aob/mcx217.

Kaddour, R., Nasri, N., M'rah, S., Berthomieu, P., Lachaâl, M., 2009. Comparative effect of potassium on K and Na uptake and transport in two accessions of *Arabidopsis thaliana* during salinity stress. Comptes Rendus Biol. 332 (9), 784–794. https://doi.org/10.1016/j.crvi.2009.05.003.

Kan, X., Ren, J., Chen, T., Cui, M., Li, C., Zhou, R., Zhang, Y., Liu, H., Deng, D., Yin, Z., 2017. Effects of salinity on photosynthesis in maize probed by prompt fluorescence, delayed fluorescence and P700 signals. Environ. Exp. Bot. 140, 56–64. https://doi.org/10.1016/j.envexpbot.2017.05.019.

Kataria, S., Verma, S.P., 2018. Salinity stress responses and adaptive mechanisms in major glycophytic crops: the story so far. In: Kumar, V., et al. (Eds.), Salinity Responses and Tolerance in Plants, vol. 1. Springer, pp. 1–40. https://doi.org/10.1007/978-3-319-75671-4_1.

Kerstiens, G., 1996. Cuticular water permeability and its physiological significance. J. Exp. Bot. 47 (12), 1813–1832. https://doi.org/10.1093/jxb/47.12.1813.

Khare, T., Kuma, V., Kavi Kishor, P.B., 2015. Na^+ and Cl^- ions show additive effects under NaCl stress on induction of oxidative stress and the responsive antioxidative defense in rice. Protoplasma 252, 1149–1165. https://doi.org/10.1007/s00709-014-0749-2.

Koyro, H.-W., Hussain, T., Huchzermeyer, B., Khan, M.A., 2013. Photosynthetic and growth responses of a perennial halophytic grass *Panicum turgidum* to increasing NaCl concentrations. Environ. Exp. Bot. 91, 22–29. https://doi.org/10.1016/j.envexpbot.2013.02.007.

Latz, A., Mehlmer, N., Zapf, S., Mueller, T.D., Wurzinger, B., Pfister, B., Csaszar, E., Hedrich, R., Teige, M., Becker, D., 2013. Salt stress triggers phosphorylation of the Arabidopsis vacuolar K^+ channel TPK1 by calcium-dependent protein kinases (CDPKs). Mol. Plant 6, 1274–1289. https://doi.org/10.1093/mp/sss158.

Liu, Y., Zhang, X., Tran, H., Shan, L., Kim, J., Childs, K., Ervin, E.H., Frazier, T., Zhao, B., 2015. Assessment of drought tolerance of 49 switchgrass (*Panicum virgatum*) genotypes using physiological and morphological parameters. Biotechnol. Biofuels 8 (1), 1–18. https://doi.org/10.1186/s13068-015-0342-8.

Luo, Y., Zhao, X., Zhou, R., Zuo, X., Zhang, J., Li, Y., 2011. Physiological acclimation of two psammophytes to repeated soil drought and rewatering. Acta Physiol. Plant. 33 (1), 79–91. https://doi.org/10.1007/s11738-010-0519-5.

Maricle, B.R., Maricle, K.L., 2018. Photosynthesis, stomatal responses, and water potential in three species in an inland salt marsh in Kansas, USA. Flora 244–245, 1–7. https://doi.org/10.1016/j.flora.2018.05.001.

Metcalfe, C.R., 1960. Anatomy of the Monocotyledons. Clarendon Press, Oxford, p. 731p. https://doi.org/10.1126/science.133.3467.1817-a.

Munns, R., Tester, M., 2008. Mechanisms of salinity tolerance. Annu. Rev. Plant Biol. 59 (1), 651–681. https://doi.org/10.1146/annurev.arplant.59.032607.092911.

Munns, R., Wallace, P.A., Teakle, N.L., Colmer, T.D., 2010. Measuring soluble ions concentrations (Na^+, K^+ e Cl^-) in salt treated plants. In: Clifton, N.J. (Ed.), Plant Stress Tolerance: Methods and Protocols, vol. 639. Humana Press. Springer, pp. 371–382. https://doi.org/10.1007/978-1-60761-702-0_23.

Murata, N., Allakhverdiev, S.I., Nishiyama, Y., 2012. The mechanism of photoinhibition in vivo: Re-evaluation of the roles of catalase, alpha-tocopherol, non-photochemical quenching and electron transport. Biochim. Biophys. Acta Bioenerg. 1817 (8),1127–1133. https://doi.org/10.1016/j.bbabio.2012.02.020.

Netondo, G.W., Onyango, J.C., Beck, E., 2004. Sorghum and salinity: II. Gas exchange and chlorophyll fluorescence of sorghum under salt stress. Crop Sci. 44, 806–811. https://doi.org/10.2135/cropsci2004.7970.

Pan, T., Liu, M., Kreslavski, V.D., Zharmukhamedov, S.K., Nie, C., Yu, M., Kuznetsov, V. V., Allakhverdiev, S.I., Shabala, S., 2020. Non-stomatal limitation of photosynthesis by soil salinity. Crit. Rev. Environ. Sci. Technol. 1–35. https://doi.org/10.1080/10643389.2020.1735231.

Percey, W.J., McMinn, A., Bose, J., Breadmore, M.C., Guijt, R.M., Shabala, S., 2016. Salinity effects on chloroplast PSII performance in glycophytes and halophytes. Funct. Plant Biol. 43 (11), 1003–1015. https://doi.org/10.1071/FP16135.

Pottosin, I., Shabala, S., 2016. Transport across chloroplast membranes: optimizing photosynthesis for adverse environmental conditions. Mol. Plant 9 (3), 356–370. https://doi.org/10.1016/j.molp.2015.10.006.

Rivelli, A.R., Lovelli, S., Perniola, M., 2002. Effects of salinity on gas exchange, water relations and growth of sunflower (*Helianthus annuus*). Funct. Plant Biol. 29, 1405–1415. https://doi.org/10.1071/PP01086.

Santos Júnior, U.M. dos, Gonçalves, J.F., Strasser, R.J., Fearnside, P.M., 2015. Flooding of tropical forests in central Amazonia: what do the effects on the photosynthetic apparatus of trees tell us about species suitability for reforestation in extreme environments created by hydroelectric dams? Acta Physiol. Plant. 37 (8), 166. https://doi.org/10.1007/s11738-015-1915-7.

Sasi, S., Venkatesh, J., Daneshi, R.F., Gururani, M.A., 2018. Photosystem II extrinsic proteins and their putative role in abiotic stress tolerance in higher plants. Plants 7 (4), 100. https://doi.org/10.3390/plants7040100.

Shabala, L., Mackay, A., Tian, Y., Jacobsen, S.-E., Zhou, D., Shabala, S., 2012. Oxidative stress protection and stomatal patterning as components of salinity tolerance mechanism in quinoa (*Chenopodium quinoa*). Physiol. Plantarum 146 (1), 26–38. https://doi.org/10.1111/j.1399-3054.2012.01599.x.

Shabala, S., Pottosin, I., 2014. Regulation of potassium transport in plants under hostile conditions: implications for abiotic and biotic stress tolerance. Physiol. Plantarum 151 (3), 257–279. https://doi.org/10.1111/ppl.12165.

Sharma, P., Jha, A.B., Dubey, R.S., Pessarakli, M., 2012. Reactive oxygen species, oxidative damage, and antioxidative defense mechanism in plants under stressful conditions. Journal of Botany 1–26. https://doi.org/10.1155/2012/217037, 2012.

Shelke, D., Nikalje, G., Nikam, T., Maheshwari, P., Punita, D., Rao, K., Kavi Kishor, P., Suprasanna, P., 2019. Chloride (Cl^-) uptake, transport, and regulation in plant salt tolerance. In: Roychoudhury, A., Tripathi, D. (Eds.), Molecular Plant Abiotic Stress. Molecular plant abiotic stress: biology and biotechnology. Wiley, pp. 241–268. https://doi.org/10.1002/9781119463665.ch13.

Shi, H., Quintero, F.J., Pardo, J.M., Zhu, J.-K., 2002. The putative plasma membrane Na$^+$/H^+ antiporter SOS1 controls long-distance Na^+ transport in plants. Plant Cell 14, 465–477. https://doi.org/10.1105/tpc.010371.

Shone, M.G.T., Clarkson, D.T., Sanderson, J., 1969. The absorption and translocation of sodium by maize seedlings. Planta 86 (4), 301–314. https://doi.org/10.1007/BF00388956.

Siringam, K., Juntawong, N., Cha-Um, S., Kirdmanee, C., 2013. Exogenous application of potassium nitrate to alleviate salt stress in rice seedlings. J. Plant Nutr. 36 (4), 607–616. https://doi.org/10.1080/01904167.2012.754032.

Spurr, A.R., 1969. A low-viscosity epoxy resin embedding medium for electron microscopy. J. Ultra. Res. 26, 31–43. https://doi.org/10.1016/S0022-5320(69)90033-1.

Strasser, R.J., Srivastava, A., Tsimilli-Michael, M., 2000. The fluorescence transient as a tool to characterize and screen photosynthetic samples. In: Yunus, M., Pathre, U., Mohanty, P. (Eds.), Probing Photosynthesis: Mechanisms, Regulation and Adaptation. Taylor and Francis, London, pp. 445–483.

Strasser, R.J., Tsimilli-Michael, M., Srivastava, A., 2004. Analysis of the chlorophyll *a* fluorescence transient. In: Papageorgiou, G.C., Govindjee (Eds.), Advances in Photosynthesis and Respiration, vol. 19. Springer, pp. 321–362. https://doi.org/10.1007/978-1-4020-3218-9_12.

Sudhir, P.R., Pogoryelov, D., Kovacs, L., Garab, G., Murthy, S.D., 2005. The effects of salt stress on photosynthetic electron transport and thylakoid membrane proteins in the cyanobacterium *Spirulina platensis*. J. Biochem. Mol. Biol. 38 (4), 481–485. https://doi.org/10.5483/BMBRep.2005.38.4.481.

Tavakkoli, E., Rengasamy, P., McDonald, G.K., 2010. High concentrations of Na^+ and Cl^- ions in soil solution have simultaneous detrimental effects on growth of faba bean

under salinity stress. J. Exp. Bot. 61, 4449–4459. https://doi.org/10.1093/jxb/erq251.

Valença, D.C., Moura, S. M. de, Travassos-Lins, J., Alves-Ferreira, M., Medici, L.O., Ortiz-Silva, B., Macrae, A., Reinert, F., 2020. Physiological and molecular responses of *Setaria viridis* to osmotic stress. Plant Physiol. Biochem. 155, 114–125. https://doi.org/10.1016/j.plaphy.2020.07.019.

V'ery, A.A., Sentenac, H., 2003. Molecular mechanisms and regulation of K^+ transport in higher plants. Annu. Rev. Plant Biol. 54, 575–603. https://doi.org/10.1146/annurev.arplant.54.031902.134831.

Wang, X-g., Zhao, X-h., Jiang, C-j., Li, C-h., Cong, S., Wu, D., Chen, Y-q., Yu, H-q., Wang, C-y., 2015. Effects of potassium deficiency on photosynthesis and photoprotection mechanisms in soybean (*Glycine max* (L.) Merr.). Journal of Integrative Agriculture 14 (5), 856–863. https://doi.org/10.1016/S2095-3119(14)60848-0.

Yamane, K., Kawasaki, M., Taniguchi, M., Miyake, H., 2008. Correlation between chloroplast ultrastructure and chlorophyll fluorescence characteristics in the leaves of rice (*Oryza sativa* L.) grown under salinity. Plant Prod. Sci. 11, 139–145. https://doi.org/10.1626/pps.11.139.

Yamane, K., Taniguchi, M., Miyake, H., 2012. Salinity-induced subcellular accumulation of H_2O_2 in leaves of rice. Protoplasma 249 (2), 301–308. https://doi.org/10.1007/s00709-011-0280-7.

Yan, K., Shao, H., Shao, C., Chen, P., Zhao, S., Brestic, M., Chen, X., 2013. Physiological adaptive mechanisms of plants grown in saline soil and implications for sustainable saline agriculture in coastal zone. Acta Physiol. Plant. 35 (10), 2867–2878. https://doi.org/10.1007/s11738-01301325-7.

Yermanos, D.M., Francois, L.E., Tammandoni, T., 1967. Effects of salinity on the development of jojoba. Econ. Bot. 21, 69–80. https://doi.org/10.1007/BF02897177.

Yusuf, M.A., Kumar, D., Rajwanshi, R., Strasser, R.J., Tsimilli-Michael, M., Govindjee, Sarin, N.B., 2010. Overexpression of y-tocopherol methyl transferase gene in transgenic *Brassica juncea* plants alleviates abiotic stress: physiological and chlorophyll *a* fluorescence measurements. Biochimica et Biophysica Acta, Amsterdam 1797, 1428–1438. https://doi.org/10.1016/j.bbabio.2010.02.002.

Zhang, H.H., Xu, N., Wu, X., Wang, J.F., Ma, S., Li, X., Sun, G., 2018. Effects of four types of sodium salt stress on plant growth and photosynthetic apparatus in sorghum leaves. J. Plant Interact. 13 (1), 506–513. https://doi.org/10.1080/17429145.2018.1526978.

Zhao, C., Zhang, H., Song, C., Zhu, J.-K., Shabala, S., 2020. Mechanisms of plant responses and adaptation to soil salinity. Innovation 1 (1), 100017. https://doi.org/10.1016/j.xinn.2020.100017.

Zhao, D., Oostherhuis, D.M., Bednarz, C.W., 2001. Influence of potassium deficiency on photosynthesis, chlorophyll content, and chloroplast ultrastructure of cotton plants. Photosynthetica 39, 103–109. https://doi.org/10.1023/A:1012404204910.

Zörb, C., Senbayram, M., Peiter, E., 2014. Potassium in agriculture – status and perspectives. J. Plant Physiol. 171, 656–669. https://doi.org/10.1016/j.jplph.2013.08.

Appendixes - Supplemental files

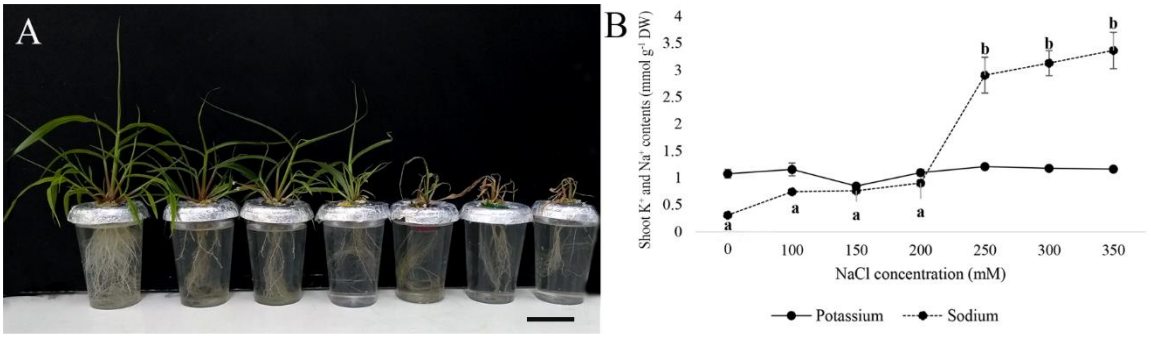

Appendix 1. *S. viridis* plants submitted to increasing concentrations of sodium chloride (NaCl) ranging from 0 to 300 mM. A. From left to right plants exposed to 0, 100, 150, 200, 250, 300 and 350mM of NaCl 120 h after treatments imposition; B. Potassium and sodium accumulation in shoot tissues 120 h after treatments imposition. Scale bar: 6cm.

CAPÍTULO 4 – ARTIGO II

NaCl- and KCl-induced effects on ion relations, photosynthesis and growth of *Chloris gayana*

Artigo em preparação para submissão

NaCl- and KCl-induced effects on ion relations, photosynthesis and growth of *Chloris gayana*

Ana Carolina Mendes Bezerra[1], Lukasz Kotula[2], Bianca Ortiz-Silva[3], Leonardo Oliveira Medici[4], Fernanda Reinert[1] and Timothy D. Colmer[2]

[1] Universidade Federal do Rio de Janeiro/IB −Dept. of Botany, Av. Carlos Chagas Filho, 373 − Ilha do Fundão −21941-902 − Rio de Janeiro, RJ – Brazil;

[2] School of Agriculture and Environment, The University of Western Australia, 35 Stirling Highway, Perth, WA 6009, Australia;

[3] Universidade Federal do Rio de Janeiro- NUMPEX-Bio, Estrada de Xerém, 27- Duque de Caxias − 25245-390− Rio de Janeiro, RJ – Brazil;

[4] Universidade Federal do Rural Rio de Janeiro − Dept. of Physiological Sciences, Rod. BR 465, km 7 − 23897-000 − Seropédica, RJ – Brazil.

ABSTRACT

Soil salinization is a widespread environmental problem that impacts agriculture. We assessed comparative responses of growth, physiology, and ion distribution of two Rhodes grass (*Chloris gayana)* cultivars, Callide and Reclaimer, in response to high NaCl salinity and KCl. Plants were grown under different saline regimes (0, 200, 400, and 600 mM NaCl + 1 or 10 mM KCl). Exposure of both cultivars to NaCl concentrations equal to or higher than 200 mM triggered response mechanisms such as the ability to accumulate inorganic solutes, stomata closure, and secretion (up to 70%) of the retained Na^+ onto the leaf surface. For Reclaimer, KCl induced positive effects in leaf photochemistry under 0 and 200 mM NaCl, as illustrated by OJIP-bands and JIP-test parameters. However, such improvements did not result in greater biomass accumulation or net photosynthesis compared to the corresponding treatments under 1 mM KCl, which may not justify the KCl application. For Callide, the opposite was observed. Even though salinity induced-stress triggered biomass reduction of up to 70% in 600 mM NaCl plants of both cultivars remained photosynthetically active under all treatments. Data reported here can provide the foundation for future research, especially if combined with genomic, proteomic, and metabolomic studies for a better understanding of salt tolerance mechanisms. Our data reinforce that Rhodes grass is an auspicious crop under saline environments and can be central in conservation programs considering soil

desalinization.

Key-words: Rhodes grass - Callide – Reclaimer – chlorophyll *a* fluorescence – gas exchange

1. Introduction

Soil salinity affect more than 1 billion hectares of land worldwide (Ivushkin et al., 2019) distressing crops performance through impacts on plant growth and yield (Munns and Tester, 2008). Climate change scenarios predict increase of land salinization that will impose a threat to agricultural production affecting more than 600 million people by 2100 (Kotula et al., 2020; Munns et al., 2020). Salt tolerance of crops may be increased by exploiting variation in salt tolerance within existing crops or by exploiting mitigation strategies in halophytic plants that that could be used to develop new crops (Colmer et al, 2005; Munns et al., 2006; Shabala, 2013).

Due to the osmotic and ionic components of salinity, acclimation to saline environments can result in reduced water uptake, turgor, nutritional disorders, and, therefore, growth. To thrive in such environments, plants depend on the conservation of hydric (osmotic adjustment) and ionic homeostasis (salt exclusion and compartmentalization) (Zhao et al., 2020). Plants can adjust osmotically by increasing the concentration of osmolytes, reducing water potential and maintaining water uptake (Deilein et al., 2014). Such reduction can be achieved either by absorbing and compartmentalizing ions abundantly present in the saline soil solution (ex. Na^+ and Cl^-) in the vacuoles and/or by synthesizing osmolytes compatible with its metabolism in the cytoplasm, an energetically expensive process (Tester and Davenport, 2003). Rhodes grass (*Chloris gayana* Kunth) is a salt-tolerant Poaceae with C_4-phosphoenolpyruvate carboxykinase (PCK) metabolism (Omoto et al., 2010) used as pasture in subtropical regions (Suttie, 2000). Excretion of salt through salt glands on both sides of leaf lamina has been associated with high salinity tolerance of the species, reported as capable of excluding almost twice the amount of sodium present in its leaves even under high levels of salinity (Oi et al., 2012; Oi et al., 2013).

Besides that, plants require a range of macro and micronutrients and all of them possess a specific role in plants' metabolism (Subbarao et al., 2003). The essentiality of a nutrient rests on plants' inability to complete their life cycle without it (Arnon and Stout, 1939). Potassium is an essential nutrient that participates in several physiological functions in

plant' metabolism and is often associated with acclimation to stressful environments (Hasanuzzaman et al., 2018). Because of their similar physicochemical properties, K^+ and Na^+ ions compete for common absorption and transport sites in the root and cellular membranes; high concentrations of Na^+ ions often reduce K^+ uptake (Wakeel, 2013).

It is widely accepted that the maintenance of adequate K^+/Na^+ ratios is essential for salt tolerance (Assaha et al., 2017; Shabala and Pottosin, 2014). K^+ is known to fulfill roles in both stomatal and non-stomatal effects on plant photosynthesis (Hatam et al., 2020; Pottosin and Shabala, 2016). However, K^+ fulfills specific and non-specific roles in plant' metabolism. Non-specific functions can be performed by other monovalent cations such as Na^+ depending on the species and genotypes (Wakeel, 2013; Subbarao et al., 2003). The use of Na^+ ions as an osmoticum in the vacuole, for example, will reduce the required critical level of tissue [K] (Mian et al., 2011). In earlier studies, a relationship of growth rate with the content of Na^+ and K^+ indicated that Rhodes grass might have the capability of using other cations, such as sodium, in place of potassium for some physiological and metabolic functions (Smith, 1974). Furthermore, Na^+ is also described as an essential nutrient in some C_4 species (Ohnishi et al., 1990). The essential role of sodium seems to be linked with specificities of the C_4 pathways of photosynthesis through the Na^+/pyruvate co-transport system into chloroplasts of the subgroups NAD-malic enzyme and PCK (Aoki and Kanai, 1997), necessary for the regeneration of phosphoenolpyruvate and CO_2 fixation (Ohnishi et al., 1990).

Understanding the association between ionic relations and growth of Rhodes grass, can help the comprehension of important questions related to the mechanisms of salt tolerance of the species. The K^+/Na^+ selectivity and strategies to cope with salt, conversely, can contribute to the elucidation of potassium physiological and metabolic roles and the influence of NaCl in plant metabolism. In the future, these results can help develop important tools for salt tolerance in non-halophytic species. This study attempts to investigate the ionic interaction between the effects of NaCl-salinity and KCl on photosynthesis and ion distribution and its effects on the growth of a moderate-sensitive (Callide) and tolerant (Reclaimer) cultivar of Rhodes grass. The data reported here suggest that Rhodes grass is an auspicious crop at low-quality soils and can be fundamental in conservation programs considering soil desalinization.

2. Material and methods

2.1. Seed germination and growth conditions

The experiment was conducted between October and December under natural sunlight at 30 ºC (day)/ 25 ºC (night) in a glasshouse located at the University of Western Australia (UWA), Perth WA, Australia (31º57' S, 115º47' E). Seeds of two Rhodes grass (*Chloris gayana*) cultivars, Callide and Reclaimer, were surface-sterilized with 0.5% sodium hypochlorite solution for 5 min and rinsed 3 times with deionized water. We used a modified nutrient solution adapted from Kotula et al., 2015, containing the following macronutrients and micronutrients (mM): $CaSO_4.2H_2O$ (1.5); $MgSO_4.7H_2O$ (0.4); $Ca(NO_3)_2.4H_2O$ (1.5); KNO_3 (0.75); NH_4NO_3 (0.625); KH_2PO_4 (0.2); $Na_2O_3Si.9H_2O$ (0.1); Fe-EDTA (0.05); KCL (0.05); H_3BO_3 (0.025); $MnSO_4.H_2O$ (0.002); $ZnSO_4.7H_2O$ (0.002); $CuSO_4.5H_2O$ (0.0005); $Na_2MoO_4.2H_2O$ (0.0005); $NiSO_4.7H_2O$ (0.001). The solution was buffered with 1.0 mM MES (2-[N-morpholino]ethanesulfonic acid) and pH was adjusted to 6.5 using NaOH. Seeds were germinated on plastic mesh floating on 25% strength aerated nutrient solution in darkness for 4 days. On the 4th day, the nutrient solution was changed to 50% in strength and the seedling were exposed to natural sunlight. The seedlings were transplanted to pots containing full-strength nutrient solution adapted from Kotula et al. (2015) when the 4th leaf was fully expanded (~10 days after germination).

Plants were grown in hydroponic continuously-aerated system in individual 5 L pots covered with aluminum foil. Salt treatments were imposed after 7 days of the transplant. In a factorial scheme, 4 pots of plants of each Callide and Reclaimer cultivars were exposed to sodium chloride (NaCl; 0, 200, 400, and 600 mM) and potassium chloride (KCl; 1 and 10 mM) combinations (0 mM NaCl + 1 mM KCl; 0 mM NaCl + 10 mM KCl; 200 mM NaCl + 1 mM KCl; 200 mM NaCl + 10 mM KCl; 400 mM NaCl + 1 mM KCl; 400 mM NaCl + 10 mM KCl; 600 mM NaCl + 1 mM KCl; 600 mM NaCl + 10 mM KCl) totaling 64 experimental units (2 cultivars × 4 NaCl treatments × 2 KCl treatments × 4 replicates). Each pot contained a total of 3 plants. The NaCl treatments were imposed by adding 100 mM NaCl every 24 h until final concentrations of NaCl had been achieved. From the first addition of NaCl, the experiment was conducted for 40 days and nutrient solution was renewed every 7 days. Non-invasive measurements, as chlorophyll *a* fluorescence, were performed in more than one replicate per pot.

2.2. Biomass accumulation

Samples for biomass accumulation were taken at the time treatments were imposed (initial; 7 days after seedlings transplantation; 4th leaf fully expanded) and after 25 days of treatments (32 days after seedlings transplantation). At sampling, shoots were washed with deionized water while roots of salt-treated plants were rinsed with mannitol solution equivalent to the NaCl levels to avoid osmotic shock (100, 200 and 300 mM mannitol + 1.5 mM $CaSO_4$ for 200, 400 and 600 mM NaCl treatments, respectively) and roots from non-saline controls were rinsed with 1.5 mM $CaSO_4$. To assess dry weight, harvested biomass was oven-dried at 70º C for 72 h to a constant weight. Water content was estimated from fresh and dry weight data to calculate mL H_2O g^{-1} dry weight. Values of shoot and root fresh weight are presented in the supplementary material (Table S1). Relative growth rates were calculated using the equation $RGR = (\ln DW_2 - \ln DW_1\ )\ (t_2 - t_1)^{-1}$ (Hunt, 1982), where: DW_1 (g) is the total dry mass (shoot and root) before treatments were imposed; DW_2 (g) is the total dry mass at the final harvest; t_1 is the time (days) when the dry mass was firstly assessed and, t_2 is the time (days) of the final harvest.

2.3. Tissue ion analysis

Root and shoot tissues were oven-dried and ground to a fine powder for Na^+ and K^+ analyses following Munns et al. (2010). Samples of about 100 mg of dried tissue were extracted in 0.5 M HNO_3 (10 mL) by shaking for 48 h in the dark at room temperature. Diluted samples of the extracts were analyzed for Na^+ and K^+ using a flame photometer (Flame Photometer 410, Sherwood, Cambridge, UK).

2.4. Leaf washing

At 24 days after treatment application, the third fully expanded leaf of *C. gayana* was washed with deionized water to remove the salt from the leaf surface. At 25 days of treatments (1 day after leaf washing), the leaf blades from third leaf were excised and placed in falcon-type tubes containing 10 mL of deionized water and shaken to remove salts from the surface. The leaf blades were removed and oven-dried. Concentrations of Na^+ and K^+ were assessed in both the leaf blade of the excised leaves and the washing solution using a flame photometer (Flame Photometer 410, Sherwood, Cambridge, UK), as described above, to estimate ion retention and secretion of K^+ and Na^+ ions in *C. gayana* leaves.

2.5. Leaf sap osmotic potential

Leaf blade of the third fully expanded leaf was collected and immediately placed into a 2 mL air-tight cryovial, frozen in liquid N_2, and stored at –20º C for further analysis. Leaf samples were thawed and sap was extracted using a simple hand-operated press. About 20 µL of leaf sap was collected and the measurements were conducted using a freezing point depression Fiske 210 osmometer (Advanced Instruments Inc., Norwood, MA).

2.6. Estimated contribution of ions (K^+ and Na^+) to the leaf sap osmotic potential

Estimation of contribution of K^+ and Na^+ ions to the leaf sap osmotic potential was calculated as = $(\frac{([ion]\ per\ sample\ water\ content) * 100}{osmotic\ potential})$, in mmol L^{-1} (Garthwaite et al., 2005). Values of sample water content refer to plant shoot measurements described above (difference between fresh and dry weight; item 2.2).

2.7. Gas exchange and chlorophyll a fluorescence measurements

Gas exchange measurements were performed on the 2nd fully expanded leaf of *C. gayana* using an LI-6400XT open gas-exchange system (LI-COR Biosciences Inc., Lincoln, NB, USA) at a photosynthetically active radiation of 1,500 µmol photons m^{-2} s^{-1} (light saturated), leaf chamber temperature of 30º C, 60–70% relative humidity and CO_2 concentrations of 400 (ambient) and 800 (elevated) µmol mol^{-1}.

Measurements of chlorophyll *a* fluorescence transients were done in intact fully expanded dark-adapted leaves (2nd fully expanded) using a Pocket PeA portable fluorometer (Hansatech Instruments, King's Lynn, Norfolk, UK). Fluorescence was inducted by a pulse of saturating light (3,500 µmol photons m^{-2} s^{-1}) during one second of illumination (10 µs to 1 s) in the 2nd fully expanded leaf. Measurements were conducted in the morning (from 10 to 11 a.m.) after dark adaptation for at least 20 min. Intensities from 50 (minimum fluorescence, F_O) 100, 300 µs, 2, and 30 ms to the highest intensity F_M (maximum fluorescence) were analyzed using the JIP-test parameters (Strasser et al., 1995; Strasser et al., 2004). The plotted fluorescence values were the average of eight measurements from each treatment.

To compare events reflected in the OJ, OI, and IP phases, the transients were normalized as relative variable fluorescence: $W_t = (F_t - F_0) / (F_J - F_0)$, $W_{OI} = (F_t - F_0) / (F_I - F_0)$ and $W_{IP} = (F_t - F_I) / (F_P - F_I)$ (Yusuf et al., 2010). Difference kinetics from relative variable fluorescence data were also calculated ($\Delta W = W_{recovery} - W_{control}$), following the

procedures of Yusuf et al. (2010) to disclose K- and L-bands between the steps W_{OJ} (K-band; 300 µs) and W_{OK} (L-band; 150 µs). To plot the normalized curves (W_{OJ}, W_{OK}, JIP radar) and observe the influence of all of the treatments the data was normalized based on the fluorescence transients of plants grown with the normal nutrient solution at an intermediary KCl level (4 mM).

2.8. Data analysis

The normal distribution of all data and homogeneity of variances was previously verified using the Cochran homogeneity test. Box-cox transformation was used when needed. Results were submitted to three- (factors: 'cultivar', 'NaCl' and 'KCl') and two-way (factors: 'NaCl' and 'KCl') analysis of variance - ANOVA ($p \leq 0.05$). In the presence of significant difference, Scott-Knott's test was used to determine the significance at $p \leq 0.05$. The analysis was carried out by processing experimental data in the software STATISTICA and Sisvar (Federal University of Lavras, Lavras, Brazil). To investigate groupings Principal Component Analysis (PCA) was carried out using the PAST 3 software (PAleontological STatistics).

3. Results

3.1.PCA

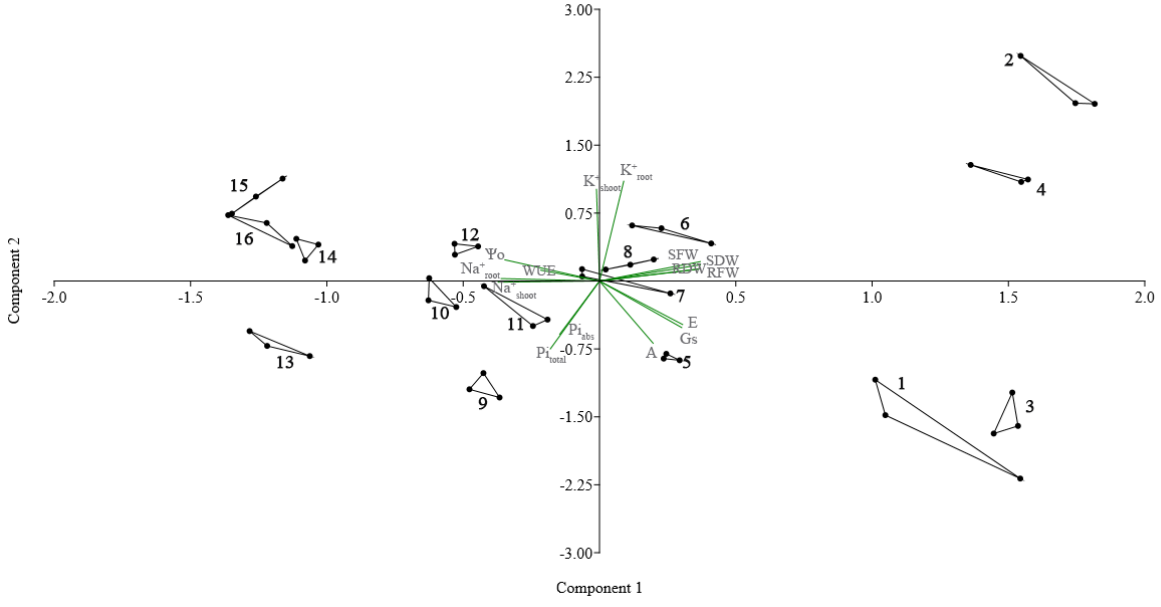

Figure 1. Principal component analysis (PCA) of Rhodes Grass (*Chloris gayana*) cv. Callide (A) and Reclaimer (B) grown in aerated nutrient solution under different saline regimes (0, 200, 400, and 600 mM) with 1 or 10 mM KCl. Treatments were imposed on 15-day-old plants

and samples were taken after 25 days of treatment. Axes is in eigenvalue scale. **1** – cv. Callide, 0 mM of NaCl + 1 mM KCl; **2** - cv. Callide, 0 mM of NaCl + 10 mM of KCl; **3** – cv. Reclaimer, 0 mM of NaCl + 1 mM KCl; **4** - cv. Reclaimer, 0 mM of NaCl + 10 mM of KCl; **5-** cv. Callide, 200 mM of NaCl + 1 mM of KCl**; 6** - cv. Callide, 200 mM of NaCl + 10 mM of KCl; **7-** cv. Reclaimer, 200 mM of NaCl + 1 mM of KCl**; 8** - cv. Reclaimer, 200 mM of NaCl + 10 mM of KCl; **9** - cv. Callide, 400 mM of NaCl + 1 mM of KCl; **10** - cv. Callide, 400 mM of NaCl + 10 mM of KCl; **11** - cv. Reclaimer, 400 mM of NaCl + 1 mM of KCl; **12** - cv. Reclaimer, 400 mM of NaCl + 10 mM of KCl; **13** - cv. Callide, 600 mM of NaCl + 1 mM of KCl; **14** - cv. Callide, 600 mM of NaCl + 10 mM of KCl; **15** - cv. Reclaimer, 600 mM of NaCl + 1 mM of KCl; **16** - cv. Reclaimer, 600 mM of NaCl + 10 mM of KCl; Na^{+}_{shoot}: shoot Na^{+} concentration; Na^{+}_{root}: root Na^{+} concentration. K^{+}_{shoot}: shoot K^{+} concentration; K^{+}_{root}: root K^{+} concentration; SFW: shoot fresh weight; SDW: shoot dry weight; RFW: root fresh weight; RDW: root dry weight; PI_{abs} and PI_{total}: performance indexes of chlorophyll *a* fluorescence (JIP-test); *A*: photosynthesis; *E*: transpiration; g_s: stomatal conductance; WUE: water use efficiency; Ψo: osmotic potential of the leaf sap.

A principal component analysis (PCA) was carried out to identify the main variables responsible for grouping treatments (Fig. 1). The first and second components (PC1 and PC2) explained, respectively, 56.6 and 16.6% of the total variation among individuals. The main characteristics responsible for grouping the individuals exposed to the highest levels of NaCl were the sodium (Na^{+}) content in the whole plant and the osmotic potential, while the groups submitted to the lowest levels of NaCl the accumulation of biomass and gas exchange parameters were more determinant. Considering the K^{+} concentration available in the nutrient solution, the main characteristics responsible for the separation of groups were the potassium (K^{+}) content in the whole plant, gas exchange, and performance indexes of chlorophyll *a* fluorescence parameters. Cultivars' groupings presented similar behavior, except when considering the highest level of NaCl (600 mM) concomitant with the lowest level of KCl (1mM), in this case, levels of sodium and osmotic potential were more relevant to the separation of Callide's groups and photosynthetic JIP-parameters were responsible for the separations of Reclaimer's groups.

3.2. Biometric traits

Increase in NaCl levels negatively impacted biomass accumulation. Shoot fresh weight (SDW) of Callide was not significantly affected by 200 mM NaCl + 1 KCl mM treatment, but decreased -0.6-fold (relative to non-saline control) under 400 mM NaCl + 1 mM KCl treatment and -0.9-fold (relative to non-saline control) at the highest salt level (600 mM NaCl with 1 mM KCl). Application of 10 mM KCl improved SDW in non-saline plants 0.3-fold but

under 200, 400 and 600 mM of NaCl caused, respectively, decreases of -0,4-, -0.7- and -0.9-fold compared to non-saline controls + 10 KCl.

Control plants with 1 mM of KCl presented a final average of shoot dry mass of 21.3 g plant^{-1} for Reclaimer cultivar. Reclaimer displayed decreases of -0.3-fold in SDW when exposed to 200 mM of NaCl + 1 mM KCl and -0.7 and -0.8-fold for 400 mM NaCl and 600 mM NaCl, respectively (Table 1). No significant differences were observed between 1 and 10 mM KCl at the same the NaCl levels. Root dry weight (RDW) of both cultivars were decreased, relative to non-saline control, on average -0.6-fold in 200 mM NaCl + 1 mM KCl, 0.7-fold in 400 mM NaCl + 1 mM KCl and -0.8-fold in 600 mM NaCl + 1 mM KCl. The higher availability of KCl (10 mM) also did not affect RDW of the roots with the NaCl levels, except for non-saline controls in cv. Callide where 10 mM KCl increased RDW 0.1-fold

The shoot water content (SWC) of both Callide and Reclaimer showed progressive reductions in response to NaCl + KCl treatments. Control plants with 1 mM of KCl presented a final average of shoot water content of 58.8 g plant^{-1} for Callide cultivar and 61.9 g plant^{-1} for Reclaimer cultivar. The presence of 10 mM of KCl increased the shoot water content by about 0.6 and 0.3-fold in non-saline controls for Callide and Reclaimer, respectively. The 200 mM NaCl + 1 mM KCl treatment did not affect the SWC of Callide cultivar but exposure to 400 mM and 600 mM of NaCl decreased SWC, respectively, by -0.4 and -0.8-fold compared to non-saline control + 1 mM KCl (Table 1). Reclaimer displayed decreases of -0.3-fold in SDW when exposed to 200 mM of NaCl + 1 mM KCl and -0.7 and -0.9-fold for 400 mM NaCl and 600 mM NaCl + 1 mM KCl, respectively (Table 1). Except for non-saline controls, the application of 10 mM of KCl did not affect the water content in both cultivars at all salinity levels.

Root water content (RWC) of both cultivars were decreased, relative to non-saline control + 1 mM KCl, on average by -0.4-fold in 200 mM NaCl + 1 mM KCl, -0.7-fold in 400 mM NaCl + 1 mM KCl and -0.8-fold in 600 mM NaCl + 1 mM KCl in cv. Callide. For the cv. Reclaimer, RWC was reduced by on average -0.4-fold in 200 and 400 mM NaCl + 1 mM KCl and -0.7-fold in 600 mM NaCl + 1 mM KCl. In non-saline controls of Reclaimer cultivar addition of 10 mM of KCl in the nutrient solution led to a 0.2-fold increase in RWC, but in the other treatments, the availability of 10 mM KCl did not improve the accumulation of water in roots (Table 1).

Table 1. Dry weights and water content of shoot and roots of two Rhodes Grass (*Chloris gayana*) cultivars, Callide and Reclaimer, grown in aerated nutrient solution under different saline regimes (0, 200, 400, and 600 mM NaCl) with 1 or 10 mM potassium chloride.

		Shoot dry weight (g)		**Root dry weight (g)**		**Shoot water content (g)**		**Root water content (g)**	
	NaCl (mM)	*KCl (mM)*							
Cultivar		*1*	*10*	*1*	*10*	*1*	*10*	*1*	*10*
Callide	*0*	19.3+2.2^{Ab}	25.8±1.9^{Aa}	3.6±0.5^{Ab}	4.2±0.5^{Aa}	55.8±9.2^{Ab}	89.4±24.6^{Aa}	36.3±4.1^{A}	41.3±7.3^{A}
	200	17.0±2.2^{A}	14.8±2.2^{B}	1.6±0.1^{B}	1.7±0.3^{B}	54.0±4.1^{A}	50.6±8.4^{A}	21.8±4.9^{B}	23.8±5.5^{B}
	400	7.3±2.6^{B}	7.8±2.3^{C}	0.9±0.1^{C}	1.1±0.3^{C}	32.3±6.3^{B}	24.1±0.3^{B}	11.9±2.2^{C}	13.0±4.1^{C}
	600	4.1±0.6^{C}	3.3±1.1^{D}	0.5±0.1^{C}	0.6±0.2^{D}	10.2±2.1^{C}	8.0±3.8^{C}	5.8±1.8^{C}	7.5±2.8^{C}
Reclaimer	*0*	21.3±2.6^{Ab}	25.4±2.3^{Aa}	3.1±0.7^{A}	3.0±0.2^{A}	61.9±15.5^{Ab}	81.9±15.5^{Aa}	27.5±1.0^{Ab}	33.4±5.1^{Aa}
	200	14.5±2.5^{B}	14.2±2.9^{B}	1.5±0.3^{B}	1.4±0.2^{B}	45.6±9.2^{B}	43.2±12.3^{B}	18.3±4.4^{B}	17.0±3.1^{B}
	400	6.7±1.3^{C}	8.8±2.2^{C}	1.2±0.3^{B}	1.1±0.2^{B}	18.7±3.6^{C}	24.4±5.1^{C}	16.2±3.8^{B}	16.7±4.2^{B}
	600	3.3±0.9^{D}	3.8±1.0^{D}	0.5±0.1^{C}	0.7±0.2^{C}	3.8±1.0^{D}	8.8±2.4^{D}	5.5±1.5^{C}	8.6±1.7^{C}

Upper case letters represent significant differences among NaCl levels within the same KCl level (column) using the Scott-Knott test at $p < 0.05$, and lowercase letters represent significant difference between the two KCl levels at the same level of NaCl (rows) using the F-test at $p < 0.05$. Treatments were imposed on 15-day-old plants and samples were taken after 25 days of treatment. Means ± standard deviation (n =8). There was a significant cultivar × NaCl × KCl interaction for shoot SWC at p <0.01 and RWC at p <0.05 (three-way ANOVA). Additional statistical analysis is given in Supplementary material (Table S2).

Total plant relative growth rate (RGR) during the treatment period (25 days) was ~0.16 g g^{-1} day^{-1} for both cultivars grown in non-saline solution with either 1 or 10 mM KCl (Fig. 2A and B). The RGR of both cultivars decreased as the NaCl concentration in the nutrient solution increased regardless of KCl level (albeit the mean was not statistically different between 0 mM NaCl + 1 KCl and 200 mM NaCl + 1 mM KCl; 400 mM NaCl +1 mM KCl and 600 mM NaCl +1 M KCl; and 200 mM NaCl + 10 mM KCl and 400 mM NaCl + 10 mM KCl for Callide and between 200 + 10 and 400 mM NaCl + 10 mM KCl for Reclaimer).

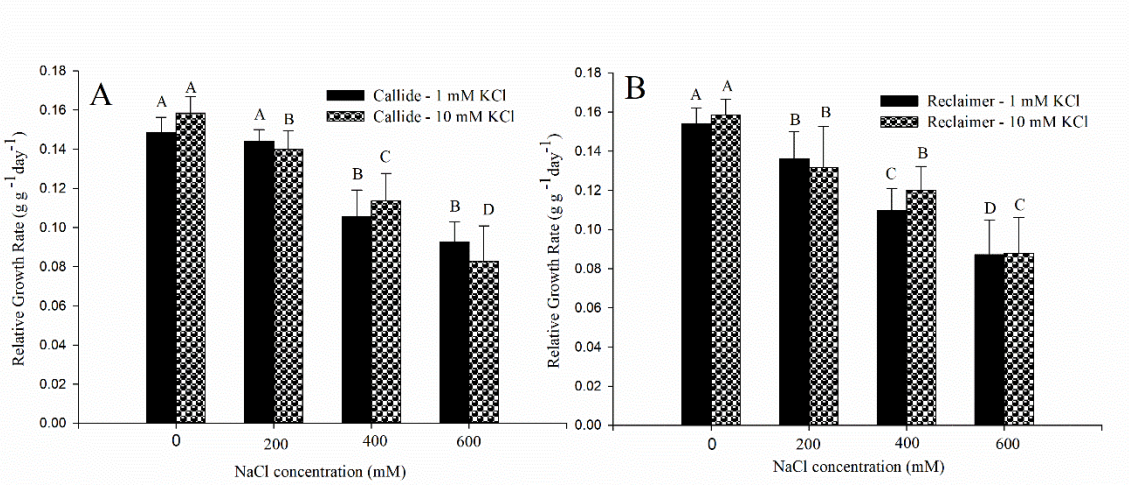

Figure 2. Total plant relative growth rate (RGR) of Rhodes Grass (*Chloris gayana*) cv. Callide (A) and Reclaimer (B) grown in aerated nutrient solution under different saline regimes (0, 200, 400, and 600 mM NaCl) with 1 or 10 mM KCl. Uppercase letters represent significant difference at $p \leq 0.05$ among levels of NaCl within the same KCl level as tested by the Scott-Knott test. No significant difference was observed between the two levels of KCl at the same level of NaCl. Treatments were imposed on 15-day-old plants and samples were taken after 25 days of treatment. Mean ± standart deviation (n = 8). Additional statistical analysis is given in Supplementary material (Table S2).

3.3. Concentrations of Na^+ and K^+ in shoots and roots

The imposition of NaCl treatment in the presence of either 1 or 10 mM KCl in the nutrient solution had a direct impact on the Na^+ and K^+ accumulation in shoots and roots (Figs. 3 and 4). In general, the exposure to NaCl increased the amount of Na^+ in both plant tissues regardless of the presence of KCl (Fig. 3A and 3C). In Callide, the concentration of Na^+ in shoots increased from on average 303 µmol g^{-1} DW in non-saline solution and reached average values of 2,194 µmol g^{-1} DW in the 600 mM NaCl treatment for both KCl levels. In roots of Callide, the Na concentrations increased from ~ 196 µmol g^{-1} DW in non-saline solution to on average 1,500 µmol g^{-1} DW in 400 and 600 mM NaCl regardless KCl availability. The addition of 10 mM KCl reduced [Na^+] of 200 mM treated plants leding to a

fold change of -0.26 in the roots cv. Callide. The patter of accumulation of Na^+ in shoots and roots of Reclaimer was similar to that of Callide, with shoot and root Na concentrations increasing as the NaCl in the nutrient solution increased (Fig. 3B, D). Application of 10 mM KCl reduced shoot Na^+ accumulation by -0.61 and -0.14-fold in non-saline control and 600 mM NaCl treatments (Fig. 3B), respectively, and augmented root Na^+ accumulation 0.2-fold in plants exposed to 400 mM NaCl (Fig. 3D).

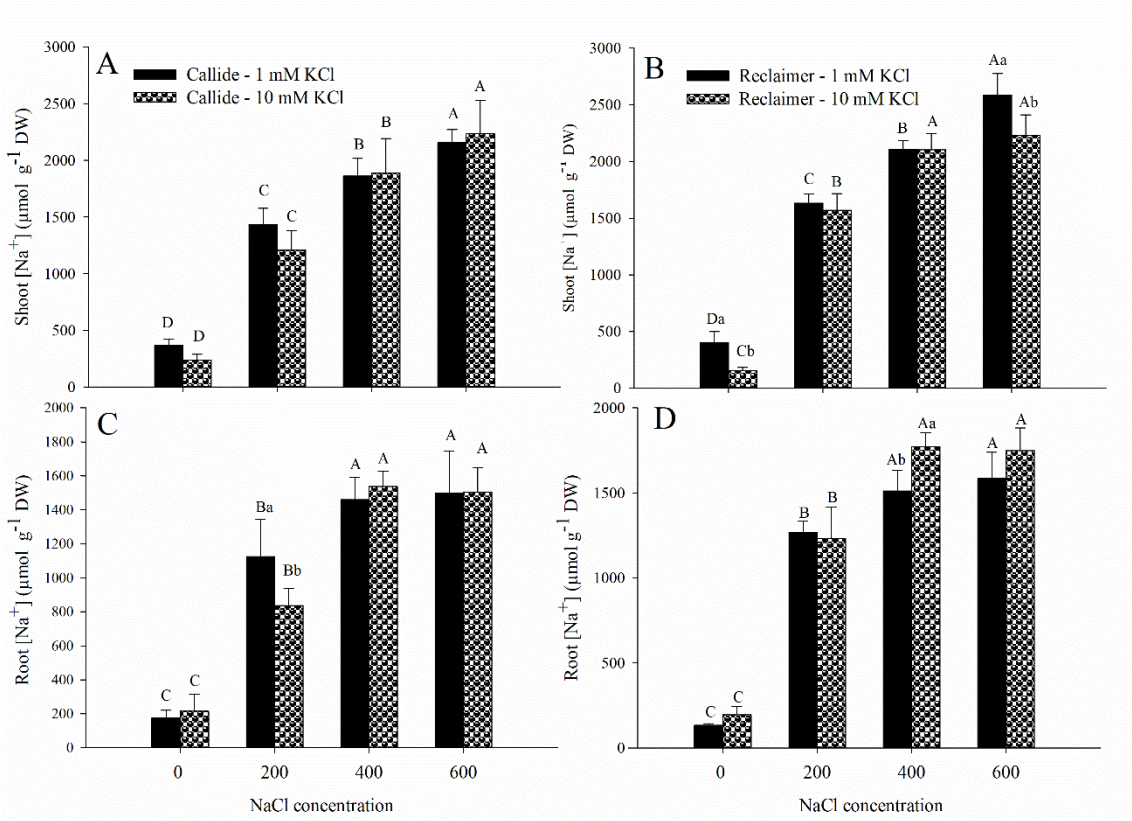

Figure 3. Sodium (Na^+) concentrations in shoots (A, B) and roots (C, D) of Rhodes Grass (*Chloris gayana*) cv. Callide (A, C) and Reclaimer (B, D) grown in aerated nutrient solution under different saline regimes (0, 200, 400, and 600 mM NaCl) with 1 or 10 mM KCl. Upper case letters represent significant differences among NaCl levels within the same KCl level using the Scott-Knott test $p < 0.05$ and lower case letters represent significant difference between the two levels of KCl at the same level of NaCl using the F-test at $p < 0.05$. Treatments were imposed on 15-day-old plants and samples were taken after 25 days of treatment. Mean ± standart deviation (n = 4). There was a significant cultivar × NaCl × KCl interaction for root [Na] at p <0.001. Additional statistical analysis is given in Supplementary material (Table S3).

In plants of cv. Callide exposed to 1 mM KCl, the shoot K^+ concentration showed similar pattern to that of Na. The shoot [K] was the lowest in plants grown in non-saline solution (221 µmol g^{-1} DW). Exposure to 200 mM NaCl led to a 0.9-fold increase and on average 1.8-fold increase in 400 and 600 mM NaCl treatments (Fig. 4A). When plants were grown with 10 mM KCl, the shoot K concentration was 1,005 µmol g^{-1} DW in non-saline

solution. Addition of 200 mM NaCl resulted in a -0.43-fold decrease in shoot [K] and on average -0.27-fold decrease in both 400 and 600 mM NaCl treatments, relative to non-saline control + 10 mM KCl. Compared to the same NaCl treatments + 1 mM KCl, plants submitted to 0 NaCl + 10 mM KCl, 200 NaCl + 10 mM KCl and 600 NaCl + 10 mM KCl showed increases of about 4, 0.4 and 0.3-fold in the shoot [K] (Fig. 3A). In roots of Callide plants grown with 1 mM KCl, the K concentration was on average 98 µmol g^{-1} DW in 0, 200 and 400 mM NaCl and increased to 271 µmol g^{-1} DW in 600 mM NaCl (Fig. 4C). Application of 10 mM KCl increased root [K] about 7-fold in non-saline solution (829 µmol g^{-1} DW). Root [K] in 200 mM NaCl was 236 µmol g^{-1} DW and on average 357 µmol g^{-1} DW in 400 and 600 mM NaCl. The greater availability of KCl in the nutrient solution (10 mM) increased root K^+ concentration by 7-fold in non-saline controls, 3-fold in 200 mM NaCl, 2-fold in 400 mM NaCl and 0.4-fold in 600 mM NaCl, as compared to 1 mM KCl treatment (Fig. 3C).

In Reclaimer cv., K accumulation in shoot and roots showed different patterns in plants grown with either 1 or 10 mM KCl. In plants exposed to 1 mM KCl, the shoot [K] was the lowest in 0 and 200 mM NaCl treatments (on average 351 µmol g^{-1} DW) and increased to ~ 613 µmol g^{-1} DW in 400 and 600 mM NaCl. Similarly, in roots the [K] was 116 µmol g^{-1} DW in non-saline solution and increased to ~ 199 µmol g^{-1} DW in 200 and 400 mM NaCl and 357 µmol g^{-1} DW in 600 mM NaCl. Application of 10 mM of KCl increased shoot K^+ accumulation 2- and 0.6-fold in plants under 0 and 200 mM of NaCl, respectively, as compared to 1 mM KCl treatment (Fig. 4B). In roots, application of 10 mM KCl increased K^+ levels by 6-fold in non-saline control, 1-fold in 200 mM NaCl and 0.7-fold in 400 mM NaCl (Fig. 4D). In roots grown with 10 mM KCl, the [K] was the highest in non-saline solution 814 µmol g^{-1} DW and decreased to 310 µmol g^{-1} DW in 200 and on average to 423 µmol g^{-1} DW in 400 and 600 mM NaCl. (Fig. 4B and 4D).

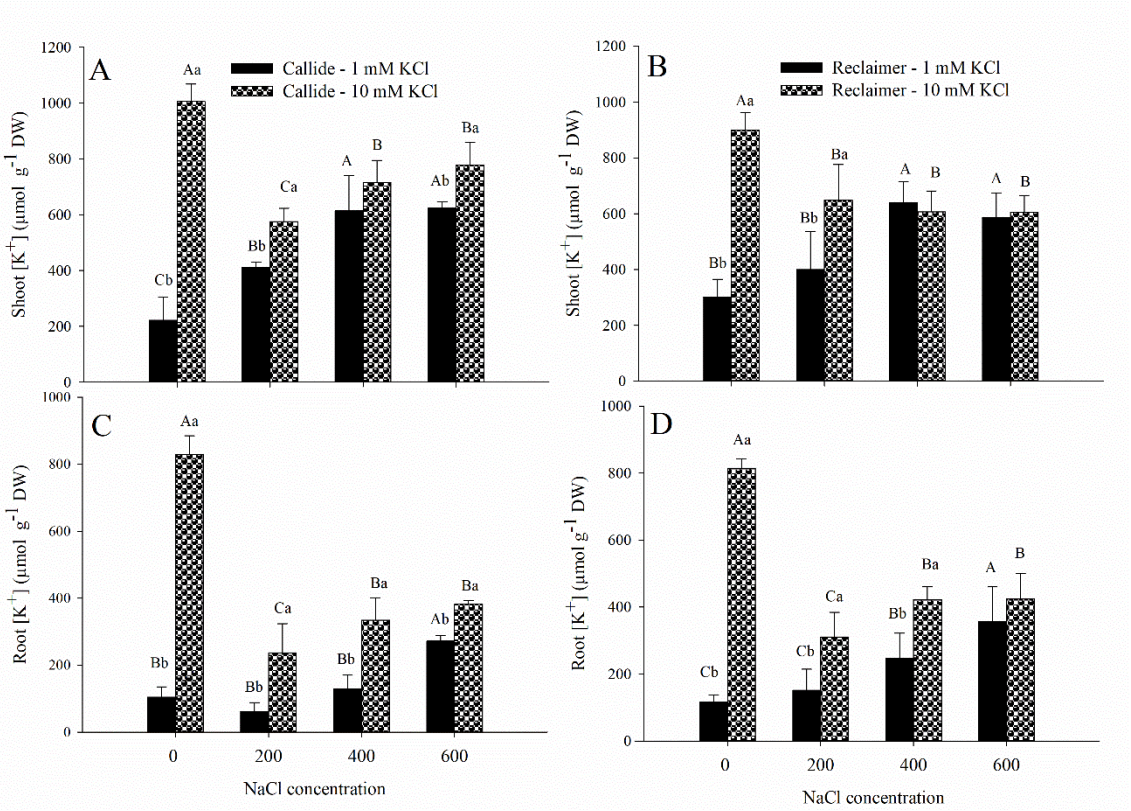

Figure 4. Potassium (K^+) concentrations in shoots and roots of Rhodes Grass (*Chloris gayana*) cv. Callide (A, C) and Reclaimer (B, D) grown in aerated nutrient solution under different saline regimes (0, 200, 400, and 600 mM NaCl) with 1 or 10 mM KCl. Upper case letters represent significant differences among NaCl levels within the same KCl level using the Scott-Knott test $p < 0.05$ and lower case letters represent significant difference between the two levels of KCl at the same level of NaCl using the F-test at $p < 0.05$. Mean ± standart deviation (n = 4). Treatments were imposed on 15-day-old plants and samples were taken after 25 days of treatment. There was a significant cultivar × NaCl × KCl interaction for root [K] at p <0.001. Additional statistical analysis is given in Supplementary material (Table S3).

Shoot K/Na ratio was on average 0.6 and 0.8 in non-saline controls + 1 mM KCl and on average 0.3 in 200 mM, 400 mM NaCl and 600 mM NaCl with 1 mM KCl for plants of cv. Callide and Reclaimer (Table 2). Application of 10 mM KCl increased the shoot K/Na ratio on average 6-fold in non-saline controls for both cultivars but did not affect K/Na ratio in 200, 400 and 600 mM NaCl treatments, compared to the respective NaCl level + 1 mM KCl (Table 2). Similarly in roots, K/Na ratio was on average 0.4 in non-saline controls, 200, 400 and 600 mM NaCl + 1 mM KCl. Application of 10 mM KCl increased K/Na 6- and 4-fold for Callide and Reclaimer cultivars, respectively, in non-saline controls but did not affect K/Na ratio in 200, 400 and 600 mM NaCl treatments, compared to the respective NaCl level + 1 mM KCl (Table 2).

Table 2. K^+/Na^+ ratios in shoots and roots of Rhodes Grass (*Chloris gayana*) cv. Callide and Reclaimer grown in aerated nutrient solution under different saline regimes (0, 200, 400, and 600 mM) with 1 or 10 mM KCl.

Cultivar	*NaCl (mM)*	**K^+/Na^+ ratio**			
		Shoot		Root	
		KCl (mM)			
		1	*10*	*1*	*10*
Callide	*0*	0.62 ± 0.2^{b}	4.33 ± 0.7^{Aa}	0.63 ± 0.3^{b}	4.62 ± 1.0^{Aa}
	200	0.30 ± 0.07	0.50 ± 0.09^{B}	0.50 ± 0.01	0.28 ± 0.1^{B}
	400	0.33 ± 0.05	0.38 ± 0.02^{B}	0.19 ± 0.02	0.21 ± 0.03^{B}
	600	0.29 ± 0.02	0.35 ± 0.06^{B}	0.19 ± 0.03	0.25 ± 0.02^{B}
Reclaimer	*0*	0.75 ± 0.04^{b}	5.81 ± 0.5^{Aa}	0.86 ± 0.1^{b}	4.40 ± 1.2^{Aa}
	200	0.25 ± 0.09	0.41 ± 0.06^{B}	0.12 ± 0.05	0.25 ± 0.07^{B}
	400	0.30 ± 0.04	0.29 ± 0.04^{B}	0.16 ± 0.04	0.23 ± 0.03^{B}
	600	0.23 ± 0.04	0.27 ± 0.04^{B}	0.22 ± 0.05	0.24 ± 0.05^{B}

Upper case letters represent significant differences among NaCl levels within the same KCl level using the Scott-Knott test $p < 0.05$ and lower case letters represent significant difference between the two KCl levels at the same level of NaCl using the F-test at $p < 0.05$. Treatments were imposed on 15-day-old plants and samples were taken after 25 days of treatment. Mean ± standart deviation (n = 4). There was a significant cultivar × NaCl × KCl interaction for shoot K/Na ratio at p <0.05 and for root K/Na ratio at p <0.001 (three-way ANOVA). Additional statistical analysis is given in Supplementary material (Table S3).

3.4. Leaf washing

Exposure to increasing concentrations of NaCl in nutrient solution augmented the amount of retained sodium in the cv. Callide from 128 µmol g^{-1} DW in non-saline control + 1 KCl to 549 µmol g^{-1} DW in 600 mM NaCl + 1 mM KCl in the second youngest fully expanded leaf of *C. gayana* and also increased amounts of leaf secreted ions from on average 5 µmol g^{-1} DW day^{-1} to 417 µmol g^{-1} DW day^{-1} in leaves of non-saline control and 600 mM NaCl + 1 mM KCl, respectively (Table 3). Addition of 10 mM KCl, reduced retained [Na] - 0.9-fold in non-saline controls and led to a fold change of 0.3 in 600 mM NaCl. Secretion of sodium in 200 mM NaCl + 1 KCl was about 1-fold higher compared to 200 mM NaCl + 10 KCl plants (Table 3).

In Reclaimer, the [Na] in leaves was on average 179 g^{-1} DW in non-saline controls + 1 mM KCl and, 412 g^{-1} DW, 722 g^{-1} DW and 971 g^{-1} DW in plants exposed to 200, 400 and, 600 mM NaCl, respectively. Plants of cv. Reclaimer submitted to 10 mM KCl [Na] reduced -

0.5 and -0.3-fold in non-saline control and 600 mM NaCl, respectively. Under the lowest KCl concentration (1 mM) secretion of sodium was on average 53 in non-saline controls, 477 in 200 mM NaCl and 656 in 400 and 600 mM NaCl (Table 3). Exposure to 10 mM KCl augmented [Na] 0.9-fold in non-saline controls but levels of KCl did not significantly affected the secretion of Na in the other treatments (200, 400 and 600 mM NaCl).

In Callide, the retained [K] in leaves of plants under 1 mM KCl was on average 384 µmol g^{-1} DW in non-saline controls and 842 µmol g^{-1} DW in 200, 400 and 600 mM NaCl (Table 3). Application of 10 mM KCl, increased the retained [K] on average 2-fold in non-saline control, 0.7-fold in 200 of NaCl and 0.3-fold in 600 mM NaCl as compared to 1 mM KCl treatment. By contrast, application of 10 mM KCl did not affect the retained [K] at 400 mM NaCl. Amounts of secreted K^+ were on average 12 µmol g^{-1} DW day^{-1} in non-saline controls and 88 µmol g^{-1} DW day^{-1} under 200, 400 and 600 Mm NaCl, irrespective of KCl (Table 3).

Retention of K in leaves of plants of cv. Reclaimer under 1 mM KCl was on average 925 µmol g^{-1} DW in non-saline controls and 684 µmol g^{-1} DW in plants exposed to 200, 400 and 600 mM KCl. The addition of 10 mM KCl led to a fold change of 0.7-fold in non-saline controls, but did not affect the other NaCl treatments (Table 3). Secreted [K] in non-saline controls under the lowest KCl concentration (1 mM), were on average 19 µmol g^{-1} DW day^{-1} in non-saline controls, 31 µmol g^{-1} DW day^{-1} in 200 Mm NaCl, 138 µmol g^{-1} DW day^{-1} in 400 Mm NaCl and, 72 µmol g^{-1} DW day^{-1} in 600 Mm NaCl. The highest KCl concentration (10 mM) augmented K secretion in ~1-fold per day in non-saline controls and 2-fold per day under 200 mM NaCl but did not significantly altered K secretion under 400 and 600 mM NaCl (Table 3).

Table 3. Concentration (µmol g^{-1} DW) and secretion (µmol g^{-1} DW day^{-1}) of Na^+ and K^+ in detached second youngest fully expanded leaves of two Rhodes Grass (*Chloris gayana*) cultivars (Callide and Reclaimer) grown under different saline regimes (0, 200, 400, and 600 mM NaCl) at 1 or 10 mM KCl.

		cv. Callide				**cv. Reclaimer**			
		Na^+		**K^+**		**Na^+**		**K^+**	
		KCl (mM)							
	NaCl (mM)	1	10	1	10	1	10	1	10
Retained	*0*	128 ± 27^{Ca}	15.4 ± 7^{Db}	384 ± 85^{Bb}	1033 ± 287^{a}	179 ± 75^{Da}	90 ± 36^{Cb}	915 ± 174^{Ab}	1600 ± 149^{Aa}
	200	228 ± 55^{C}	209 ± 28^{C}	701 ± 191^{Ab}	1190 ± 186^{a}	412 ± 144^{C}	432 ± 83^{B}	676 ± 162^{B}	658 ± 196^{B}
	400	410 ± 86^{B}	345 ± 63^{B}	844 ± 138^{A}	1086 ± 104	722 ± 103^{B}	672 ± 169^{A}	710 ± 99^{B}	815 ± 42^{B}
	600	549 ± 52^{Ab}	706 ± 137^{Aa}	983 ± 125^{Ab}	1310 ± 129^{a}	971 ± 146^{Aa}	702 ± 65^{Ab}	666 ± 53^{B}	664 ± 111^{B}
Secreted	*0*	5 ± 2.5^{B}	8 ± 4^{C}	6 ± 3.1^{B}	18 ± 6^{B}	53 ± 0.6^{Cb}	102 ± 9^{Ca}	19 ± 3^{Cb}	43 ± 12^{a}
	200	498 ± 90^{Aa}	228 ± 59^{Bb}	96 ± 37^{A}	61 ± 23^{A}	477 ± 81^{B}	470 ± 69^{B}	30.9 ± 6^{Cb}	87 ± 38^{a}
	400	384 ± 31^{A}	368 ± 130^{A}	83 ± 39^{A}	94 ± 33^{A}	632 ± 72^{A}	672 ± 51^{A}	138 ± 59^{B}	97 ± 48
	600	417 ± 106^{A}	468 ± 51^{A}	99 ± 24^{A}	97 ± 29^{A}	680 ± 89^{A}	620 ± 85^{A}	72 ± 28^{A}	92 ± 36

Upper case letters represent significant differences among NaCl levels within the same KCl level (column) using the Scott-Knott test $p < 0.05$ and lower case letters represent significant difference between the two KCl levels at the same level of NaCl (rows) using the F-test at $p < 0.05$. Treatments were imposed on 15-day-old plants and samples were taken from the 3rd fully expanded leaf after 25 days of treatment. Leaves were washed with deionized water one day before harvest. Means ± standard deviation (n =8). There was a significant cultivar × NaCl × KCl interaction at p <0.001 for retained and secreted [Na] and, for retained [K] (three-way ANOVA). Additional statistical analysis is given in supplementary material (Table S4).

3.5. Osmotic potential of the leaf sap

The leaf sap osmotic potential was more negative as the concentration of NaCl in the nutrient solution increased (Fig. 5). In cultivar Callide the leaf sap osmotic potential was on average –1.0 MPa in non-saline solution and–1.9 MPa in 200 mM NaCl at both KCl levels. The increase in NaCl concentration in nutrient solution further decreased the osmotic potential in cv. Callide. In 400 mM NaCl the osmotic potential was –2.5 MPa in 400 NaCl + 1 mM KCl and -3.0 MPa in 400 mM NaCl + 10 mM KCl. Under 600 mM of NaCl the osmotic potential was -3.5 and -4 MPa in plants with 1 and 10 mM KCl, respectively (Figure 5A).

In Reclaimer, the osmotic potential was -1.0 or -1.3 MPa in non-saline controls, -1.6 or -2.4 MPa in 200 mM NaCl, and -2.5 or -3.0 MPa in 400 mM NaCl, when plants were grown with 1 or 10 mM KCl, respectively (Fig. 5B). At the 600 mM NaCl, the leaf sap osmotic potential was similar (-3.0 MPa) to that in 400 mM NaCl when plants were grown with 10 mM KCl, but decreased to –4.9 MPa in 600 mM NaCl + 1 mM KCl (Fig. 5B).

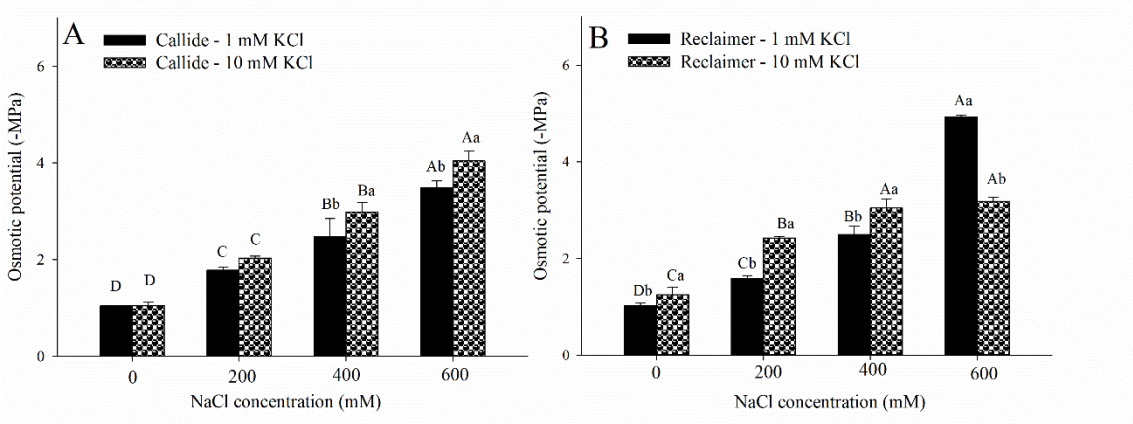

Figure 5. Leaf sap osmotic potential in shoots of Rhodes Grass (*Chloris gayana*) cv. Callide (A) and Reclaimer (B) grown in aerated nutrient solution under different saline regimes (0, 200, 400, and 600 mM NaCl) with 1 or 10 mM KCl. Upper case letters represent significant differences among NaCl levels within the same KCl level using the Scott-Knott test $p < 0.05$ and lower case letters represent significant difference between the two levels of KCl at the same level of NaCl using the F-test at $p < 0.05$. Mean ± standart deviation (n = 4). Treatments were imposed on 15-day-old and samples were taken after 25 days of treatment. Leaf sap osmotic potential was measured by using a freezing-point depression osmometer. There was a significant cultivar × NaCl × KCl interaction at $p < 0.001$ for osmotic potential (three-way ANOVA). Additional statistical analysis is given in Supplementary material (Table S5).

3.6. Contribution of ions (Na^+ and K^+) to the leaf sap osmotic potential

In order to evaluate if Na and K are major determinants of osmotic adjustment, the contribution of these ions to the leaf osmotic potential was calculated. In Callide, the

estimated contribution of Na^+ to the leaf sap osmotic potential was 16% and 2% in the non-saline treatments, but with 1 or 10 mM KCl, respectively. In plants that received 1 mM KCl, the estimated contribution of Na^+ to the leaf sap osmotic potential was, on average, 15% irrespective of NaCl added to the growth medium. Exposure to 10 mM KCl reduced the estimated contribution of Na^+ to the leaf sap osmotic potential by -0.9-fold in non-saline treatments (controls). In contrast, in 200 mM NaCl + 10 mM KCl, the estimated contribution of Na^+ to the leaf sap osmotic potential augmented 3-fold compared to 0 mM NaCl + 10 mM KCl and, in 400 and 600 mM NaCl + 10 mM KCl, the increase was on average 6-fold (Table 4). The contribution of K^+ ions showed an opposite pattern in response to KCl levels. In plants exposed to 1 mM KCl the contribution of K^+ ions to the osmotic potential was 30% in non-saline control treatment and, on average, 19% in three levels of NaCl. In plants that received 10 mM KCl, the contribution of K^+ to the leaf sap osmotic potential augmented 1-fold in the non-saline control treatment. Under 400 mM the contribution of K^+ to the leaf sap osmotic potential was reduced -0.5-fold and, under 200 and 600 mM NaCl decreased -0.8-fold as compared to 0 mM NaCl + 10 mM KCl. Different levels of KCl did not influence the contribution of both K^+ and Na^+ to the leaf sap osmotic potential when considering the two levels of KCl at the same level of NaCl, except when considering non-saline controls in the cv. Callide (Table 4).

In Reclaimer, the estimated contribution of Na^+ to the leaf sap osmotic potential was 18% and 7% in the non-saline treatments, but with 1 or 10 mM KCl, respectively, a reduction of ~ 1.5-fold due to 10 mM KCl. Under 1 mM KCl the augment in [NaCl] did not result in higher contribution of Na^+ ions for the osmotic potential (Table 4). In plants that received 10 mM KCl, however, the estimated contribution of Na^+ ions for the osmotic potential was on average 16.6% a fold increase of 1.3 as compared to 0 mM NaCl + 10 mM KCl. The contribution of K^+ ions to the osmotic potential was on average 30% in non-saline controls exposed to 1 mM KCl and 62% in non-saline controls exposed to 10 mM KCl (1-fold increase). The estimated contribution of K^+ ions to the osmotic potential in plants submitted to 1 mM KCl was on average 14% to 200, 400, and 600 mM NaCl. While in plants submitted to 10 mM KCl, the estimated contribution of K^+ ions to the osmotic potential was on average 24% in 200 mM, 400 and 600 mM NaCl (Table 4). Under 400 mM NaCl application of 10 mM KCl led to a fold increase of 1.6 as compared to the same treatment + 1 mM KCl.

Table 4. Estimated contribution of ions (Na^+ and K^+) to the leaf sap osmotic potential (%) of two Rhodes Grass (*Chloris gayana*) cultivars, Callide and Reclaimer, grown in aerated nutrient solution under different saline regimes (0, 200, 400, and 600 mM NaCl) with 1 or 10 mM KCl.

		cv. Callide				**cv. Reclaimer**			
		Na^+		**K^+**		**Na^+**		**K^+**	
		KCl (mM)							
	NaCl (mM)	1	10	1	10	1	10	1	10
Contribution to leaf sap osmotic potential (%)	*0*	16.1±5.5^{Aa}	2.0±0.7^{Cb}	29.9±4.6^{Ab}	58.7±6.7^{Aa}	18.0±7.2^{a}	7.0±3.6^{Bb}	28.8±4.6^{Ab}	62.4±6.7^{Aa}
	200	10.4±3.1^{B}	8.0±1.7^{B}	18.8±6.8^{B}	27.6±9.7^{B}	17.2±6.0	17.0±4.3^{A}	18.6±2.3^{B}	21.9±3.0^{B}
	400	7.7±2.8^{B}	11.1±3.2^{A}	19.6±7.5^{B}	15.3±6.2^{C}	20.8±6.9	16.5±5.8^{A}	11.4±3.1^{Bb}	29.5±8.3^{Ba}
	600	11.0±1.6^{B}	16.0±5.8^{A}	18.6±7.0^{B}	12.4±1.4^{C}	21.6±2.7	16.4±1.2^{A}	12.5±0.9^{B}	20.4±8.8^{B}

Upper case letters represent significant differences among NaCl levels within the same KCl level (column) using the Scott-Knott test $p < 0.05$ and lower case letters indicate significant difference between the two levels of KCl at the same level of NaCl (rows) using the F-test at $p < 0.05$. Treatments were imposed on 15-day-old plants and samples were taken after 25 days of treatment. The values of sample water content used in the calculations refer to measurements recorded in plant' shoot. Means ± standard deviation (SE) (n =4). There was a significant cultivar × NaCl × KCl interaction at $p<0.05$ for contribution of K^+ to leaf sap osmotic potential (three-way ANOVA). Additional statistical analysis is given in Supplementary material (Table S5).

3.7. Chlorophyll a fluorescence transients

The effect of NaCl and KCl on the photosynthetic electron transfer, especially the activity of PSII units, was studied using chlorophyll *a* fluorescence analysis. Fluorescence kinetics analysis (OJIP; Fig. 6) of the Callide cultivar, despite the loss of intensity, shows that treatments presented the typical polyphasic shape indicating that all plants remained photosynthetically functional. Callide cultivar submitted to 400 mM NaCl + 1 mM KCl suffered the range of variations of the relative fluorescence intensity at F_o, F_J, F_I, and F_M points and non-saline controls of cv. Callide and 40 mM NaCl + 10 mM NaCl showed reductions in the points F_J, F_I, and F_M (Fig. 6A and Table 5). Under 600 mM NaCl + 10 mM KCl plants of the Callide cultivar also showed significant reductions on each characteristic point on the OJIP curve, and the lower KCl availability (1 mM) favored the maintenance of OJIP to control levels in the highest NaCl treatment (Fig. 6A and Table 5).

Figure 6B shows that the shape of OJIP curve was also maintained for the Reclaimer cultivar in all treatments with loss of fluorescence intensities. However, unlike the Callide cultivar, the addition of 10 mM KCl in plants under 0 mM of NaCl did not reduce the intensity of fluorescence at any OJIP major points. Under 200 mM NaCl + 10 mM KCl, the initial fluorescence, Fo, was 402 (a.u.) and, the lower availability of KCl (200 mM NaCl + 1 mM KCl treatment) reduced Fo by ~19% (Fig. 6B). Plants submitted to 200 mM NaCl +1 mM KCl also presented reductions in the points F_J, F_I and F_M and showed significant changes at the points F_I and F_M when grown with 200 mM NaCl + 10 mM KCl. Reductions at the points F_I and F_M were also observed in plants grown with 400 mM NaCl (irrespective of KCl) and at the point F_J under 400 mM NaCl + 10 mM KCl (Fig. 6B and Table 5). At the highest NaCl treatment (600 mM), the lower availability of KCl caused reductions in fluorescence from F_J to F_M, while 10 mM KCl caused a reduction I step but led to values close to the control. at all the other points of OJIP-curve (Fig. 6B and Table 5).

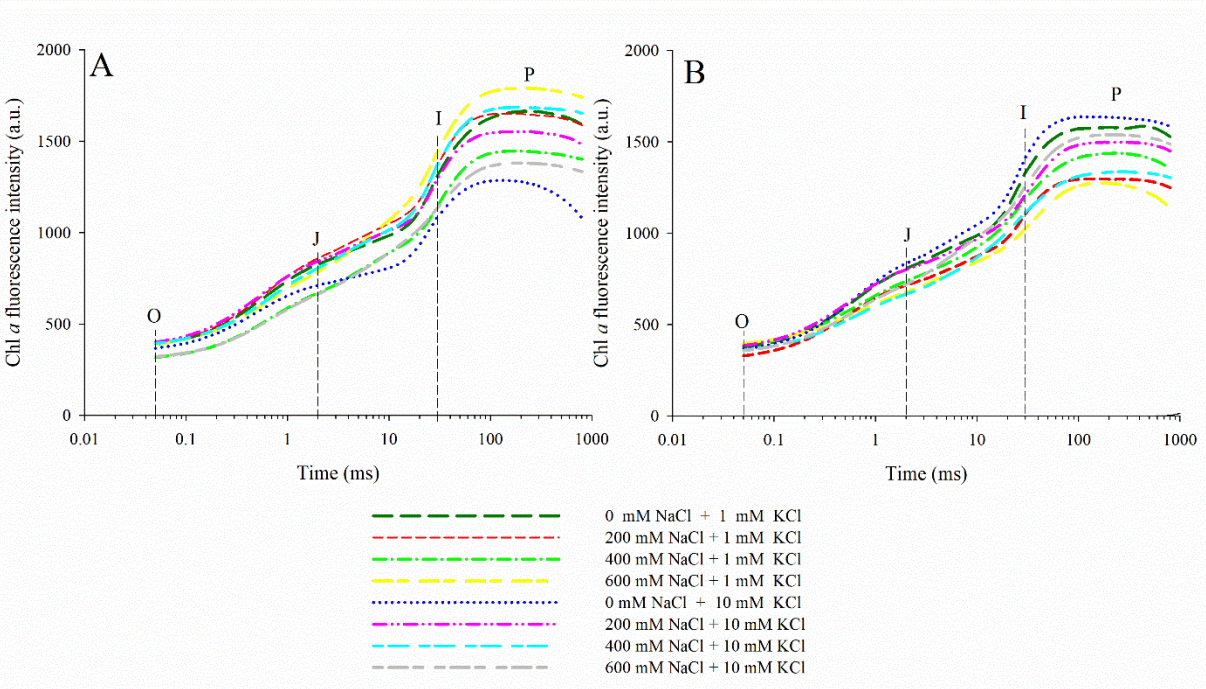

Figure 6. Effects of different saline regimes (0, 200, 400, and 600 mM NaCl) and 1 or 10 mM KCl on OJIP curves of Rhodes Grass (*Chloris gayana*) cv. Callide (A) and Reclaimer (B) grown in aerated nutrient solution. Treatments were imposed on 15-day-old plants and readings were performed in the 2nd fully expanded leaves in the morning (from 10 to 11 a.m.) after dark adaptation for at least 20 min after 24 days of treatment. Each curve is the average of eight replicates.

Table 5. Chlorophyll *a* fluorescence intensity in OJIP-steps O (F_0), J (F_J), I (F_I), and P (F_M) of Rhodes Grass (*Chloris gayana)* cv. Callide and Reclaimer grown in aerated nutrient solution under different saline regimes (0, 200, 400, and 600 mM NaCl) with 1 or 10 mM KCl.

		F_0		**F_J**		**F_I**		**F_M**	
	NaCl (mM)	*KCl (mM)*							
Cultivar		*1*	*10*	*1*	*10*	*1*	*10*	*1*	*10*
Callide	*0*	390±16.6^{A}	368±15.2^{A}	827±16.6^{Aa}	712±27.9^{Bb}	1312±101^{Aa}	1085±81.6^{Bb}	1664±128^{Aa}	1267±43.3^{Bb}
	200	395±25.4^{A}	401±31.1^{A}	860±65.9^{A}	843±46.1^{A}	1368±103^{A}	1296±117^{A}	1646±140^{A}	1553±103^{A}
	400	318±38.8^{Bb}	395±18.3^{Aa}	671±92.9^{Bb}	807±47.8^{Aa}	1147±121^{Bb}	1373±105^{Aa}	1443±177^{Bb}	1683±53.3^{Aa}
	600	390±32.4^{Aa}	321±23.0^{Bb}	787±33.4^{Aa}	664±62.6^{Bb}	1446±43.5^{Aa}	1135±102^{Bb}	1790±76.3^{Aa}	1379±66.4^{Bb}
Reclaimer	*0*	381±9.6^{A}	361±17.5	990±51.4^{A}	1056±38.6^{A}	1341±100^{A}	1417±25.1^{A}	1597±109^{A}	1631±31.5^{A}
	200	328±45.1^{Bb}	402±27.4^{a}	875±79.6^{Bb}	1009±49.7^{Aa}	1138±131^{B}	1165±113^{C}	1290±146^{B}	1436±105^{B}
	400	389±10.9^{A}	365±31.0	923±48.9^{A}	856±73.6^{B}	1184±55.7^{Ba}	1104±30.9^{Db}	1415±53.4^{B}	1309±97.5^{B}
	600	397±59.9^{A}	358±45.8	844±104^{Bb}	979±51.2^{Aa}	1027±103^{Cb}	1259±95.3^{Ba}	1273±135^{Bb}	1539±117^{Aa}

Upper case letters represent significant differences among NaCl levels within the same KCl level (column) using the Scott-Knott test $p < 0.05$ and lower case letters represent significant difference between the two levels of KCl at the same level of NaCl (rows) using the F-test at $p < 0.05$. Treatments were imposed on 15-day-old plants and readings were performed on the 2nd fully expanded leaf in the morning (from 10 to 11 a.m.) after dark adaptation for at least 20 min after 24 days of treatment. Means ± standard deviation (n=8). There was a significant cultivar × NaCl × KCl interaction at $p < 0.001$ for F_o, F_J, F_I and F_M (three-way ANOVA). Additional statistical analysis is given in Supplementary material (Table S6).

To further evaluate and compare the effects of NaCl and KCl on the electron transport chain of *C. gayana* leaves, we normalized the OJIP curves as relative variable fluorescence and calculated the difference kinetics from relative variable fluorescence (Fig. 7 and Fig. 8). Normalized curves of the cv. Callide presented an expressive reduction in the maximum fluorescence (F_M) for control non-saline plants with 10 mM KCl, with a continuous drop after 1 second (Fig. 7A). Normalization between O-I steps, from 50 µs to 30 ms, revealed slight alterations in fluorescence curves due to exposure to salt. The relative fluorescence intensity of point J, at 2 ms, showed decreasing trends compared with the control and decrease in the relative fluorescence intensity of point I and slight loss of the polyphasic shape, at 30 ms, for 400 mM NaCL and 600 mM of NaCl (irrespective of KCl) (Fig 7C).

For the evaluation of I-P steps, two normalizations were used: one considering W_{OI} after 1ms (reflecting the size of the electron acceptors pool at the PSI acceptor side) and the other a normalization between steps I and P (allowing for the comparison among the reduction rates of the end electron acceptors' pool). Exposure to NaCl increased the reduction rates at the end of electron acceptors in plants submitted to both levels of KCl as observed for the higher amplitudes and shorter half-life with the strongest effect caused by 200 mM NaCl + 1mM KCl in the cv. Callide. The insert (Fig. 7E; $W_{OI}>1$) shows that all treatments caused a reduction in the poll size, especially for plants exposed to the lower levels of NaCl with 10 mM KCl. A drop in the maximum fluorescence (F_M) in control non-saline plants with 10 mM KCl can be noted (Fig. 7E).

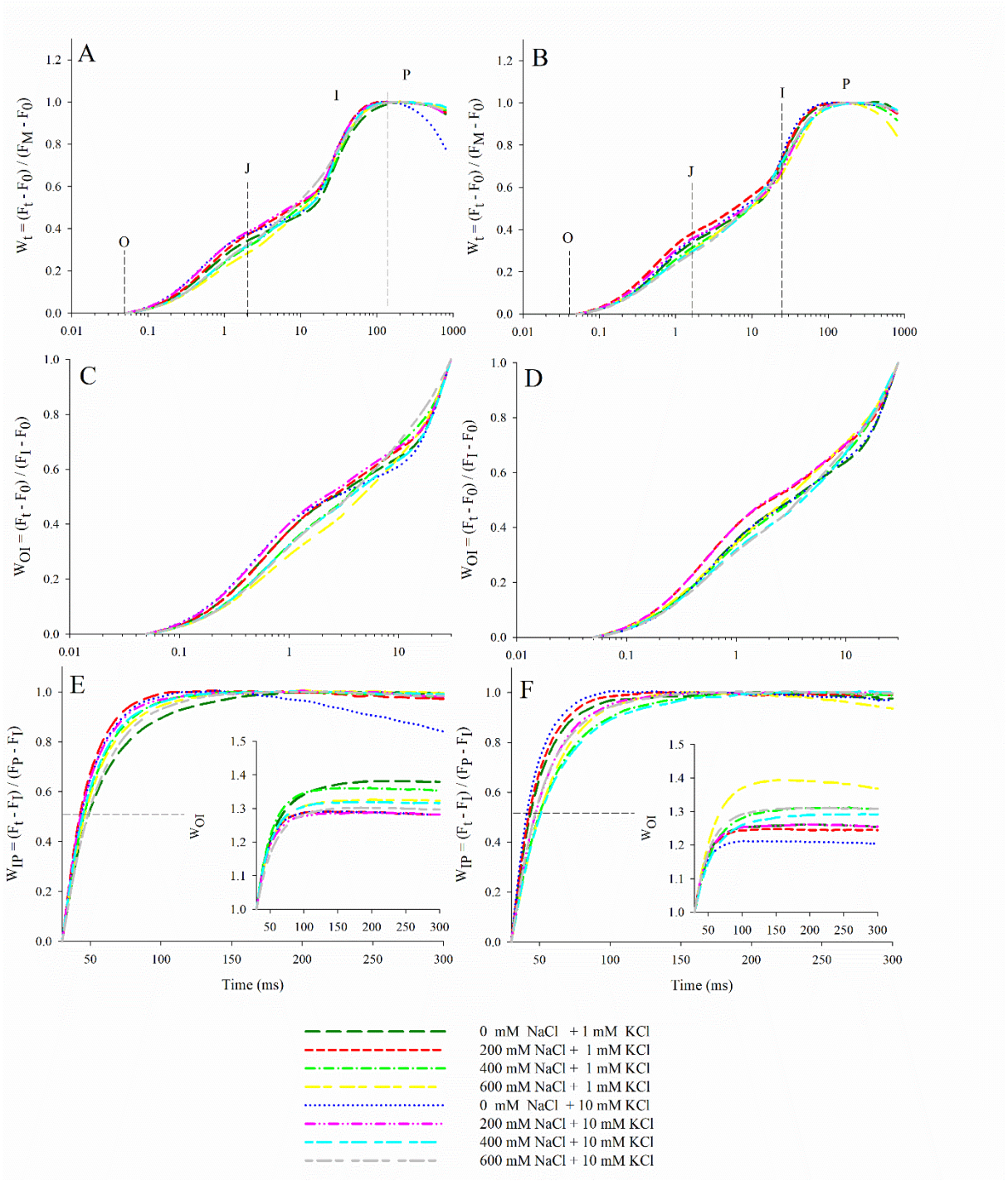

Figure 7. Transients of two cultivars of Rhodes Grass (*Chloris gayana)* cv. Callide (A, C, E) and Reclaimer (B, D, F) grown in aerated nutrient solution under different saline regimes (0, 200, 400, and 600 mM NaCl) with 1 or 10 mM KCl. A. Normalized transients between F_o and F_m in cv. Callide; B. Normalized transients between F_o and F_m in cv. Reclaimer; C. Normalized transients between F_o and F_5 in cv. Callide; D. Normalized transients between F_o and F_5 in cv. Reclaimer; E. Normalized transients between F_5 and F_m in cv. Callide; F. Normalized transients between F_5 and F_m in cv. Reclaimer. The signals were plotted on a logarithmic time scale. Treatments were imposed on 15-day-old plants and readings were

performed on the 2nd fully expanded leaf in the morning (from 10 to 11 a.m.) after dark adaptation for at least 20 min after 24 days of treatment. Each curve is the average of eight replicates.

Control (0 mM NaCl + 1 mM KCl) plants of the cv. Reclaimer presented a typical OJIP with well-defined steps and, although salt induced slight modifications in OJIP-curve, none of the salt treatments or extra KCl altered its shape (Fig. 7B). Normalization between O-I steps exposed a trend of increase in the J-step for 200 mM NaCl (irrespective of KCl) (Fig. 7D). Evaluation between steps I and P induced two different rates of reduction of electron's acceptor on the end PSI. Application of 400 and 600 mM NaCl (irrespective of KCl) and the 200 mM + 10 mM KCl resulted in a lower rate at the end electron acceptors' pool with the bigger half-time, as indicated by the crossing of the curves with the horizontal dashed line drawn at W_{IP}=0.5. The strongest effect was caused by the 400 mM NaCl (Fig. 7F). After 1ms (W_{OI} – insert), the pool size was reduced with higher amplitudes in control plants with extra KCl (Fig. 7F). Increased electron acceptor pool on PSI was observed as a response to the highest level of NaCl − the higher the NaCl concentration the larger was the rise in electron acceptor pool on the PSI and this effect was more pronounced in plants that did not receive extra KCl (Fig. 7F)

Alterations in OJIP curves are reflected in the presence of a positive K-band to the Callide plants (Fig. 8A). Maximum amplitudes of positive K-bands were observed in plants submitted to 0 and 200 mM NaCl with 10 mM KCl (Fig. 8A). Positive hidden L-bands (~150 μs) were detected under all NaCl and KCl regimes, indicating connectivity loss between PSII units (Fig. 8C). The most pronounced effect was observed in Callide plants exposed to 600 mM NaCl + 1 mM KCl treatment (Fig. 8C).

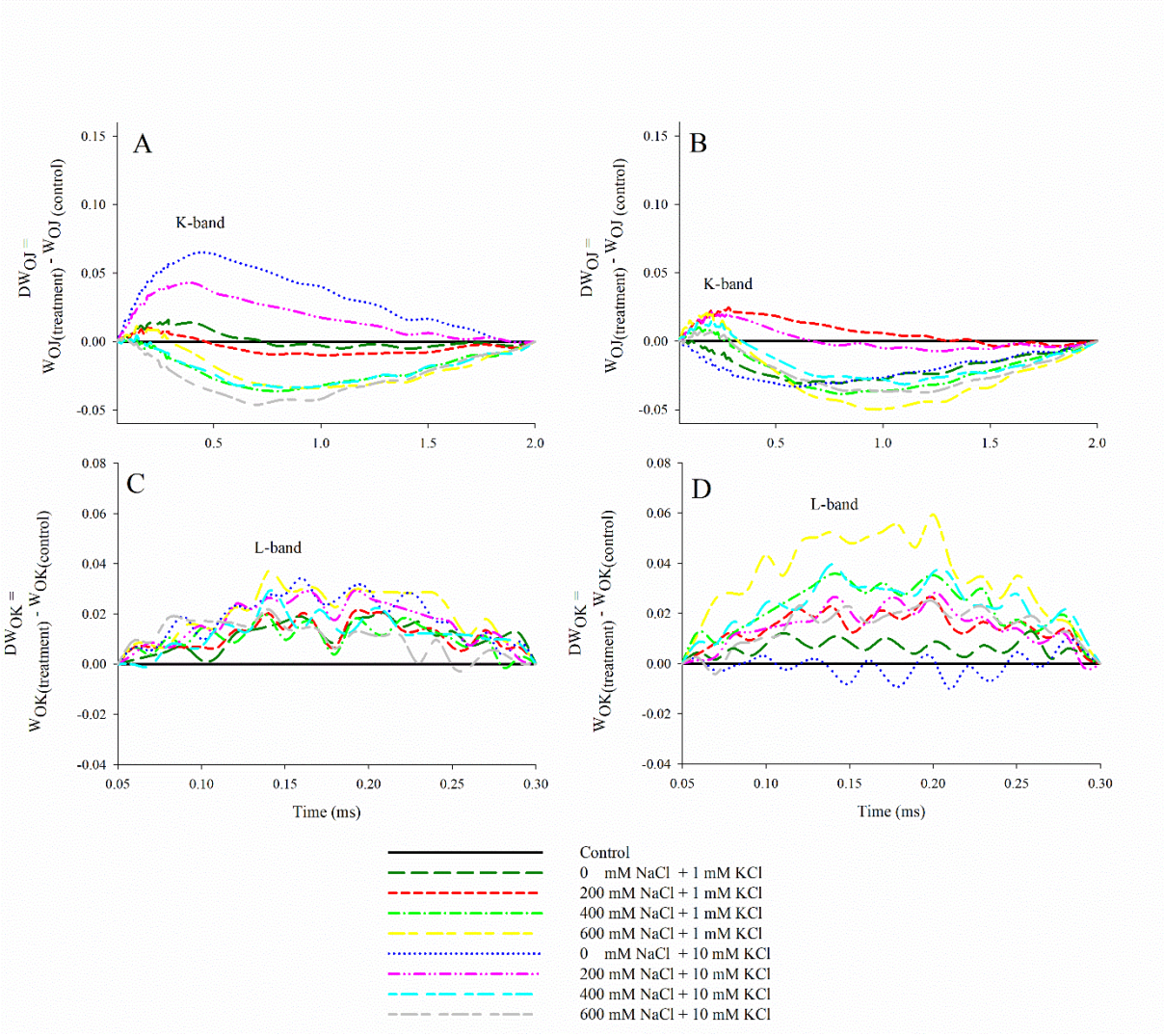

Figure 8. Transients of two cultivars of Rhodes Grass (*Chloris gayana*) cv. Callide (A, C) and Reclaimer (B, D) grown in aerated nutrient solution under different saline regimes (0, 200, 400, and 600 mM NaCl) with 1 or 10 mM KCl. A. The PF transient curves normalized between F_o and F_J, expressed as $W_{OJ} = [(F_t-F_o)/(F_J-F_o)]$, cv. Callide; B. The PF transient curves normalized between F_o and F_J, expressed as $W_{OJ} = [(F_t-F_o)/(F_J-F_o)]$, cv. Reclaimer; C. The PF transient curves normalized between F_O and F_K, presented as $W_{OK} = [(F_t-F_O)/(F_K-F_O)]$, cv. Callide; D. The PF transient curves normalized between F_O and F_K, presented as $W_{OK} = [(F_t-F_O)/(F_K-F_O)]$, cv. Reclaimer. The signals were plotted on a logarithmic time scale. Treatments were imposed on 15-day-old plants and readings were performed in the 2nd fully expanded leaf in the morning (from 10 to 11 a.m.) after dark adaptation for at least 20 min after 24 days of treatment. Each curve is the average of eight replicates.

Positive K- and L-bands (Figs. 8B, D) were also observed in the cultivar Reclaimer in response to NaCl application under both KCl regimes indicating, respectively, OEC

inactivation and/or increase in the functional size PSII antenna complex and loss of energy connectivity between PSII units. Amplitude of K-band was slightly reduced due to 10 mM KCl in the low and the highest level of NaCl (200 and 600 mM, respectively) and worsened in the 400 mM + 10 mM KCl treatment (Fig. 8D). Higher availability of KCl (10 mM) in the nutrient solution of plants submitted to the lowest level of NaCl (0 mM) had a positive effect on both donor and acceptor sides of PSII, as can be seen by the presence of a more negative K- and L- bands (Figs. 8B, D).

Effects of NaCl and KCl on JIP-test parameters shown that the lower levels of NaCl (0 and 200 mM) with 10 mM KCl induced negative effects in the specific fluxes per reaction center in Callide with increases in the absorption (ABS/RC), trapping (TR_o/RC), and dissipation (DI_o/RC) fluxes (Fig. 9A). The area between the OJIP curve and line F_o=F_M and reductions of the final electron acceptor on the acceptor side of photosystem I (Re_o/RC) and photosynthetic performance indexes (PI_{abs} and PI_{total}) were also reduced by these treatments (Fig. 10A). Performance index PI_{abs} of increased on average 28% under 400 and 600 mM NaCl as compared to non-saline control irrespective of KCl level (Table 6). Under the lowest NaCl levels (0 and 200 mM NaCl) the presence of 10 mM KCl reduced PI_{abs} by on average 42%. PI_{total} was augmented in plants exposed to 600 mM NaCl at both KCl levels and 400 mM NaCl + 10 mM KCl. The availability of 10 mM KCl reduced PI_{total} of Callide non-saline plants (52%) and 600 mM NaCl (34%) (Fig. 9 and Table 6).

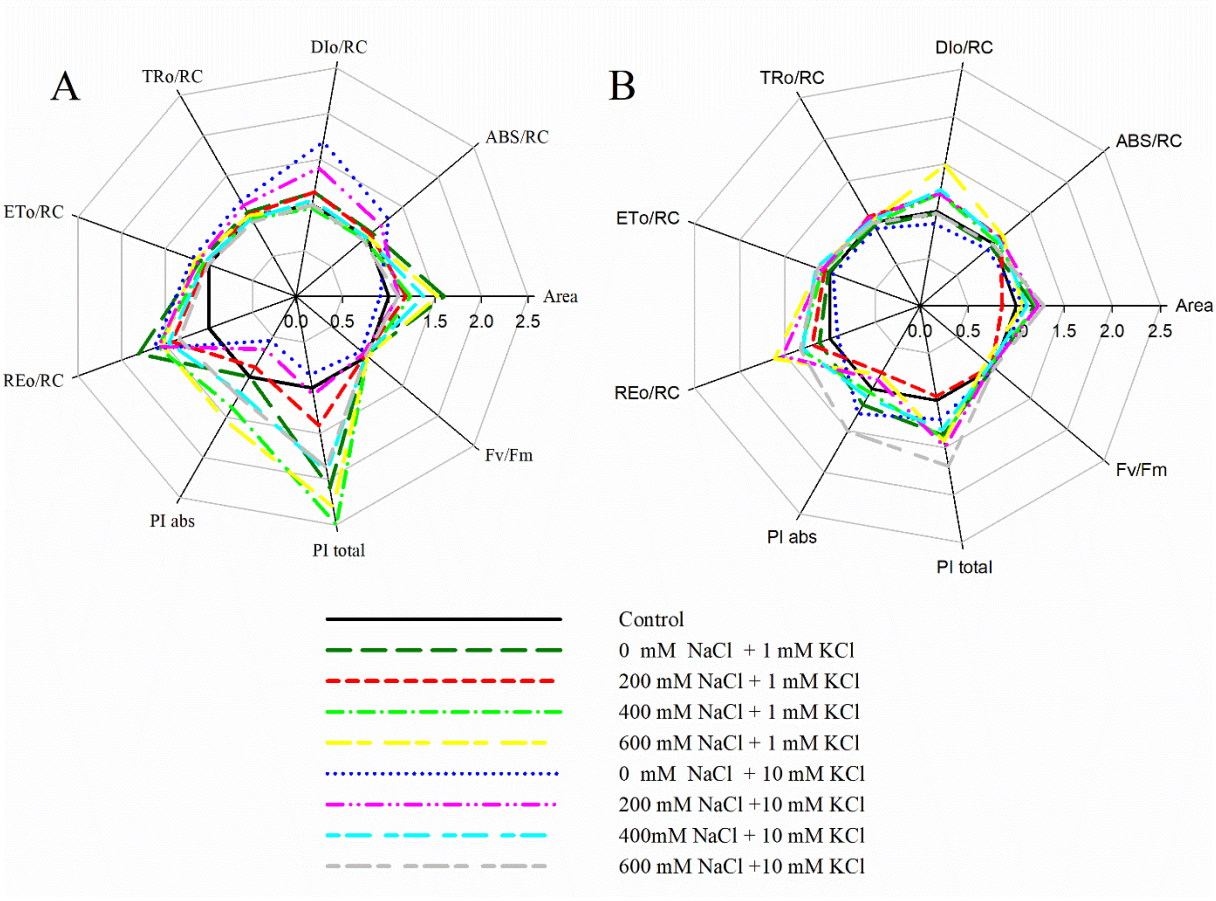

Figure 9. JIP test parameters of two cultivars of Rhodes Grass (*Chloris gayana*) cv. Callide (A) and Reclaimer (B) grown in aerated nutrient solution under different saline regimes (0, 200, 400, and 600 mM NaCl) with 1 or 10 mM KCl. Treatments were imposed on 15-day-old plants and readings were performed in the 2nd fully expanded leaf in the morning (from 10 to 11 a.m.) after dark adaptation for at least 20 min after 24 days of treatment. Each radar line is the average of eight replicates.

For Reclaimer, the more pronounced effects with increases in specific fluxes per reaction center were observed in the treatments 600 mM NaCl + 1 mM KCl (Fig. 10B). Performance index, PI_{abs}, was reduced for plants from 200 to 600 mM NaCl under the lowest availability of KCl, and PI_{total} was augmented 35% as compared to non-saline control under the highest KCl availability (Fig. 10B; Table 6). The quantum efficiency of photosystem II (F_V/F_M) was not sensible to any of the treatments or cultivars tested (Fig. 10A and 10B).

Table 6. JIP parameters of chlorophyll *a* fluorescence of two cultivars of Rhodes Grass (*Chloris gayana*) cv. Callide and Reclaimer grown in aerated nutrient solution under different saline concentrations (0, 200, 400, and 600 mM NaCl) with 1 or 10 mM KCl.

		PIabs		**PItotal**	
	NaCl (mM)	*KCl (mM)*			
Cultivar		*1*	*10*	*1*	*10*
Callide	*0*	3.5 ± 0.4^{Ba}	1.9 ± 0.1^{Bb}	2.5 ± 0.5^{Ba}	1.2 ± 0.3^{Bb}
	200	3.8 ± 0.2^{Ba}	2.3 ± 0.4^{Bb}	2.0 ± 0.2^{B}	1.3 ± 0.1^{B}
	400	4.3 ± 0.5^{A}	4.5 ± 0.6^{A}	2.8 ± 0.3^{B}	2.4 ± 0.5^{A}
	600	4.7 ± 1.0^{A}	4.3 ± 0.8^{A}	3.5 ± 0.8^{Aa}	2.3 ± 0.9^{Ab}
Reclaimer	*0*	3.8 ± 0.8^{A}	3.9 ± 0.6	1.9 ± 0.6	1.5 ± 0.5^{B}
	200	2.6 ± 0.3^{B}	3.0 ± 0.3	1.2 ± 0.2	1.7 ± 0.4^{B}
	400	3.1 ± 0.2^{B}	3.1 ± 0.2	1.8 ± 0.2	1.7 ± 0.3^{B}
	600	2.9 ± 0.9^{B}	3.5 ± 0.9	1.8 ± 0.6	2.3 ± 0.5^{A}

Upper case letters represent significant differences among NaCl levels within the same KCl level (column) using the Scott-Knott test $p < 0.05$ and lower case letters represent significant difference between the two levels of KCl at the same level of NaCl (rows) using the F-test at $p < 0.05$. Treatments were imposed on 15-day-old plants and readings were performed in the 2nd fully expanded leaf in the morning (from 10 to 11 a.m.) after dark adaptation for at least 20 min after 24 days of treatment. Means ± standard deviation (n=8). There was a significant cultivar × NaCl × KCl interaction at $p < 0.001$ for PI_{total} and at $p < 0.05$ for PI_{abs} (three-way ANOVA). Additional statistical analysis is given in Supplementary material (Table S6).

3.8. Leaf gas exchange

Gas exchange measurements showed different performances in response to different cultivars and salinity regimes. The photosynthetic rates (*A*) at ambient CO_2 level when plants were grown in non-saline solutions at both levels of KCl were on average 35 µmol CO_2 m^{-2} s^{-1} for Callide and 38 µmol CO_2 m^{-2} s^{-1} for Reclaimer. The *A* was not affected by 400 mM NaCl treatments at either KCl levels in both cultivars but it was reduced when plants were grown with 200 mM NaCl with either 1 or 10 mM KCl (with exception for Reclaimer in 200 mM NaCl +10 mM KCl) by on average -0.4- and -0.3-fold of controls for Callide and Reclaimer, respectively and by -0.5 of non-saline controls for both cultivars at 600 mM NaCl. The photosynthetic rates did not significantly increase for either cultivar when measurements were conducted at elevated external CO_2 (800 µmol s^{-1}), when compared with *A* at the ambient

CO_2 level of 400 μmol mol^{-1} (Table 7).

Stomatal conductance (g_s) at ambient CO_2 level was on average 0.23 mol (H_2O) m^{-2} s^{-1} in Callide grown with 0 mM NaCl at both KCl levels. Exposure to 200 and 400 led to a g_s reduction of -0.3-fold and 600 mM NaCl treatments reduced g_s -0.6-fold of controls, respectively. In Reclaimer, the g_s was similar in non-saline control, 200 and 400 mM NaCl treatments at both levels of KCl with an average of 0.16 mol (H_2O) m^{-2} s^{-1} but it was reduced to 0.07 mol (H_2O) m^{-2} s^{-1} by imposition of 600 mM NaCl. Elevation of CO_2 to 800 μmol s^{-1} reduced g_s on average 0.5-fold in Callide for 0, 200 and 400 mM NaCl treatments irrespective of KCl, relative to g_s at ambient CO_2, at corresponding treatment combinations (Table 7).

The ratio of intercellular to external CO_2 concentration (C_i/C_a) was reduced by NaCl. For Callide *Ci/Ca* was on average 0.30 for non-saline plants and 0.24 for 200 mM NaCl treated plants. Exposure to 400 and 600 mM NaCl treatments reduced C_i/C_a by on average -0.6-fold at both KCl levels. For Reclaimer, C_i/C_a was on average of 0.24 in non-saline controls at both KCl levels, imposition of 200 mM NaCl + 10 KCl and 400 mM of NaCl (irrespective of KCl) reduced *Ci/Ca* by -0.3-fold and C_i/C_a declined by -0.6-fold at 600 mM of NaCl (irrespective of KCl). All measurements performed under elevated external CO_2 (800 μmol mol^{-1}) were responsive and reduced with regard to salt in a similar way to measurements performed in ambient CO_2 (Table 7).

In Callide, at ambient CO_2 level *WUE* of non-saline + 1 mM KCl was on average 7.8 mmol CO_2 $mmol^{-1}$ H_2O irrespective of KCl and exposure to 400 and 600 mM NaCl led to a 0.3-fold increment in *WUE* (Fig. 10A). At the highest KCl level (10 mM), the increment in NaCl levels did not affect *WUE*. In the cv. Reclaimer, WUE under non-saline + 1 mM KCl was on average 10.3 mmol CO_2 $mmol^{-1}$ H_2O and NaCl levels did not affected *WUE*. The augment in KCl availability, hovewer, caused a -0.3-fold reduction in *WUE* in non-saline controls and a 0.4-fold increase in 200 mM NaCl (Fig. 10A).

In general, values of *WUE* were incremented about 1-fold in measurements performed under elevated CO_2 (Fig. 10). *WUE* in plants of cv. Callide exposed to 400 and 600 mM NaCl in the highest KCl level (10 mM) was on average 19 mmol CO_2 $mmol^{-1}$ H_2O, while for non-saline controls and 200 mM NaCl was 14 mmol CO_2 $mmol^{-1}$ H_2O. Additionally, plants submitted to 10 mM of KCl plants exhibited a -0.2-fold decrease in 200 mM NaCl and 0.2-fold in increase in *WUE* under 600 mM NaCl as compared to the same treatments under 1

mM KCl (Fig. 10B). In Reclaimer, WUE was on average 13 in non-saline control, irrespective of KCl. Exposure to 400 mM + 1 KCl, however, improved WUE about 0.3-fold as compared to the other saline and non-saline treatments under 1 mM KCl. Under 10 mM KCl, WUE was improved about 0.4-fold as compared to non-saline control in response to the treatments 200, 400 and 600 mM of NaCl (Fig. 10D).

Table 7. Gas exchange parameters measured at a CO_2 concentration of 400 µmol mol^{-1} and 800 µmol mol^{-1} for two Rhodes grass (*Choris gayana*) cultivars, Callide and Reclaimer grown under different saline regimes (0, 200, 400 and, 600 mM NaCl) and 1 or 10 mM KCl.

		cv. Callide					
External CO_2	*NaCl (mM)*	**Net photosynthetic rates (*A*, µmol CO_2 m^{-2} s^{-1})**		**Stomatal conductance (g_s, mol (H_2O) m^{-2} s^{-1})**		**C_i/C_a (ratio of intercellular to ambient CO_2 concentration)**	
		1	*10*	*1*	*10*	*1*	*10*
400 µmol mol^{-1}	*0*	37.0 ± 5.0^{A}	33.2 ± 6.1^{A}	0.25 ± 0.01^{A}	0.20 ± 0.03^{A}	0.34 ± 0.05^{A}	0.28 ± 0.03^{A}
	200	27.9 ± 2.1^{B}	20.2 ± 3.4^{B}	0.18 ± 0.01^{Ba}	0.11 ± 0.01^{Bb}	0.24 ± 0.07^{B}	0.24 ± 0.04^{A}
	400	34.0 ± 7.4^{A}	30.7 ± 5.7^{A}	0.18 ± 0.05^{B}	0.15 ± 0.03^{A}	0.16 ± 0.04^{C}	0.11 ± 0.01^{B}
	600	20.1 ± 4.8^{B}	22.9 ± 2.4^{B}	0.07 ± 0.02^{C}	0.09 ± 0.0^{B}	0.14 ± 0.05^{C}	0.10 ± 0.08^{B}
800 µmol mol^{-1}	*0*	40.2 ± 4.9^{A}	36.3 ± 6.8^{A}	0.11 ± 0.06	0.09 ± 0.02	0.32 ± 0.1^{A}	0.36 ± 0.06^{A}
	200	31.7 ± 2.1^{Aa}	23.9 ± 5.6^{Bb}	0.10 ± 0.02	0.06 ± 0.01	0.26 ± 0.03^{A}	0.23 ± 0.01^{B}
	400	36.0 ± 2.9^{A}	32.0 ± 4.3^{A}	0.09 ± 0.00^{a}	0.07 ± 0.01	0.17 ± 0.03^{B}	0.10 ± 0.01^{C}
	600	21.4 ± 4.1^{B}	25.2 ± 2.2^{B}	0.06 ± 0.00	0.06 ± 0.00	0.15 ± 0.04^{B}	0.11 ± 0.05^{C}

cv. Reclaimer							
External CO_2	*NaCl (mM)*	**Net photosynthetic rates (*A*, µmol CO_2 m^{-2} s^{-1})**		**Stomatal conductance (g_s, mol (H_2O) m^{-2} s^{-1})**		**C_i/C_a (ratio of intercellular to ambient CO_2 concentration)**	
		1	*10*	*1*	*10*	*1*	*10*
400 µmol mol^{-1}	*0*	32.9 ± 6.3^{A}	27.7 ± 3.9^{A}	0.17 ± 0.03^{A}	0.18 ± 0.02^{A}	0.21 ± 0.03^{B}	0.26 ± 0.04^{A}
	200	22.5 ± 8.9^{B}	30.2 ± 1.9^{A}	$0.13\pm.0.04^{A}$	0.16 ± 0.02^{A}	0.36 ± 0.04^{Aa}	0.16 ± 0.06^{Bb}
	400	33.7 ± 1.8^{A}	28.3 ± 1.9^{A}	0.17 ± 0.01^{A}	0.13 ± 0.01^{A}	0.15 ± 0.03^{B}	0.19 ± 0.04^{B}
	600	15.5 ± 2.8^{B}	15.7 ± 4.8^{B}	0.07 ± 0.01^{B}	0.07 ± 0.02^{B}	0.11 ± 0.03^{B}	0.09 ± 0.04^{C}
800 µmol mol^{-1}	*0*	38.9 ± 4.0^{Aa}	30.1 ± 3.8^{Ab}	0.16 ± 0.01^{Aa}	0.13 ± 0.01^{Ab}	0.48 ± 0.05^{A}	0.49 ± 0.01^{A}
	200	20.1 ± 7.1^{Bb}	30.3 ± 2.2^{Aa}	0.09 ± 0.03^{B}	0.10 ± 0.01^{B}	0.35 ± 0.1^{Ba}	0.21 ± 0.07^{Bb}
	400	36.9 ± 2.3^{Aa}	29.9 ± 1.4^{Ab}	0.09 ± 0.01^{B}	0.08 ± 0.00^{C}	0.17 ± 0.03^{C}	0.17 ± 0.05^{B}
	600	17.0 ± 1.3^{B}	17.3 ± 1.4^{B}	0.04 ± 0.00^{C}	0.04 ± 0.00^{D}	0.16 ± 0.03^{C}	0.12 ± 0.08^{B}

Upper case letters represent significant differences among NaCl levels within the same KCl level (column) using the Scott-Knott test $p < 0.05$ and lower case letters represent significant difference between the two levels of KCl at the same level of NaCl (rows) using the F-test at $p < 0.05$. Treatments were imposed on 15-day-old plants and readings were performed in the second youngest fully expanded leaf after 24 days of treatment. Means ± standard deviation (n =4). There was a significant cultivar × NaCl × KCl interaction at $p < 0.001$ for net photosynthetic rates (*A)* and *Ci/Ca* ratio and at $p < 0.05$ for stomatal conductance (g_s) in measurements performed at elevated CO_2 concentration (800 µmol mol^{-1}) (three-way ANOVA). Additional statistical analysis is given in Supplementary material (Table S7).

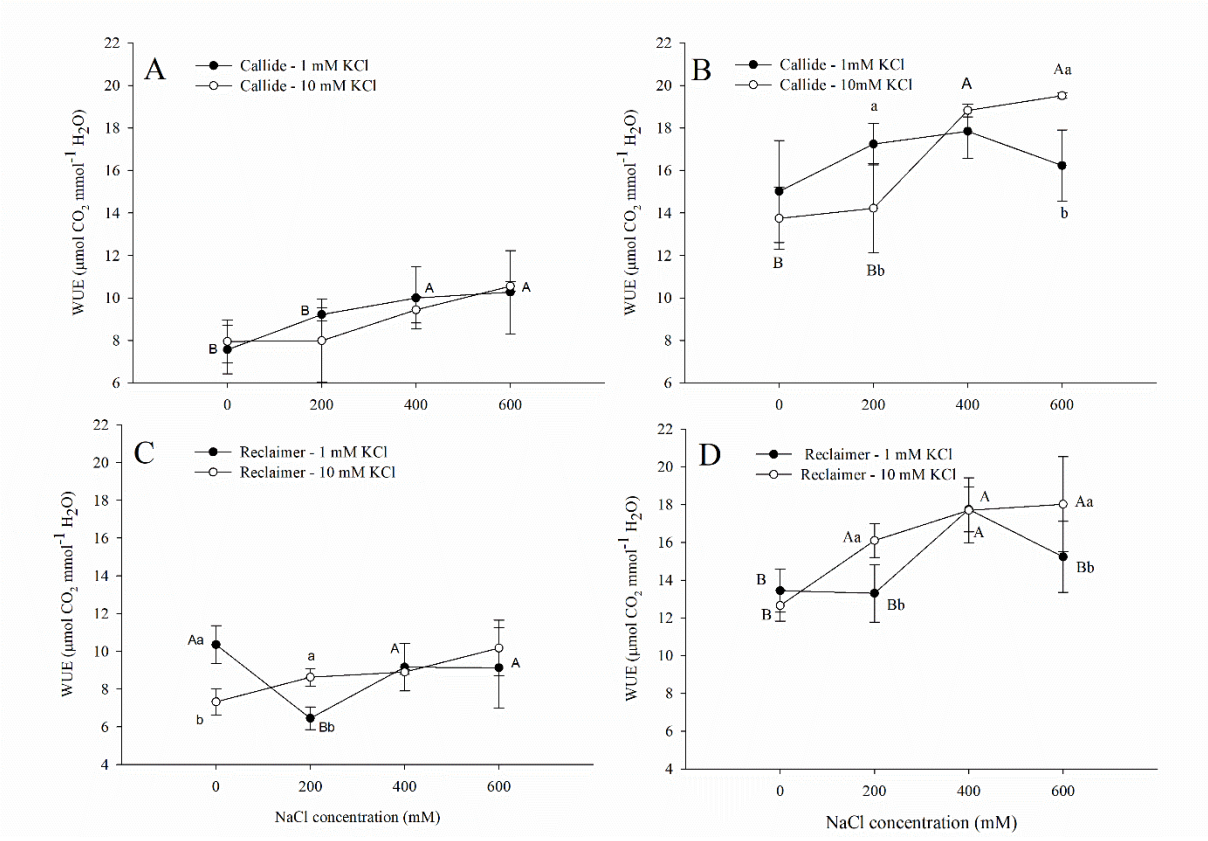

Figure 10. Water use efficiency (*WUE*; ratio of net photosynthetic rates and transpiration rates) measured at a CO_2 concentration of 400 µmol mol^{-1} (A, C) and 800 µmol mol^{-1} (B, D) Measurements were conducted for two Rhodes grass (*Choris gayana*) cultivars, Callide (A, B) and Reclaimer (C, D) grown in aerated nutrient solution under different saline regimes (0, 200, 400, and 600 mM NaCl) with 1 or 10 mM KCl. Upper case letters represent significant differences among NaCl levels within the same KCl level using the Scott-Knott test $p < 0.05$ and lower case letters represent significant difference between the two levels of KCl at the same level of NaCl using the F-test at $p < 0.05$. Treatments were imposed on 15-day-old plants and readings were performed on the second youngest fully expanded leaves after 24 days of treatment. Means ± standard deviation (n =4). There was a significant cultivar × NaCl × KCl interaction at $p < 0.05$ for *WUE* ratio in measurements performed at elevated CO_2 concentration (800 µmol mol^{-1}) (three-way ANOVA). Additional statistical analysis is given in Supplementary material (Table S7).

4. Discussion

Known for its ability to withstand saline/sodic soil conditions, Rhodes grass is a forage grass reported to possess intra and interspecific cultivar variability in response to salt stress (Luca et al., 2001). Here, we observed several mechanisms to cope with salinity stress: 1) ability to accumulate high amounts of inorganic solutes, contributing to osmotic adjustment; 2) stomata closure without impairing carbon assimilation per leaf area, increasing the

efficiency of water use; secretion of up to 70% of the retained Na^+ onto the leaf surface and, 4) reduction of growth, diminishing plant transpiration total area. Osmotic adjustment and ion exclusion have been correlated with salt tolerance in several grasses in the subfamily Chloridoideae (Marcum, 1999). Contrary to our data, the evaluation of the physiological causes for reduced productivity in Rhodes grass cv. Boma revealed that net assimilation rate per leaf area remained almost unchanged during long periods of exposure to 200 mM of NaCl (~60 days). Leaf area and its ratio per unit plant mass, however, were rapidly responsive to salt stress with great depressive impact on growth rate (Luca et al., 2001). Even though the reduction of biomass accumulation is considered one of the main deleterious effects in crops cultivated in saline soils (Deinlein et al., 2014), in terms of plant biology it represents an important strategy to cope with excessive salt, by reducing leaf transpiration area and, therefore, helping to maintain plant water status through its lower demand for water (Chaves et al., 2009).

Here, we observed an increment in the accumulation of sodium ions in both shoot and root associated with increasing level of external salinity in both Rhodes cultivars. Recognized as a salt-tolerant C_4 species, *Chloris gayana*, was reported to accumulate Na in their tissues (Ando and Masaoka, 1985; Kobayashi et al, 2010; Luca et al., 2001; Kopittke et al., 2009). Our results point to a reduction in leaf sap osmotic potential in response to increasing salinity and accumulation of sodium (~ 1.7-fold more negative in 400 mM and 2.7-fold more negative in 600 mM NaCl in the cv. Callide; and, 1.4-fold more negative in 400 mM NaCl, irrespective of KCl and 3.7-fold more negative in 600 mM NaCl + 1 KCl in cv. Reclaimer. Uptake and accumulation of Na^+ in barley plants was central to tolerate salt stress by accumulating salt in the leaves for osmotic adjustment (Mian et al., 2011). Even though *C. gayana* was earlier reported to accumulate Na^+, the energy required for the uptake, storage and exclusion of these solutes ended up affecting growth when compared with plants cultivated in non-saline environments, leading to decreased growth (up to 70%) in the treatments with 400 and 600 mM NaCl. This result is consistent with other reports (Kopittke et al., 2009; Luca et al., 2001).

Reduction in biomass accumulation in response to increased salinity was not always accompanied by decreases in rates of carbon assimilation, especially in plants treated with 400 mM of NaCl. This might indicate that growth reduction could have occurred as a result of

redirection and conservation of energy to activities that guarantee the survival during salinity stress rather than as a response to a lack of energy due to impairments in the photosynthetic processes. Adoption of several energy-requiring processes for plant acclimation, as the synthesis of compatible osmolytes and, ion compartmentalization and excretion might be responsible for both plant growth reduction and survival (Flowers and Colmer, 2008; Kopittke et al., 2009). Leaf washing analysis indicated that high amounts of sodium were excluded through the salt glands, which, on the one hand, may have had a significant role in avoiding the accumulation of excessive quantities of the ion in the leaves and, on the other hand, diverged the species' energy demand for activities other than growth.

In Callide cultivar, the higher levels of NaCl treatments (400 and 600 mM) in the nutrient solution augmented the retention of sodium and potassium in the leaf tissue. Contrary to what was observed with the Callide cultivar, the shoot accumulation of K^+ in cv. Reclaimer under low KCl was low even in the absence of NaCl and was progressively reduced in the presence of NaCl. A similar result was reported for two natural accessions (Columbia-0 and NOK2) of *Arabidopsis thaliana* (L.) Heynh. subjected to increase in potassium fertilization, where only one of the accessions was responsive to the external extra potassium (Kaddour et al., 2009). The accession of *A. thaliana* NOK2 was sensitive to additional potassium fertilization restoring K^+ net uptake to nearly control values in the presence of 50 mM of NaCl. However, contrary to our results, the increase in potassium was correlated with a decrease of about 25% in the sodium content of NOK2 leaves and increased plant biomass not only in the absence of NaCl (15% increase in final biomass) but also in the presence of NaCl (30% increase in final biomass), demonstrating the protective effect conferred by the increase in K-fertilization. Maintenance of K^+ uptake and transport in Callide plants even under the highest levels of NaCl, suggests the presence of a strong selectivity for the uptake of K^+. The interactions among the external levels of the nutrients in the soil and/or nutrient solution are determinant on its uptake (Assaha et al., 2017) and selective transport systems are strongly associated with salt tolerance (Kaddour et al., 2009). High-affinity uptake and transport systems (HAT) possess high specificity for K^+ and are associated with its uptake at very low K^+ concentrations. Low-affinity K^+ uptake (LAT) is linked with K^+ uptake and transport in the mM range (up to 50 mM) (Assaha et al., 2017; Maathuis et al., 1997).

The impairment of the electron transport chain, especially considering PSII activity, is

normally compromised by ion leakage and the passage of toxic ions into the chloroplast (Pan et al., 2020). It may lead to inactivation of key photosynthetic enzymes, dissociation of photosynthetic intrinsic and extrinsic proteins necessary to the activity of the photosystems, damage to photosystems complexes, and pigment degradation (Chaves et al., 2009), characterizing the non-stomatal limitation of photosynthesis. Halophytes species, however, are known for its ability to maintain [Na^+] about 20 times higher than glycophytes species without causing major injuries to plant metabolism as well as efficiently regulate the passage of potential toxic ions to the chloroplast keeping it to a torable level (Flowers et al., 2015).

Our results point out that in the cv. Callide the presence of 10 mM KCl injured the electron transport chain of plants treated with less NaCl (0 and 200 mM), with possible toxic effect from the excessive accumulated potassium in *C. gayana* leaves (from ~221 to 1000 µmol g^{-1} DW^{-1}, in plants treated with 0 mM of NaCl). These plants showed an increase in absorption indices per reaction center and reductions in performance indexes PI_{abs} and PI_{total} (JIP-test), a lower inflection in the OJIP points (especially F_M), and presented positive hidden K and L-bands with greater amplitude compared to other treatments. Furthermore, the increase in DIo/RC rates about 70% higher than the ABS/RC rise indicates a possible inactivation of a parcel of Q_A-reducing centers (Valença et al., 2020; Yusuf et al., 2010). Furthermore, the increase in [K] concomitant with low levels of [Na] in the leaf tissue did not favor leaf photochemistry nor carbon assimilation rates of these plants. Low levels of Na^+ were already associated with a reduction in PSII activity of the C_4 species *Amaranthus tricolor* L. (Johnston et al., 1989) and *Kochia childsii* Hort. (Grof et al.,1989). Similarly, in pot trials with *C. gayana* cv. Pioneer, the amount of potassium in shoots to achieve maximum growth was progressively reduced as the level of sodium increased from 0 to 400 mg per pot, since the potassium concentration was above a critical value that could not be replaced by other cations (0.5% of the dry matter) (Smith, 1974). In the cv. Reclaimer, however, the higher availability of KCl (10 mM) associated with the lower levels of NaCl (0 and 200) induced positive effects in the photosynthetic electron transport chain as indicated by the presence of positive K- and L- hidden bands and JIP-test parameters.

A notable increase in photosynthetic index PI_{total}, due to exposure to high levels of NaCl, was observed in both cultivars. Cv. Callide also presented augment in PI_{abs} as a response to 400 and 600 mM NaCl. PI_{abs} is a product of terms expressing the performance of

the PSII reaction center from the energy absorption to the reduction of intersystem electrons acceptor and, PI_{total} is a multiparametric variable associated with the photosynthetic performance from energy absorption to the reduction of PSI final electron acceptors (Yusuf et al., 2010). Increases in PI_{abs} due to exposure to stresses such as oil (Reinert et al., 2016) and herbicide (Sousa et al., 2014) were described, however, such increases were not sustained over time and could be considered a tentative of the plant to overcompensate the stress. Under salinity, PI_{abs} and PI_{total} are often described as sensitive parameters to assess decreases in the photochemical efficiency of photosynthetic electron transport in NADP-ME C_4 plants (Bussotti et al., 2010; Bezerra et al., 2021).

The different responses of the performance indexes observed here may also have occurred as an attempt to overcompensate the stress, which would not be sustained for much more longer. ce of permanent impairments in electrons transport under salinity, leading to more efficient reHowever, the evaluation of the chloroplast ultrastructure of *C. gayana* under saline conditions showed preservation of bundle sheath (BS) cells with well-developed grana (Omoto et al., 2010). In the chloroplasts of mesophyll cell, in contrast, it was observed swelling of thylakoids and grana unstacking (Omoto et al., 2010). The well-developed grana observed in BS cells associated with its high preservation may have been a decisive factor in the avoidangulation of photosynthetic electron transport between the two photosystems. It is not known why salinity caused ultrastructural changes to chloroplasts in mesophyll cells but not in chloroplasts of bundle sheath cells (Omoto et al., 2010). These authors suggest that investigation of the expression of stress-inducible genes, such as a salt-inducible gene encoding glycine-rich RNA-binding protein (GR-RBP), in plants with different C_4 metabolism might be a path to elucidate this differential sensitivity. The different sensitivity can also be a result of higher production of reactive oxygen species in mesophyll cells as compared to bundle sheath cells, as observed in maize during salt stress (Omoto et al., 2013). Although our data do not indicate photoinhibition and/or permanent damage to the electron transport chain even in plants grown with 600 mM NaCl whether the preservation of BS cells would be maintained under such high levels of salt is yet to be confirmed.

In some C_4 species, sodium is an essential nutrient to guarantee plants' growth and performance (Subbarao et al., 2003). Sodium stimulating growth through enhanced photosynthesis was also reported to the C_4 grasses *Panicum coloratum* L. (Matoh and Murata,

1990) and *Panicum antidotale* Retz. (Hussain et al., 2020). Furthermore, even though leaf Na^+ concentrations were at least 6-fold higher under high salinity levels (400 and 600 mM) chloroplast Na^+ concentration may have been kept at much lower levels, therefore, not compromising photosynthesis. Halophytes exposed to saline levels equal to or higher than 300 mM were reported to accumulate Na^+ in leaves about 4-fold higher than the Na^+ amount found in its chloroplasts (Flowers et al., 2015).

Analysis of the quantum efficiency of PSII (F_V/F_M; JIP-test), a common index used to evaluate plants' response to stress was not sensitive to any of the treatments applied, failing to indicate either damage and energy conservation throughout the photosynthetic electron transport chain. The insensitivity of this parameter to stressful conditions was also reported under drought, nitrogen deficiency and contamination with oil (Reinert, 2016; Oukarroum et al., 2007; Živcak et al., 2014) indicating the need for more detailed analysis, using other parameters, for the correct detection of alterations in leaf photochemistry.

During salt stress, photosynthesis can be affected via stomatal and non-stomatal factors (Chaves et al., 2009). Due to its leaf anatomy and carbon concentration mechanism, the decreased CO_2 availability caused by stomatal closure is not normally associated with reduction in net photosynthesis of C_4 species (Ghannoum, 2009; Maricle and Maricle, 2018). Accordingly, except for Callide plants treated with 200 mM of NaCl + 1 KCl, our results assessed under elevated CO_2 do not point for stomatal limitation, as increases in *A* in most treatments were non-significant, suggesting that CO_2 availability was not the main limiting factor in the reduction of carbon assimilation. Earlier reports of gas exchange measurements have shown that the C_4 photosynthesis is nearly saturated at ambient CO_2 (Maricle and Maricle, 2018) and that improvements in photosynthesis associated with elevated CO_2 occur mainly due to enhancement in water relations through modified stomatal conductance (Conley et al. 2001). Likewise, in our study elevated external CO_2 caused one-fold increases in WUE. In *Panicum turgidum* Forssk, also reported as a high salt-tolerant C_4 species, however, high salinity (500 mM) led to a significant decrease in water use efficiency which was mainly attributed to non-stomatal limitation of photosynthesis (Koyro et al., 2013).

Although both Callide and Reclaimer cultivars presented similar responses to the salts, the interaction between different levels of NaCl and KCl led to different outcomes depending on the cultivar. Higher accumulation of K in leaves of Callide grown with 10 mM KCl as

compared to 1 mM KCl exposed to the lower levels of NaCl (0 and 200 mM of NaCl) harmed leaf photochesmitry, as indicated by increases in DI_o and ABS/RC, decreases in photosynthetic indexes and, the presence of high positive hidden bands. Contrary to that, 10 mM of KCl improved leaf photochemistry of cv. Reclaimer presenting positive impacts on both donor and acceptor side of the PSII, especially for the non-saline treatment. However, although the availability of K^+ in the nutrient solution affected chlorophyll *a* transient parameters of plants of both cultivars not all parameters were sensitive to plants' overall improvement nor improvements were converted in superior net photosynthesis or growth.

5. Conclusions

Rhodes grass contrasting cultivars showed variation dependent on the level of retained potassium and severity of salt stress and presented several acclimation strategies to cope with the high salinity. The lower dependence of Callide cultivar on high levels of potassium can be an important indicator for the use and cultivation of the species in salinized environments and becoming a target for molecular studies considering the expression of selective K^+-transport under low K^+. Although the increased KCl availability has had some positive effects in leaf photochemistry of plants under 0 and 200 mM NaCl in the Reclaimer cultivar, as indicated by the presence of negative hidden bands and JIP-parameters, the use of additional potassium fertilization might be not justified considering the slight or nonexistent improvements in net photosynthesis and biomass accumulation. In cv. Reclaimer, leaf photochemistry and carbon assimilation phases of photosynthesis were highly tolerant to high levels of salt (plants were not affected up to 600 mM NaCl) indicating that the cultivar might be central in conservation programs, cultivation in saline environments, and studies of the regulation of membrane transport and ion compartmentalization. It is important to note, however, that although alterations were detected in both cultivars in response to NaCl and KCl levels, it did not result in photoinhibition in any of the treatments and plants were photosynthetically active even under the highest levels of salt.

6. References

Ando, T., Masaoka, Y. 1985. Interspecific differences in sodium accumulation and requirement among forage crops. Soil Science and Plant Nutrition 31 (4): 601-610. https://doi.org/10.1080/00380768.1985.10557468.

Aoki, N., Kanai, R. 1997. Reappraisal of the role of sodium in the light-dependent active

transport of pyruvate into mesophyll chloroplasts of C_4 plants. Plant and Cell Physiology 38: 1217-1225. https://doi.org/10.1093/oxfordjournals.pcp.a029108.

Arnon, D.I., Stout, P.R. 1939. The essentiality of certain elements in minute quantity for plants with special reference to copper. Plant Physiology 14: 371-375. http://doi.org/10.1104/pp.14.2.371

Assaha, D.V.M., Ueda, A., Saneoka, H., Al-Yahyai, R., Yaish, M. W., 2017. The role of Na^+ and K^+ transporters in salt stress adaptation in glycophytes. Frontiers in Physiology 8, 509. https://doi.org/10.3389/fphys.2017.00509.

Bezerra, A.C.M., Valença, D.C., Junqueira, N.E.G., Hüther, C.M., Borella, J., Pinho, C.F., Ferreira, M.A., Medici, L.O., Ortiz-Silva, B., Reinert, F. 2021. Potassium supply promotes the mitigation of NaCl-induced effects on leaf photochemistry, metabolism and morphology of *Setaria viridis.* Plant Physiology and Biochemistry 160: 193-210. https://doi.org/10.1016/j.plaphy.2021.01.021.

Bussotti, F., Desotgiu, R., Pollastrini, M., Cascio, C., 2010. The JIP test: a tool to screen the capacity of plant adaptation to climate change. Scandinavian Journal of Forest Research 25 (8), 43-50. https://doi.org/10.1080/02827581.2010.485777.

Chaves, M.M., Flexas, J., Pinheiro, C., 2009. Photosynthesis under drought and salt stress: regulation mechanisms from whole plant to cell. Annals of Botany 103, 551-560. https://doi.org/10.1093/aob/mcn125.

Colmer, T.D., Munns, R., Flowers, T.J. 2005. Improving salt tolerance of wheat and barley: future prospects. Australian Journal of Experimental Agriculture 45: 1425-1443. https://doi.org/10.1071/EA04162.

Conley, M.M., Kimball, B.A., Brooks, T.J., Pinter Jr, P.J., Hunsaker, D.J., Wall, G.W., Adam, N.R., LaMorte, R.L., Matthias, A.D., Thompson, T.L., Leavitt, S.W., Ottman, M.J., Cousins, A.B., Triggs, M. 2001. CO_2 enrichment increases water-use efficiency in sorghum. New Phytologist 151: 407-412. https://doi.org/10.1046/j.1469-8137.2001.00184.x.

Deinlein, U., Stephan, A.B., Horie, T., Luo, W., Xu, G., Schroeder, J.I. 2014. Plant salt-tolerance mechanisms. Trends in Plant Science 19 (6), 371-379. https://doi.org/10.1016/j.tplants.2014.02.001.

Flowers, T.J., Colmer, T.D. 2008. Salinity tolerance in halophytes. New Phytologist, 179: 945-963. https://doi.org/10.1111/j.1469-8137.2008.02531.x

Flowers, T.J., Munns, R., Colmer, T.D. 2015. Sodium chloride toxicity and the cellular basis of salt tolerance in halophytes. Annals of Botany, 115: 419-431. https://doi.org/10.1093/aob/mcu217.

Garthwaite, A.J., Bothmer, R. von, Colmer, T.D. 2005. Salt tolerance in wild *Hordeum* species is associated with restricted entry of Na^+ and Cl^- into the shoots. Journal of Experimental Botany, 56 (419): 2365-2378. https://doi.org/10.1093/jxb/eri229.

Ghannoum, O. 2009. C_4 photosynthesis and water stress. Annals of Botany 103: 635–644. https://doi.org/10.1093/aob/mcn093.

Grof, C.P., Johnston, M., Brownell, P. F. 1989. Effect of sodium nutrition on the ultrastructure of chloroplasts of C_4 plants. Plant Physiology, 89: 539–543. https://doi.org/10.1104/pp.89.2.539

Hasanuzzaman, M., Bhuyan, M.H.M., Nahar, K., Hossain, M.S., Mahmud, J.A., Hossen, M.S., Masud, A.A.C., Moumita, Fujita, M., 2018. Potassium: a vital regulator of plant responses and tolerance to abiotic stresses. Agronomy 8 (31), 1-29. https://doi.org/10.3390/agronomy8030031.

Hatam, Z., Sabet, M.S., Malakoutim M.J., Mokhtassi-Bidgoli, A., Homaee, M., 2020. Zinc and potassium fertilizer recommendation for cotton seedlings under salinity stress based in gas exchange and chlorophyll fluorescence responses. South African Journal of Botany 130, 155-164. https://doi.org/10.1016/j.sajb.2019.11.032.

Hunt, R. 1982. Plant growth curves. The functional approach to plant growth analysis. London: Edward Arnold.

Hussain, T., Koyro, H-W, Zhang, W., Liu, X., Gul, B., Liu, X., 2020. Low salinity improves photosynthetic performance in *Panicum antidotale* under drought stress. Frontiers in Plant Science 11, 481. https://doi.org/10.3389/fpls.2020.00481.

Ivushkin, K., Bartholomeusa, H., Bregta, A.K., Pulatovb, A., Kempenc, B., Sousac, L., 2019. Global mapping of soil salinity change. Remote Sensing of Environment 231, 111260. https://doi.org/10.1016/j.rse.2019.111260.

Johnston, M., Grof, C.P.L., Brownell, P.F. 1989. Chlorophyll a/b ratios and photosystem activity of mesophyll and bundle sheath fractions from sodium-deficient C_4 plants. Australian Journal of Plant Physiology 16: 449–457. http://doi.org/10.3389/fpls.2020.559876.

Kaddour, R., Nasri, N., M'rah, S., Berthomieu, P., Lachaâl, M., 2009. Comparative effect of potassium on K and Na uptake and transport in two accessions of *Arabidopsis thaliana* during salinity stress. Comptes Rendus – Biologies 332 (9), 784-794. https://doi.org/10.1016/j.crvi.2009.05.003.

Kobayashi, H., Masaoka, Y., Takahashi, Y., Ide, Y., Sato, S. 2010. Ability of salt glands in Rhodes grass (*Chloris gayana* Kunth) to secrete Na^+ and K^+. Soil Science and Plant nutrition 53 (6): 764-771. https://doi.org/10.1111/j.1747-0765.2007.00192.x.

Kopittke, P.M., Kopittke, R.A., Menzies, N.W. 2009. Measurement and interpretation of salinity tolerance in four perennial grasses. Journal of Plant Nutrition 32 (1): 30-43. https://doi.org/10.1080/01904160802530995.

Kotula, L., Caparros, P.G., Zörb, C., Colmer, T.D., Flowers, T.J. 2020. Improving crop salt tolerance using transgenic approaches: An update and physiological analysis. Plant Cell and Environment 43 (12): 2932-2956. https://doi.org/10.1111/pce.13865.

Kotula, L., Clode, P.L., Striker, G.G., Pedersen, O., Läuchli, A., Shabala, S., Colmer, T.D. 2015. Oxygen deficiency and salinity affect cell-specific ion concentrations in adventitious roots of barley (*Hordeum vulgare*). New Phytologist 208 (4): 1114-1125. https://doi.org/10.1111/nph.13535.

Koyro, H.-W., Hussain, T., Huchzermeyer, B., Khan, M.A., 2013. Photosynthetic and growth responses of a perennial halophytic grass *Panicum turgidum* to increasing NaCl concentrations. Environmental and Experimental Botany 91, 22–29. http://dx.doi.org/10.1016/j.envexpbot.2013.02.007.

Luca, M. de, Seffino, G., Grunberg, K., Salgado, M., Còrrdoba, A., Luna, C., Ortega, L., Rodriguez, A., Castagnaro, A., Taleisnik, E. 2001. Psysiological causes for decreased productivity under high salinity in Boma, a tetraploid *Chloris gayana* cultivar. Australian Journal of Agriculture Research 52 (9): 903-910. https://doi.org/10.1071/AR00190

Maathuis, F.J.M., Ichida, A.M., Sanders, D., Schroeder, J.I. 1997. Roles of higher plant K^+ channels. Plant Physiology 114 (4): 1141–1149. http://doi.org/10.1104/pp.114.4.1141.

Marcum, K.B. 1999. Salinity tolerance mechanisms of grasses in the subfamily Chloridoideae. Crop Science 39: 1153–1160. https://doi.org/10.2135/cropsci1999.0011183X003900040034x.

Maricle, B.R., Maricle, K.L., 2018. Photosynthesis, stomatal responses, and water potential in three species in an inland salt marsh in Kansas, USA. Flora 244-245, 1-7. https://doi.org/10.1016/j.flora.2018.05.001.

Matoh, T., Murata, S. 1990. Sodium stimulates growth of *Panicum coloratum* through enhanced photosynthesis. Plant Physiology 92: 1169-1173. http://doi.org/10.1104/pp.92.4.1169.

Mian, A.A., Senadheera, P., Maathuis, F.J. 2011. Improving crop salt tolerance: anion and cation transporters as genetic engineering targets. Plant Stress 5 (1): 64–72.

Munns, R., James, R. A., Läuchli, A. 2006. Approaches to increasing the salt tolerance of wheat and other cereals. Journal of Experimental Botany 57: 1025-1043. https://doi.org/10.1093/jxb/erj100.

Munns, R., Passioura, J.B., Colmer, T.D., Byrt, C. 2020. Osmotic adjustment and energy limitations to plant growth in saline soil 225: 1091-1096. https://doi.org/10.1111/nph.15862.

Munns, R., Tester, M., 2008. Mechanisms of salinity tolerance. Annual Review of Plant Biology, 59 (1), 651-681. https://doi.org/10.1146/annurev.arplant.59.032607.092911.

Munns, R., Wallace, P.A., Teakle, N.L., Colmer, T.D., 2010. Measuring soluble ions concentrations (Na^+, K^+ e Cl^-) in salt treated plants. In: Clifton, N.J. (ed.) Plant stress tolerance: methods and protocols. Humana Press. Springer 639, 371-382. https://doi.org/10.1007/978-1-60761-702-0_23.

Ohnishi, J., Flugge, U.I, Heldt, H.W., Kanai, R. 1990. Involvement of $Na^{+/}$ in active uptake of

pyruvate in mesophyll chloroplasts of some C_4 plants. Na^{+}/pyruvate cotransport. Plant Physiology 94: 950-959. https://doi.org/10.1104/pp.94.3.950.

Oi, T., Hirunagi, K., Taniguchi, M., Miyake, H. 2013. Salt excretion from the salt glands in Rhodes grass (*Chloris gayana* Kunth) as evidenced by low-vacuum scanning electron microscopy. Flora 208: 52-57. http://dx.doi.org/10.1016/j.flora.2012.12.006.

Oi, T., Taniguchi, M., Miyake, H. 2012. Morphology and ultrastructure of the salt glands on the leaf surface of Rhodes grass (*Chloris gayana* Kunth). International Journal of Plant Sciences 173 (5): 454-463. https://doi.org/10.1086/665588.

Omoto, E., Nagao H, Taniguchi M, Miyake H. 2013. Localization of reactive oxygen species and change of antioxidant capacities in mesophyll and bundle sheath chloroplasts of maize under salinity. Physiologia Plantarum 149: 1–12. https://doi.org/10.1111/ppl.12017.

Omoto, E., Taniguchi, M., Miyake, H. 2010. Effects of salinity stress on the structure of bundle sheath and mesophyll chloroplasts in NAD-malic enzyme and PCK type C_4 plants. Plant Production Science 13 (2): 169-176. https://doi.org/10.1626/pps.13.169.

Oukarroum, A., Madidi, S.E., Schansker, G., Strasser, R.J., 2007. Probing the responses of barley cultivars (*Hordeum vulgare* L.) by chlorophyll a fluorescence OLKJIP under drought stress and re-watering. Environmental and Experimental Botany, 60: 438–446. http://dx.doi.org/10.1016/j.envexpbot.2007.01.002.

Pan, T., Liu, M., Kreslavski, V.D., Zharmukhamedov, S.K., Nie, C., Yu, M., Kuznetsov, V.V., Allakhverdiev, S.I., Shabala, S., 2020. Non-stomatal limitation of photosynthesis by soil salinity. Critical Reviews in Environmental Science and Technology 1-35. https://doi.org/10.1080/10643389.2020.1735231.

Pottosin, I., Shabala, S., 2016. Transport across chloroplast membranes: Optimizing photosynthesis for adverse environmental conditions. Molecular Plant 9 (3), 356–370. https://doi.org/10.1016/j.molp.2015.10.006.

Reinert, F., Pinho, C.F., Ferreira, M.A. 2016. Diagnosing the level of stress on a mangrove species (*Laguncularia racemosa*) contaminated with oil: A necessary step for monitoring mangrove ecosystems. Marine Pollution Bulletin 113: 94-99. https://doi.org/10.1016/j.marpolbul.2016.08.070.

Shabala, S. 2013. Learning from halophytes: physiological basis and strategies to improve abiotic stress tolerance in crops. Annals of Botany, 112: 1209-1221. https://doi.org/10.1093/aob/mct205.

Shabala, S., Pottosin, I., 2014. Regulation of potassium transport in plants under hostile conditions: implications for abiotic and biotic stress tolerance. Physiologia Plantarum 151 (3), 257-279. https://doi.org/10.1111/ppl.12165.

Smith, F.W. 1974. The effect of sodium on potassium nutrition and ionic relations in Rhodes grass. Australian Journal of Agricultural Research 25: 407-414. https://doi.org/10.1071/AR9740407.

Sousa, C.P., Pinto, J.J.O., Martinazzo, E.G., Perboni, A.T., Farias, M.E., Bacarin, M.A., 2014. Chlorophyll *a* fluorescence in rice plants exposed of herbicides of group imidazolinone. Planta Daninha. 32: 141–150. http://dx.doi.org/10.1590/S0100-83582014000100016.

Strasser, R.J., Srivastava, Govindjee. 1995. Polyphasic chlorophyll *a* fluorescence transient in plants and cyanobacteria. Photochemistry and Photobiology, 61 (1): 32-42. https://doi.org/10.1111/j.1751-1097.1995.tb09240.x

Strasser, R.J., Tsimilli-Michael, M., Srivastava, A., 2004. Analysis of the chlorophyll *a* fluorescence transient. In: Papageorgiou, G.C., Govindjee (eds.) Advances in Photosynthesis and Respiration, Springer 19, 321-362. https://doi.org/10.1007/978-1-4020-3218-9_12.

Subbarao, G.V., Ito, O., Berry, W.L., Wheeler, R.M. 2003. Sodium-a functional plant nutrient. Critical Reviews in Plant Science 22 (5): 391-416. https://doi.org/10.1080/07352680390243495.

Suttie, J.M. 2000. Hay and straw conservation– for small-scale farming and pastoral conditions. FAO Plant Production and Protection Series 29. Food and Agriculture Organization, Rome.

Tester, M.; Davenport, R. 2003. Na^+ Tolerance and Na^+ Transport in Higher Plants. Annals of Botany 91(5): 503-527. https://doi.org/10.1093/aob/mcg058.

Valença, D.C., Moura, S. M. de, Travassos-Lins, J., Alves-Ferreira, M., Medici, L.O., Ortiz-Silva, B., Macrae, A., Reinert, F., 2020. Physiological and molecular responses of *Setaria viridis* to osmotic stress. Plant Physiology and Biochemistry 155, 114-125. https://doi.org/10.1016/j.plaphy.2020.07.019.

Wakeel, Abdul. 2013. Potassium–sodium interactions in soil and plant under saline-sodic conditions. Journal of Plant Nutrition and Soil Science 176: 344-354. http://doi.org/10.1002/jpln.201200417.

Yusuf, M.A., Kumar, D., Rajwanshi, R., Strasser, R.J., Tsimilli-Michael, M., Govindjee, Sarin, N.B., 2010. Overexpression of y-tocopherol methyl transferase gene in transgenic *Brassica juncea* plants alleviates abiotic stress: Physiological and chlorophyll *a* fluorescence measurements. Biochimica et Biophysica Acta, Amsterdam 1797, 1428-1438. https://doi.org/ 10.1016/j.bbabio.2010.02.002.

Zhao, C., Zhang, H., Song, C., Zhu, J-K, Shabala, S., 2020. Mechanisms of plant responses and adaptation to soil salinity. The innovation 1 (1), 100017. https://doi.org/ 10.1016/j.xinn.2020.100017.

Živcak, M., Olšovská, K., Slamka, P., Galambošová, J., Rataj, V., Shao, H.B., Brestič, M., 2014. Application of chlorophyll fluorescence performance indices to assess thewheat photosynthetic functions influenced by nitrogen deficiency. Plant Soil and Environment. 60, 210–215. https://doi.org/10.17221/73/2014-PSE.

Supplementary material

Table S1. Shoot and root fresh weight of two Rhodes Grass (*Chloris gayana)* cultivars, Callide and Reclaimer, grown in aerated nutrient solution under four different NaCl regimes (0, 200, 400, and 600 mM) with 1 or 10 mM potassium chloride for 25 days. Treatments were imposed 7 days after seedlings transplant.

		Shoot fresh weight (g)		**Root fresh weight (g)**	
	NaCl (mM)	*KCl*			
Cultivar		*1*	*10*	*1*	*10*
Callide	*0*	75.1±11.1^{Ab}	115.2±25.5^{Aa}	39.8±4.2^{A}	45.5±17.6^{A}
	200	70.9±9.8^{A}	65.4±10.5^{B}	23.5±4.9^{B}	25.5±5.8^{B}
	400	39.5±8.6^{B}	31.9±9.1^{C}	12.8±2.3^{C}	14.1±4.1^{C}
	600	14.3±2.7^{C}	11.4±4.6^{D}	6.3±1.7^{C}	8.0±2.7^{C}
Reclaimer	*0*	83.3±18.0^{Ab}	107.3±14.4^{Aa}	30.6±1.0^{Ab}	36.4±5.2^{Aa}
	200	60.1±11.5^{B}	57.7±14.3^{B}	19.8±4.6^{B}	18.4±3.0^{B}
	400	25.4±4.1^{C}	33.1±6.5^{C}	17.3±3.7^{B}	17.8±4.4^{B}
	600	7.1±1.2^{D}	12.6±3.5^{D}	6.0±1.5^{C}	9.3±1.8^{C}

Upper case letters represent significant differences using the Scott-Knott test in the column at $p < 0.05$. No significant differences were observed between the two levels of KCl with each NaCl level using the F-test at $p < 0.05$. Means ± standard deviation (n =8).

Table S2. F-values of three-way ANOVA (factors: 'cultivar', 'NaCl' and 'KCl') for dry weight and water content of shoots and roots and, relative growth rate (RGR) of two Rhodes Grass (*Chloris gayana)* cultivars, Callide and Reclaimer, grown in aerated nutrient solution under four different NaCl regimes (0, 200, 400, and 600 mM) with 1 or 10 mM potassium chloride for 25 days. Treatments were imposed 7 days after seedlings transplant. NS, $p > 0.05$; *, $p \leq 0.05$; **, $p \leq 0.01$; ***, $p \leq 0.001$. Data is shown in Table 1 and Figure 2.

	Shoot dry weight (g)	**Root dry weight (g)**	**Shoot water content (g)**	**Root water content (g)**	**RGR**
Cultivar	0.050^{NS}	1.355^{NS}	4.595^{**}	4.024^{*}	0.045^{NS}
NaCl	389.429^{***}	356.597^{***}	180.416^{***}	106.429^{***}	159.931^{***}
KCl	13.561^{***}	2.304^{NS}	8.284^{**}	3.939^{NS}	1.667^{NS}
Cultivar*NaCl	2.601^{NS}	6.598^{***}	0.615^{NS}	5.849^{**}	1.383^{NS}
Cultivar*KCl	0.08^{NS}	0.681^{NS}	0.265^{NS}	0.003^{NS}	0.025^{NS}
NaCl*KCl	15.525^{***}	0.828^{NS}	11.055^{***}	$t1.038^{NS}$	2.606^{NS}
Cultivar*NaCl*KCl	3.260^{*}	1.857^{NS}	1.917^{NS}	0.214^{NS}	0.597^{NS}

Table S3. F-values of three-way ANOVA (factors: 'cultivar', 'NaCl' and 'KCl') for Sodium (Na^+) and Potassium (K^+) concentrations in shoots and roots of two Rhodes Grass (*Chloris gayana)* cultivars, Callide and Reclaimer, grown in aerated nutrient solution under four different NaCl regimes (0, 200, 400, and 600 mM) with 1 or 10 mM potassium chloride for 25 days. Treatments were imposed 7 days after seedlings transplant. NS, $p > 0.05$; *, $p \leq 0.05$; **, $p \leq 0.01$; ***, $p \leq 0.001$. Data are shown in Figures 3, 4 and 5.

	Shoot [Na] (µmol g^{-1} DW)	**Root [Na] (µmol g^{-1} DW)**	**Shoot [K] (µmol g^{-1} DW)**	**Root [K] (µmol g^{-1} DW)**	**Ratio (Shoot)**	**Ratio (Root)**
Cultivar	3.2^{NS}	7.511^{***}	2.502^{NS}	21.852^{***}	5.812^{*}	10.373^{***}
NaCl	821.00^{***}	615.722^{***}	9.904^{***}	43.196^{***}	405.315^{***}	236.775^{***}
KCl	37.8^{***}	1.602^{NS}	15.859^{***}	343.014^{***}	332.782^{***}	163.366^{***}
Cultivar*NaCl	5.333^{**}	4.224^{***}	1.936^{NS}	2.805^{*}	11.636^{***}	0.878^{NS}
Cultivar*KCl	4.001^{*}	4.400^{*}	5.082^{*}	2.592^{NS}	5.984^{*}	10.400^{***}
NaCl*KCl	21.421^{***}	3.963^{**}	52.908^{***}	61.774^{***}	286.849^{***}	20.310^{***}
Cultivar*NaCl*KCl	3.793^{*}	0.232^{NS}	2.146^{NS}	0.072^{NS}	7.530^{***}	0.773^{NS}

Table S4. F-values of three-way ANOVA (factors: 'cultivar', 'NaCl' and 'KCl') for secreted (µmol g^{-1} DW day^{-1}) and concentrated (µmol g^{-1} DW day^{-1}) Na^+ and K^+ in detached second youngest fully expanded leaves of two Rhodes Grass (*Chloris gayana)* cultivars, Callide and Reclaimer, grown in aerated nutrient solution under four different NaCl regimes (0, 200, 400, and 600 mM) with 1 or 10 mM potassium chloride for 25 days. Treatments were imposed 7 days after seedlings transplant. NS, $p > 0.05$; *, $p \leq 0.05$; **, $p \leq 0.01$; ***, $p \leq 0.001$. Data is shown in Table 2.

	Secreted [Na] (µmol g^{-1} DW)	**Retained [Na] (µmol g^{-1} DW)**	**Secreted [K] (µmol g^{-1} DW)**	**Retained [K] (µmol g^{-1} DW)**
Cultivar	102.511^{***}	90.046^{***}	0.103^{NS}	7.482^{***}
NaCl	656.284^{***}	216.977^{***}	37.220^{***}	3.859^{*}
KCl	8.17763^{***}	20.018^{***}	3.539^{NS}	66.743^{***}
Cultivar*NaCl	0.051^{NS}	1.533^{NS}	2.886^{NS}	35.378^{***}
Cultivar*KCl	35.131^{***}	0.271^{NS}	2.996^{NS}	9.579^{***}
NaCl*KCl	30.443^{***}	11.793^{***}	2.420^{NS}	10.079^{***}
Cultivar*NaCl*KCl	11.724^{***}	6.131^{***}	3.916^{*}	2.405^{NS}

Table S5. F-values of three-way ANOVA (factors: 'cultivar', 'NaCl' and 'KCl') for leaf sap osmotic potential (-MPa) and contribution of ions (K^+ and Na^+) to the leaf sap osmotic potential (%) of two Rhodes Grass (*Chloris gayana)* cultivars, Callide and Reclaimer, grown in aerated nutrient solution under four different NaCl regimes (0, 200, 400, and 600 mM) with 1 or 10 mM potassium chloride for 25 days. Treatments were imposed 7 days after seedlings transplant. NS, $p > 0.05$; *, $p \leq 0.05$; **, $p \leq 0.01$; ***, $p \leq 0.001$. Data are shown in Figure 6 and Table 3.

	Leaf sap osmotic potential (-MPa)	**Contribution of K^+ (%)**	**Contribution of Na^+ (%)**
Cultivar	9.225^{***}	0.091^{NS}	35.247^{NS}
NaCl	773.565^{***}	56.699^{***}	4.300^{***}
KCl	12.027^{***}	40.757^{***}	10.613^{***}
Cultivar*NaCl	1.644^{NS}	0.507^{NS}	1.363^{NS}
Cultivar*KCl	17.451^{***}	6.488^{*}	2.037^{NS}
NaCl*KCl	38.384^{***}	14.911^{***}	7.340^{***}
Cultivar*NaCl*KCl	57.386^{***}	2.941^{*}	2.357^{NS}

Table S6. F-values of three-way ANOVA (factors: 'cultivar', 'NaCl' and 'KCl') chlorophyll *a* fluorescence intensity in steps O (F_0), J (F_J), I (F_I), and P (F_M) and performance indexes PIabs and PItotal (JIP-test) of two Rhodes Grass (*Chloris gayana)* cultivars, Callide and Reclaimer, grown in aerated nutrient solution under four different NaCl regimes (0, 200, 400, and 600 mM) with 1 or 10 mM potassium chloride for 25 days. Treatments were imposed 7 days after seedlings transplant. NS, $p > 0.05$; *, $p \leq 0.05$; **, $p \leq 0.01$; ***, $p \leq 0.001$. Data are shown in Tables 4 and 5.

	F_0	F_J	F_I	F_M	PI_{abs}	PI_{total}
Cultivar	0.012^{NS}	2.232^{NS}	11.037^{***}	17.224^{***}	5.723^{*}	18.702^{***}
NaCl	1.087^{NS}	0.770^{NS}	3.909^{NS}	1.329^{NS}	11.753^{***}	12.136^{***}
KCl	0.092^{NS}	0.088^{NS}	1.447^{NS}	2.033^{NS}	5.419^{*}	10.569^{***}
Cultivar*NaCl	3.571^{*}	10.376^{***}	13.479^{***}	10.015^{***}	18.628^{***}	2.537^{NS}
Cultivar*KCl	0.345^{NS}	14.890^{***}	8.108^{***}	19.622^{***}	18.412^{***}	18.401^{***}
NaCl*KCl	9.971^{***}	3.225^{*}	0.742^{NS}	3.843^{*}	2.885^{*}	1.925^{NS}
Cultivar*NaCl*KCl	6.725^{***}	5.069^{***}	18.187^{***}	14.829^{***}	3.919^{*}	1.338^{NS}

Table S7. F-values of three-way ANOVA (factors: 'cultivar', 'NaCl' and 'KCl') gas exchange measurements of two Rhodes Grass (*Chloris gayana)* cultivars, Callide and Reclaimer, grown in aerated nutrient solution under four different NaCl regimes (0, 200, 400, and 600 mM) with 1 or 10 mM potassium chloride for 25 days. Treatments were imposed 7 days after seedlings transplant. NS, $p > 0.05$; *, $p \leq 0.05$; **, $p \leq 0.01$; ***, $p \leq 0.001$. Data are shown in Table 6 and Figure 10.

	Ambient CO_2 (*400* µmol s^{-1})			
	Photosynthesis (*A*, µmol CO_2 m^{-2} s^{-1})	**Stomatal conductance (g_s, mol (H_2O) m^{-2} s^{-1})**	***C_i/C_a* (ratio of intercellular to ambient CO_2 concentration)**	***WUE***
Cultivar	3.125^{NS}	3.397^{NS}	0.912^{NS}	1.066^{NS}
NaCl	22.569^{***}	34.602^{***}	32.962^{***}	7.072^{***}
KCl	1.763^{NS}	3.975^{NS}	8.046^{***}	0.209^{NS}
Cultivar*NaCl	1.831^{NS}	1.855^{NS}	4.095^{**}	1.977^{NS}
Cultivar*KCl	0.719^{NS}	2.554^{NS}	0.001^{NS}	0.262^{NS}
NaCl*KCl	1.212^{NS}	1.288^{NS}	2.749^{NS}	3.578^{*}
Cultivar*NaCl*KCl	2.506^{NS}	2.726^{NS}	6.651^{***}	2.220^{NS}
	Elevated CO_2 (*800* µmol s^{-1})			
	Photosynthesis (*A*, µmol CO_2 m^{-2} s^{-1})	**Stomatal conductance (g_s, mol (H_2O) m^{-2} s^{-1})**	***C_i/C_a* (ratio of intercellular to ambient CO_2 concentration)**	***WUE***
Cultivar	10.144^{***}	4.218^{*}	9.349^{***}	5.268^{*}
NaCl	42.487^{***}	29.924^{***}	50.978^{***}	18.210^{***}
KCl	2.411^{NS}	6.563^{*}	3.778^{NS}	1.648^{NS}
Cultivar*NaCl	0.610^{NS}	4.921^{***}	2.734^{NS}	0.124^{NS}
Cultivar*KCl	0.156^{NS}	0.622^{NS}	0.229^{NS}	1.672^{NS}
NaCl*KCl	3.152^{*}	1.094^{NS}	1.692^{NS}	3.610^{*}
Cultivar*NaCl*KCl	6.256^{***}	1.444^{NS}	1.113^{NS}	2.938^{*}

CAPÍTULO 5 – CONCLUSÃO E PERSPECTIVAS

No primeiro artigo, nossos dados demonstraram o papel fundamental do K^+ suplementar em garantir condições fisiológicas adequadas para melhor suportar a aclimatação da espécie glicófita *S. viridis*, sustentando seu crescimento sob salinidade moderada (150 mM). Nossos resultados suportam a conclusão de que a aplicação de KCl pode ser uma estratégia eficiente para neutralizar os efeitos nocivos da salinidade, mas apresenta limitações dependendo do nível de estresse aplicado. Os dados descritos aqui podem fornecer indicações para pesquisas futuras em culturas de Panicoideae C_4 e seu crescimento em condições de salinidade.

A avaliação de *C. gayana* mostrou variação dependente do cultivar, com efeitos positivos na cadeia de transporte de elétrons da presença de 10 mM KCl para a cultivar Reclaimer e efeitos deletérios para a cultivar Callide. Tal efeito positivo, no entanto, não resultou em maior acúmulo de biomassa nem em fotossíntese líquida, o que pode não justificar a utilização de maiores doses de KCl para ambas as cultivares. A resposta de plantas pertencentes a cultivar Callide aos baixos níveis de K^+ na solução nutritiva pode ser um importante indicador para o uso e cultivo do cultivar em áreas marginais, além de alvo para estudos moleculares considerando a expressão canais seletivos de K^+ em solos intemperizados. Enquanto que a cv. Reclaimer se mostrou extremamente tolerante à exposição ao NaCl e taxas de assimilação de carbono não foram reduzidas até a exposição ao maior nível de sal (600 mM). É importante notar, entretanto, que embora algumas alterações tenham sido detectadas em ambas as cultivares em resposta à aplicação de NaCl e KCl, tais alterações não resultaram em fotoinibição em nenhum dos tratamentos avaliados.

A utilização de dados de fisiologia comparativa, aliada a dados e estudos de abordagens genômica, proteômica e metabolômica, serão fundamentais para a melhor compreensão de mecanismos de tolerância ao sal e desenvolvimento de culturas tolerantes ao sal. A exploração de respostas adaptativas e mitigação em safras já existentes poderá ser vital para alcançar esse entendimento e contribuir para o desenvolvimento de culturas mais adaptadas. A realização de experimentos adicionais visando a avaliação de respostas de culturas comercias a nível de campo será fundamental para validar a resposta positiva do aumento do nível de fertilização potássica como estratégia de mitigação do estresse salino em glicófitas em culturas de Panicoideae de metabolismo C_4, além de selecionar variedades

responsivas e com maior seletividade na absorção e transporte do nutriente em condições de salinidade.

Embora a comparação direta entre as duas espécies seja dificultada por diferentes metabolismos de fotossíntese C_4, um deles apresentando necessidade específica por Na^+, associada a mudanças anatômicas e ultraestruturais, conforme anteriormente relatado na literatura, o estudo das duas espécies nos permitiu observar respostas de aclimatação ao estresse similares com diferente eficiência. O estudo de *Setaria viridis* sob 150 mM de NaCl nos permitiu observar a capacidade de aclimatação da espécie com redução da biomassa e sua capacidade de se ajustar ao longo do tempo, conforme indicado pela redução das bandas K- entre 48h e 96h, mesmo quando as plantas não receberam potássio adicional. A fertilização com KCl adicional foi eficiente em reduzir os efeitos deletérios da salinidade até 150 mM NaCl, conforme observado pelo maior acúmulo de biomassa, redução da [Na] na parte aérea das plantas e no extravasamento de eletrólitos, densidade de estômatos a nível de plantas controle, aparente recuperação de turgor nas células epidérmicas da superfície adaxial das folhas, além da presença de bandas K- e L-negativas indicando maior eficiência fotossintética entre as unidades do FSII. No entanto, a capacidade da espécie de sobreviver a ambientes salinos apresentou limite (250 mM) no qual o aumento severo na quantidade de sal na parte aérea da planta (60x maior que o das plantas controle) foi limitante, interrompendo a cadeia de transporte de elétrons fotossintética, causando fotoinibição e inibindo o crescimento de novas folhas. A avaliação do *Chloris gayana*, no entanto, mesmo quando submetido a altos níveis de salinidade, como 600 mM de NaCl, não apresentou indícios de alterações ou interrupções permanentes na cadeia de transporte de elétrons fotossintética e, embora a presença de NaCl tenha induzido redução de taxa de fotossíntese líquida, em alguns casos, todas as plantas permaneceram fotossinteticamente ativas. Nossos resultados apontam, portanto, para maior eficiência de *C. gayana* em tolerar quantidades extremamente altas de sódio em sua parte aérea e raiz (de ~300 µmol g^{-1} DW em controles não salinos para ~2200 µmol g^{-1} DW em 600 mM na cultivar Callide, e de ~400 µmol g^{-1} DW em controles não salinos para ~2400 µmol g^{-1} DW em 600 mM na cultivar Reclaimer), contribuindo para o potencial osmótico, especialmente para a cultivar Reclaimer, e indicando alta eficiência na regulação do transporte de membranas, compartimentalização e exclusão de íons.

Nosso grupo de pesquisa, liderado pela prof. Fernanda Reinert, promove estudos de

fisiologia comparativa avaliando a resposta de *S. viridis* a condições ambientais adversas, tais como estresse hídrico, estresse salino, resistência a herbicidas e estresse térmico. Como perspectiva do estudo de *S. viridis* em condições de salinidade e mitigação do estresse com extra fertilização com potássio estima-se realizar experimentos futuros de avaliação da ultraestrutura em cloroplastos sob condições de salinidade e mitigação com K^+. Adicionalmente, estudo complementar avaliando a resposta dos diferentes tipos de raiz de *S. viridis* aos mesmos tratamentos avaliados no Artigo I se encontra em andamento. Como segunda parte do Artigo II, pretendemos realizar análise anatômica e ultraestrural de *C. gayana* em condições de alta salinidade para avaliar possíveis alterações além de níveis de preservação nas células do mesofilo e bainha perivascular.